GLOBAL PORT VULNERABILITY AND SUSTAINABILITY IN A RISKY WORLD:

EMPIRICAL EVIDENCE FROM CONGESTION, NATURAL DISASTERS, AND GEOPOLITICAL TENSIONS

LI CHENGKUN

PhD

The Hong Kong Polytechnic University

2025

The Hong Kong Polytechnic University

Department of Logistics and Maritime Studies

Global Port Vulnerability and Sustainability in a Risky World: Empirical Evidence from Congestion, Natural Disasters, and Geopolitical Tensions

LI Chengkun

A thesis submitted in partial fulfilment of the requirements
for the degree of Doctor of Philosophy

July 2025

CERTIFICATE OF ORIGINALITY

I hereby declare that this thesis is my own work and that, to the best of my knowledge and belief, it reproduces no material previously published or written, nor material that has been accepted for the award of any other degree or diploma, except where due acknowledgement has been made in the text.

_____ (Signed)

LI Chengkun

_____ (Name of Student)

Abstract

Maritime transport is considered the backbone of international trade and the global economy, with ports worldwide handling 80% of global trade by volume and 70% of global trade by value. Meanwhile, ports are vulnerable to both natural and human-induced disruptions, which can severely impact the global supply chains, leading to delays in the delivery of goods, increased transportation costs, and shortages of essential commodities. This study aims to investigate the disruptions that threaten port operations and the underlying mechanisms by using high-frequency global vessel data, which are essential for developing effective countermeasures to mitigate the adverse impact on international trade and economic stability. The first chapter explores congestion internalization at ports, with a particular analysis of the distinctive aspect of berthing priority and its impact on congestion. To address concerns related to endogeneity, the empirical analysis employs an instrumental variable approach. The results reveal that higher market concentration decreases port delays, as dominant shipping lines may internalize congestion. However, the provision of berthing priority in seaports might exacerbate delays at terminals and diminish shipping lines' motivation to mitigate congestion internally. The second chapter assesses port resilience under climate-related disasters. A port vulnerability index is developed based on the duration each port takes to rebound to its pre-disaster level of port calls. Subsequent analyses show that port vulnerability is inversely associated with factors at the hinterland, port interface, and seaside levels, including hinterland industrial diversity, port size, and port connectivity within the global liner shipping network. The third chapter evaluates how geopolitical tensions influence carbon emissions at the port level. Leveraging a SYS-GMM framework, the findings indicate that rising geopolitical risks increase carbon emissions by disrupting vessel arrivals and reducing berthing efficiency. Larger-vessel ports are more exposed to such shocks, while ports with high carrier concentration display greater operational resilience due to better coordination under uncertainty. These findings provide novel insights into the sustainability of international trade under internal and external risks and offer potential avenues for enhancing trade resilience.

Acknowledgements

I would like to express my deepest gratitude to my supervisor, Dr. Yang Dong, for his invaluable guidance, encouragement, and patience throughout the course of my research. His insightful feedback and constant support have been instrumental in shaping this thesis.

I am also profoundly thankful to Prof. Pierre Cariou, from Kedge Business School, Bordeaux, France, who supervised my research during my PhD visiting period. His generous support, constructive feedback, and academic inspiration greatly enriched my research experience and broadened my perspectives.

In particular, I wish to thank Dr. Bai Xiwen from Tsinghua University, Prof. Sarah Wan Yulai from the Hong Kong Polytechnic University, and Dr. Yang Xiyi from ShanghaiTech University, who were involved in different aspects of this thesis for their constructive suggestions, helpful discussions, and generous support.

I sincerely thank external examiners of this thesis, Prof. Yang Zaili of Liverpool John Moores University and Dr. Kou Ying of Shanghai Jiao Tong University, the internal examiner, Prof. Jiang Changmin of the Hong Kong Polytechnic University, for their time, insightful feedback, and invaluable guidance on the thesis.

Finally, I am profoundly thankful to my parents, whose unwavering love, understanding, and support have sustained me throughout the entire period of my study.

This thesis would not have been possible without the support of all these individuals.

List of Tables

List of Figures

Contents

Chapter 1

Introduction

Maritime transport is considered the backbone of international trade and the global economy (UNCTAD, 2022; Verschuur et al., 2022), with ports worldwide handling 80% of global trade by volume and 70% of global trade by value (Xu et al., 2020). Ports have evolved from simple points where ships dock into central hubs that coordinate the movement of goods throughout global supply chains (Notteboom et al., 2022). Despite their central role in global logistics systems, ports are increasingly exposed to a wide range of disruptions that threaten their operational stability, including congestion, extreme weather events, and geopolitical shocks. These disruptions can destabilize global supply chains by delaying cargo movement, inflating shipping costs, and causing supply shortages. For instance, Hurricane Katrina in 2005 forced the closure of several major ports in Louisiana, leading to significant export losses for the United States, with cascading effects across global supply chains and a sharp rise in commodity prices.(UNCTAD, 2021a; Trepte and Rice Jr, 2014; Rousset and Ducruet, 2020). Similarly, the imbalance between shipping container supply and demand intensified due to the COVID-19 lockdown policy, leading to notable congestion at the Ports of Los Angeles and Long Beach as restrictions eased in August 2021, ships faced wait times of up to twelve days to berth (FinancialTimes, 2021). The delays at ports could increase the time and fuel cost of shipping lines, disrupt delivery schedules, and in turn severely impact the global supply chain efficiency and costs (CNN, 2021; UNCATD, 2022). In addition, due to the Red Sea crisis, the number of vessels calling at the Suez Canal declined by approximately 42% from its previous peak by January 2024, leading to higher freight rates, rerouting via the Cape of Good Hope, and a substantial rise in carbon emissions, resulting in as much as a 70% increase in greenhouse gas emissions on voyages between Singapore and Northern Europe (UNCTAD, 2024).

Therefore, understanding how ports respond to and recover from both internal and external disruptions has become a matter of critical importance for the resilience of global

trade systems. Ports are not only passive infrastructure nodes, they are embedded within broader economic, logistical, and geopolitical environments, which means their ability to absorb shocks and restore normal operations, what we refer to as port resilience or vulnerability, is shaped by a complex set of interrelated factors. These include, but are not limited to, port governance structures, market concentration, infrastructure capacity, connectivity in the global liner network, and hinterland integration. Fortunately, recent technological advances associated with the Automatic Identification System (AIS), which is a vessel identification system that transmits real-time information on routes of vessels, enable more adequate monitoring of port activities (McCauley et al., 2016; Kroodsma et al., 2018). Leveraging AIS vessel-level data allows for a detailed and dynamic analysis of port performance under shock conditions, thereby enabling a more systematic assessment of port vulnerability and sustainability in the face of major disruptions.

Despite a growing body of research on how ports respond to and recover from disruptions, much of the existing literature remains hazard-specific and case-based. Prior studies have typically examined individual shocks in isolation, whether natural disasters or human-related events, often relying on qualitative approaches or limited case studies. While these works provide valuable insights, what remains underdeveloped is a broader and more systematic perspective that captures port resilience across different types of disruptions using large-scale and high-frequency data. Moreover, although AIS data applications have emerged in recent years, they generally cover only a limited number of ports or shorter time horizons, which constrains their generalizability.

To address this gap, the overall aim of this dissertation is to advance understanding of how ports are affected by and respond to diverse disruptions, thereby contributing to a more comprehensive perspective on port vulnerability and sustainability. The thesis pursues three objectives: (1) to investigate how market concentration and berthing priority influence terminal-level congestion; (2) to assess the vulnerability of ports to climate-related natural disaster shocks and identify the key determinants; (3) to analyze how geopolitical risks affect port-level emissions.

The choice of these three cases is deliberate. Together, port congestion, natural disasters, and geopolitical risks capture complementary dimensions of disruptions: internal operational shocks, external environmental shocks, and externally driven political shocks. Compared with other possible hazards, such as global pandemics, these cases are both empirically tractable with available data and theoretically representative of the broader set of risks shaping port vulnerability. While each study is independent, the dissertation as a whole contributes to a coherent and multi-dimensional understanding of port vulnerability and sustainability. At the thesis level, the overall scope covers container ports as key nodes in

global trade. The specific ports analyzed vary across chapters, reflecting the nature and scale of the disruptions investigated: congestion is examined at the terminal level in selected high-throughput ports to ensure sufficient data for capturing operational decision-making; natural disasters are analyzed in ports affected by specific events; and geopolitical risks are assessed using a broader global sample.

The first chapter explores congestion internalization at international container ports, with a particular analysis of berthing priority and its impact on congestion. The shipping market is dominated by a handful of carriers. An extra visit to the terminal by a certain carrier can not only increase the waiting time of the other carriers' fleets but also hurt the operation of its own fleet. Consequently, carriers may have incentives to internalize congestion. Using high-frequency global vessel data from January 2016 to December 2020, covering 27 prominent container ports and 138 terminals, we provide evidence on the existence of congestion internalization and quantify the impact of priority provision on the incentives of internalizing congestion. To address concerns related to endogeneity, the empirical analysis employs an instrumental variable approach. The results reveal that higher market concentration decreases waiting times at terminals, as dominant shipping lines may internalize congestion. However, the provision of berthing priority in seaports might exacerbate congestion and diminish shipping lines' motivation to mitigate congestion internally.

This second chapter examines global container ports' resilience to natural disasters by integrating perspectives from the hinterland, port interface, and seaside network, which is crucial but has been absent from existing literature. A port vulnerability index is first constructed utilizing daily shipping traffic data at 735 container ports worldwide, and coordinates data of 1,768 natural disasters between 2015 and 2019. Subsequent causality analyses reveal that port vulnerability is inversely related to port infrastructure development, hinterland industrial diversity, and port connectivity in the global shipping network. Additionally, the heterogeneity tests show that the influence of these determinants on port vulnerability varies by regional economic levels, disaster types, and port functions. This chapter addresses the endogeneity problem arising from reverse causality between industrial diversity and port vulnerability, and between port connectivity and port vulnerability, respectively.

The third chapter explores the impact of geopolitical tensions on port-level carbon emissions using a monthly panel dataset covering 269 container ports across 40 countries and regions from 2016 to 2023. Employing a system generalized method of moments (SYS-GMM) estimator, this chapter finds that heightened geopolitical tensions exacerbate emissions at ports, primarily by disrupting vessel arrival schedules and lowering berthing efficiency. Further heterogeneity analyses show that ports primarily serving larger vessels are more vulnerable to geopolitical shocks, likely due to that such vessels operate on long-haul international

routes and face greater exposure to geopolitical disruptions. In contrast, ports with higher market concentration, dominated by a few major carriers, exhibit greater resilience, possibly due to stronger coordination capacities that help stabilize operations during global disruptions.

The structure of the remainder of this thesis is outlined as follows. Chapter 2 investigates the internalization of port congestion by dominant carriers, focusing on how market concentration and berthing priority policies affect port waiting times. Chapter 3 develops a port vulnerability index based on post-disaster recovery patterns in port calls, and empirically examines how factors at the hinterland, port interface, and seaside levels influence a port's ability to rebound from climate-related natural disasters. Chapter 4 examines the impact of geopolitical tensions on port-level carbon emissions, capturing how vessel rerouting and scheduling disruptions alter environmental outcomes. Chapter 5 concludes the thesis and offers suggestions for future research on maritime resilience under global uncertainty.

Chapter 2

Port Congestion Internalization and the Role of Berthing Priority

2.1 Introduction

Service providers of congestible facilities often assign priority to users (customers) with higher time valuation (i.e., per-unit-time waiting cost), which may reduce the waiting time of prioritized customers while inevitably increasing that of non-prioritized ones. The classic operation management (OM) literature considers this priority allocation problem with heterogeneous customers, where each customer has a waiting cost per unit of time c and service time distribution μ. Waiting cost minimization can be achieved by assigning priority to customers in a descending order of $c\mu$, which is known as the famous $c\mu$ rule (Cox and Smith, 1961). However, the optimality of $c\mu$ rule may not be applicable for many service systems in practice. Firstly, accurately tracking the waiting times of all customers and understanding their specific waiting cost functions is often impractical. As a result, priority allocation is frequently based on limited data and the service providers' past experiences. For example, in emergency rooms, physicians quickly assess patients' conditions and assign the priority level based on existing triage protocols rather than conducting detailed examinations for each patient. Consequently, priority is typically granted to customers perceived to require urgent service or who are considered of higher value, with these priority policies rarely changing in the short term, which is called a fixed priority policy (Ouyang et al., 2022). Secondly, customers are considered atomistic in classic OM literature. Imagine a customer joining a queue at a bank or a queue to reach the customer service at a call center. He or she makes decisions independently without considering that his or her queue joining behavior would cause subsequent customers to wait for a longer time. Few studies from the OM side consider

non-atomistic customers, and empirical evidence on the efficient effect of priority provision on queuing systems is lacking, given that existing theoretical models cannot capture all the real-world complexities.

Non-atomistic users are a common feature in the logistics process of the global supply chain. Unlike atomistic users, such as individual end-consumers, non-atomistic users consume multiple units of the service and make decisions for all the service consumption instances at the same time. Typical examples can be users of transportation facilities, such as airport runways, air cargo terminals, and container ports' berthing space. Users of these facilities are mainly operators or business clients (e.g., airlines, shipping lines, etc.), and hence, one single user may consume a large share, instead of one single unit, of the service offered by the facility. For example, a major passenger airline may operate a huge number of flights, and therefore it would care about the externality that each flight that lands on the runway (i.e., each unit of service consumption) would impose on its own other flights using the same runway system (i.e., its own other consumption units). As a result, compared with a small fringe airline with very few flights, the major airline has more incentives to refrain itself from overusing the runway during the busiest hours, though it would still not care about the externality imposed on other airlines. This partial internalization of congestion externality implies that larger users would internalize more congestion externality by smoothing the arrival times, and in the end, contribute more to overall waiting time reduction. This issue of congestion internalization has been widely discussed in the transportation economics literature (Brueckner, 2002; Mayer and Sinai, 2003; Rupp, 2009; Ater, 2012; Silva and Verhoef, 2013), which is commonly tested by the impact of market concentration on waiting time, but has not been recognized in the general OM literature on priority queuing problems. Intuitively, the provision of priority could distort non-atomistic users' congestion internalization incentives, and their strategic responses could jeopardize the intended outcomes of the priority strategy. Indeed, service providers often grant priority to users with higher market shares to ensure system utilization. This implies that the congestion internalization of those large users is more likely to be affected by the priority strategy than small users in real life, which could exacerbate the congestion and increase waiting times. In a word, theoretically, when the usage of a facility is dominated by a few large operators, granting priority could cause longer waiting times.

Compared to theoretical research, empirical studies on the effectiveness of priority strategies in improving queuing system efficiency and reducing waiting times are scarce, not to mention the test of potentially negative impacts of priority in the presence of non-atomistic users and congestion internalization. This is potentially hindered by data availability. Specifically, the main difficulty is to collect priority arrangement information, which is often not

publicly disclosed. For instance, in maritime transportation, terminal operators might grant berthing priority to larger shipping lines during congestion (Imai et al., 2003), but such information is rarely accessible (Notteboom and Rodrigue, 2017).

To fill the gap, this study empirically tests the existence of congestion internalization behaviors and explores how priority affects waiting times at congestible facilities serving non-atomistic users, using data from the container shipping industry. In our study context, the congestible facilities refer to the berth space at container terminals and are managed by terminal operators. When a container ship calls at a terminal, it will be assigned to a berth where the containers are loaded or unloaded. When the number of ships arriving at the terminal exceeds the capacity of the berthing space, ships will form a virtual queue and wait at the anchorage area for their turn to berth. The non-atomistic users are shipping lines that often operate a fleet of container ships and may have multiple vessels calling at a certain terminal within a short time window. Shipping lines being offered berthing priority can skip the virtual queue and have their vessels berthed and handled earlier upon arrival at the terminal than the vessels of the other shipping lines. By observing container ships' arrival and berthing behaviors at various terminals, we can estimate each vessel's waiting times at anchorage areas before entering berths (Bai et al., 2023a), the concentration of shipping lines' vessel calls at each terminal, and shipping lines' priority status, allowing for drawing new insights on how priority provision influences incentives to internalize congestion externality. To address the potential endogeneity problem arising from the causal relationship between market concentration and waiting times, as well as that between priority share and waiting times, we leverage an Instrument Variable (IV) approach. Besides, we examine the effect of HHI on queue length as an intuitive mechanism for congestion internalization, whereby dominant shipping lines may coordinate ship arrival schedules to alleviate terminal congestion.

The challenge of getting priority information is overcome by utilizing high-frequency vessel movement data provided by the Automatic Identification System (AIS) database. We collect all container ships' positions and movements at 138 terminals in 27 major ports worldwide from January 2016 to December 2020. This information is then merged with the Lloyd's List to identify the operating shipping line of each container ship. Then, we develop an algorithm to identify whether a shipping line has priority privilege at a certain terminal by observing the queue-skipping behaviors of its container ships. The degree of priority provision, so-called priority share hereafter, at each terminal is then defined as the traffic share of prioritized shipping lines at each terminal. Our data reveals that the average traffic share of prioritized shipping lines is around 8.35%. Figure 2.1 shows the distribution of the number of years of priority provision among terminals from 2016 to 2020. Although

18 terminals did not offer priority to any shipping lines, 61 out of 138 sampled terminals consistently provided priority to at least one shipping line throughout the five-year study period, suggesting that priority is a common strategy applied by terminal operators.

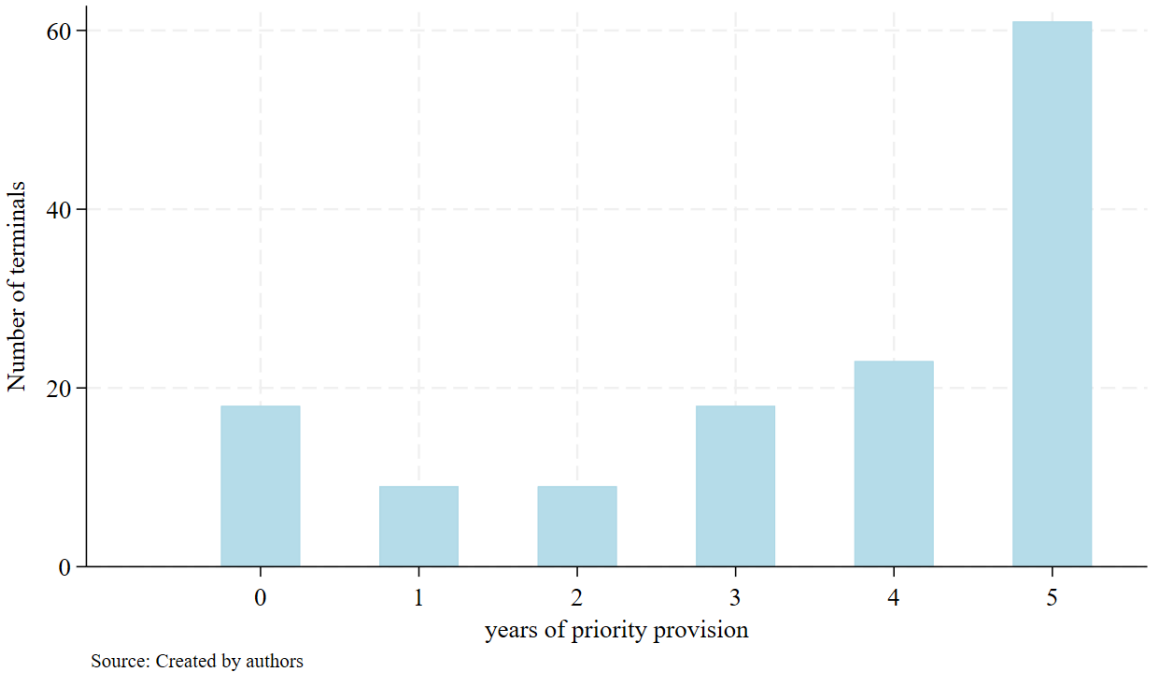

Figure 2.1: Number of terminals by years of berthing priority provision (2016 – 2020)

This study first finds that the market concentration level is negatively related to the waiting times at terminals, confirming the existence of congestion internalization. Furthermore, berthing priority provision can exacerbate berthing congestion at terminals. Specifically, an increase of 0.01-unit Herfindahl-Hirschman (HHI) index, which measures the market concentration level, leads to an average decrease of about 1.308 hours in vessel waiting time. When the sample is restricted to terminals with a fixed priority policy, a 0.01-unit increase in HHI results in an average decline of about 3.942 hours in vessel waiting time. Additionally, a 0.01-unit increase in the priority share leads to an average increase of about 6.942 hours in vessel waiting time. Moreover, when terminals with a fixed priority policy are classified into two groups based on the median priority share, we find that for terminals with a priority share lower than the median over five years, a 0.01-unit increase in HHI results in an average decrease of about 7.289 hours in vessel waiting time. In contrast, the coefficient of HHI is not significant in the group of terminals with a higher priority share than the median. This indicates that congestion internalization behaviors can be dampened by berthing priority, as the incentives for shipping lines to internalize congestion are diminished by priority provision.

The contribution of this study is multi-fold. First, it goes beyond the theoretical OM literature, which has focused on the impact of priority provision and optimal priority allocation schemes with atomistic users, by empirically examining the effects of priority provision in the presence of non-atomistic users. This empirical evidence would provide new empirical insights for future theoretical exploration of priority schemes by incorporating non-atomistic users and congestion internalization behaviors. Second, we take advantage of abundant global vessel movement data to develop an approach to identify users' priority status. This study also has direct implications for management strategies and policies to enhance the operational efficiency of congestible facilities, especially on the design of congestion pricing and priority provision schemes.

The organization of this study is outlined as follows: Section 2 reviews the relevant literature and develops hypotheses, Section 3 details the data collection and methodology employed, Section 4 discusses the findings, and Section 5 provides conclusions and implications of the study.

2.2 Literature Review and Hypothesis Development

This study engages with two strands of literature: priority in queuing systems and congestion internalization. We will discuss relevant works in each area separately before introducing the hypotheses we have developed based on the existing literature.

2.2.1 Priority in queuing

Extensive OM literature has investigated the priority schemes in queuing systems, especially on the minimization of the total waiting cost. Early work by Cobham (1954) and Cox and Smith (1961) laid the foundation by developing the well-known $c\mu$ rule, which suggests prioritizing customers in a descending order of $c\mu$ to minimize the total waiting cost. Building on this framework, later studies (Nain, 1989; Argon and Ziya, 2009) extended the analysis to accommodate more general cost structures and address challenges such as imperfect information about customer types. The above literature assumes that the waiting cost is linear to the waiting time of customers, while the linear cost function may not accurately capture situations where the waiting cost per unit time increases as the waiting time lengthens. In response, studies including Haji and Newell (1971) and further work by Van Mieghem (1995) and Mandelbaum and Stolyar (2004) proposed a generalized $c\mu$ rule. This approach prioritizes service based on the product of marginal waiting cost and service rate, effectively addressing scenarios with increasing and convex cost functions. Furthermore,

in practice, many congestible facilities default to a fixed priority policy, prioritizing certain customer types based on limited data and their experience without adjusting for real-time waiting cost dynamics. Ouyang et al. (2022) highlighted that the fixed priority policy may not always align with the objective of minimizing total waiting costs, and may yield benefits only when the proportion of prioritized customers is relatively small.

Meanwhile, empirical studies have explored queuing behaviors across diverse settings such as call centers (Yu et al., 2017), emergency departments (Song et al., 2015; Ding et al., 2019), radiological services (Singh et al., 2024), and restaurants (Tan and Staats, 2020), etc. These empirical studies have attempted to understand the decision-making process of users under priority schemes (Yu et al., 2017) and the priority routing behaviors of service providers (Ding et al., 2019). Among them, Song et al. (2015) specifically explored the differences in the impacts of pooled and dedicated queues on waiting times.

Maritime transportation research, which has long addressed berth allocation and terminal operations, offers additional insights into these issues. Studies in this field (Imai et al., 2003; Golias et al., 2009; Ursavas and Zhu, 2016; Yıldırım et al., 2020; Yu et al., 2022) incorporate berthing priority as a decision variable to minimize total terminal operation time, including handling and waiting times. More recently, Lin et al. (2024) developed a prioritized queuing mode and theoretically demonstrated that the total system cost for carriers will either remain constant or increase under the priority provision scheme, even though the carrier granted priority may enjoy a reduction in operation costs. Both Ouyang et al. (2022) and Lin et al. (2024) find that priority may increase the total waiting cost, yet some of their findings diverge due to differences in model settings. Ouyang et al. (2022) proposed a single-server queuing system with different customer types, and they suggest implementing a priority policy instead of FCFS when prioritized customers only account for a smaller proportion. Conversely, Lin et al. (2024) considered a biterminal model with two carriers and argued that the system cost increases if the prioritized carrier handles a smaller volume of shipping demand compared to the other. In Lin et al. (2024)'s model, the terminal granting priority ends up serving fewer customers (vessels), leading to a larger operational cost at the terminal without priority provision, hence the overall system cost increases. However, we are not aware of any empirical evidence on how the proportion of prioritized customers influences the efficiency of queuing systems with priority. Our study addresses this gap by providing new empirical findings on the impact of prioritized customer proportions on waiting times through a heterogeneity test.

2.2.2 Congestion internalization

This study falls right into the strand of literature examining congestion internalization when carriers are non-atomistic in the airline industry. Based on a simulation model, Daniel (1995) initially noted the potential congestion internalization behavior by dominant airlines and studied the implications of this possibility on airport congestion pricing. By comparing actual intraday traffic patterns at the Minneapolis-St. Paul airport with the simulated pattern under the internalization hypothesis, he rejected internalization and concluded that an atomistic model is more favored empirically. Since then, a number of studies have investigated congestion internalization at airports. While Daniel's work is based on a complex bottleneck model with one dominant airline and many fringe carriers, Brueckner (2002) was the first to use a neat Cournot competition model to demonstrate why each airline will internalize its own share of congestion externality through profit maximization, implying that dominant airlines (those with higher market shares) internalize more congestion externality. This finding has huge implications on how congestible airports should be regulated, as small and large airlines were treated the same in earlier airport literature. Brueckner's study, therefore, started a stream of research which builds on the Cournot competition model to derive and evaluate a wide range of airport regulation and policies such as pricing, capacity investment, slot allocation, etc., by incorporating various features, including hub-and-spoke airline network, airport non-aeronautical revenue, heterogeneous passengers, intermodal competition, to name a few. The most pioneer works of this stream are contributed by Pels and Verhoef (2004); Brueckner (2005); Zhang and Zhang (2006); Brueckner (2009), while this Cournot approach is still popular in recent airport-related theoretical studies. Considering that Daniel's study assumed a case of one dominant carrier and many fringe airlines in one airport which is different from the oligopoly Cournot competition context, Brueckner and Van Dender (2008) reconciled mixed views theoretically by modeling an airport with duopoly airlines and comparing equilibrium outcomes under three model settings: Cournot competition, Stackelberg leader with a Cournot follower, and Stackelberg leader with a fringe follower. The Cournot follower realizes that its decision would affect congestion and airfares, while the fringe follower does not, and thus the third setting best aligns with Daniel's model. Brueckner and Van Dender (2008) showed that the leader will internalize different levels of externality under the first and second settings, but it will not internalize any externality when airlines are perfect substitutes in the third setting. More importantly, even in the third setting, as long as airlines are imperfect substitutes, the leader would internalize some externality. Silva and Verhoef (2013) also showed that the fashion of competition affects internalization. They demonstrated theoretically that the level of internalization under differentiated Bertrand competition is below the prediction of Cournot model.

Scholars have also made significant efforts to explore the answer using real data, but the findings have been ambiguous. Empirical evidence in support of the internalization behavior was offered by Brueckner (2002) and Mayer and Sinai (2003) who both showed the airports dominated by a few large carriers (and hence have high airport concentration) tend to have lower delays than those served by many airlines each with a small market share (and hence have low airport concentration), other things being equal.Guo et al. (2018) found that full-service airlines' ticket price data is consistent with the internalization hypothesis, while ticket price data of low-cost airlines suggests no internalization. Morrison and Winston (2007) further found mild support to design an optimal congestion pricing scheme that accounts for carrier internalization compared to atomistic pricing, while Daniel and Harback (2008) and Rupp (2009) found no support for internalization behavior. Ater (2012) supported the internalization hypothesis when studying congestion patterns during the high flight volume period.

To the best of our knowledge, only two papers in the maritime shipping field have addressed the issue of congestion internalization. Jiang et al. (2017) built a theoretical model to analyze the congestion internalization of the shipping lines, considering the knock-on effect. Barkley and Mcleod (2022) empirically investigated the effects of increased market concentration generated by mergers on delays at congested ports in the US inland waterway system. They found that mergers decreased delays by 7% on average, indicating the presence of congestion internalization. However, they did not examine how priority provision could affect the internalization behavior of shipping firms. Furthermore, the sample they use is restricted to only local data.

The congestible facilities with non-atomistic users may change the results of classic OM literature regarding the impact of priority in congestible facilities with atomistic users due to the congestion internalization behaviors. Non-atomistic users, such as airlines and shipping lines, will consider the impact of an extra visit on the waiting times of their own fleets, and they may decrease the congestion by smoothing the arrivals. This brings a new source of complexity in understanding how priority schemes affect the efficiency of queuing systems and the waiting costs of individual users to the classic OM literature. To fill this gap, this study empirically explores the relationship between the degree of priority provision (priority share) and waiting time together by controlling for individual shipping lines' priority status (i.e., vessel priority variable) and market concentration (congestion internalization).

2.2.3 Hypothesis development

The following hypotheses are developed based on existing literature.

Many aviation studies support the existence of congestion internalization (Brueckner, 2002; Mayer and Sinai, 2003; Ater, 2012; Guo et al., 2018; Milchtaich, 2021). The shipping market is similar to the aviation market in terms of market structure and operation pattern, we expect that congestion internalization also exists in the shipping industry. Building on previous studies, we propose a basic prediction regarding the relationship between market concentration and congestion: when a shipping terminal becomes more concentrated, moving from the extreme atomistic case, the average waiting time should fall (Brueckner, 2002; Mayer and Sinai, 2003; Ater, 2012). In this paper, we follow the vast literature (Brueckner, 2002; Mayer and Sinai, 2003) in using HHI as a proxy for the extent to which congestion is internalized by carriers. HHI is computed based on the share of port calls made by shipping lines. If port calls at a particular terminal mostly come from a single shipping line (i.e., the terminal concentration measure is higher), then waiting times shall be shorter when holding the number of port calls constant. Therefore, we propose Hypothesis 1 as below:

Hypothesis 1 *Waiting times are lower at terminals with a higher level of terminal concentration measured by Herfindahl-Hirschman index (denoted HHI).*

Literature from the OM and maritime sides has both suggested concern on the impact of priority provision on system efficiency due to the excessive waiting cost caused by priority schemes. Firstly, despite many OM studies supporting that priority can minimize waiting cost by allocating priority following the well-known $c\mu$ rule, Ouyang et al. (2022) argued that queuing system performance is often worse off under a fixed priority policy, especially when customers have a quadratic cost function of waiting time. In maritime literature, Lin et al. (2024) discovered that berthing priority provision will either have no effect (if prioritized carrier operates a larger shipping demand) or increase (if prioritized carrier operates a smaller shipping demand) the total system cost (i.e., time cost and bunker consumption cost) for both carriers. Building upon the findings of Ouyang et al. (2022) and Lin et al. (2024), we expect that the priority provision may increase the waiting time of those carriers who have no agreement with the terminal while reducing the waiting time for prioritized carriers, and the average waiting time is expected to increase. Based on prior discussion, our second hypothesis is as follows:

Hypothesis 2 *The increased priority provision will result in increased average waiting times.*

Without a priority scheme, each shipping line internalizes the proportion of externality of one additional ship equivalent to its market share. When the priority scheme is adopted, the shipping lines' incentive to internalize the congestion externality would be affected. While we are not aware of any theoretical study on this issue, intuitively, the expected waiting time for prioritized vessels shall be shorter compared to the no-priority case, implying less incen-

tive for priority shipping lines to internalize congestion externality. Although non-priority shipping lines may expect higher expected waiting times and be willing to internalize more externality, as priority is commonly granted to shipping lines with large traffic shares at the terminal, the reduction of congestion internalization could be substantial and dominating. Therefore, we expected that there would be a cancelling effect of berthing priority on congestion internalization, and our third hypothesis is as follows:

Hypothesis 3 *The amount of congestion internalization is affected by the priority share provided by the terminal. Specifically, the positive relationship between terminal concentration and average amount of internalization is dampened by priority provision.*

2.3 Data and Methodology

This section presents the data sources, the construction of key variables, and the econometric models employed to examine our hypotheses.

2.3.1 Data

The primary data source we use for the empirical study is Automatic Identification System (AIS) data. AIS is an automatic tracking system installed onboard vessels that was originally designed for ship collision avoidance. It provides detailed information about the real-time movements of all ocean-going ships and enables the study of micro-behaviors of individual ships. Specifically, AIS data records a vessel's static (e.g., vessel identification number), dynamic (e.g., time stamp, latitude, longitude, speed), and voyage-related (e.g., draught, destination) information (Yang et al., 2019). We collect global vessel movement data of all container vessels with deadweight tonnage (DWT) over 1000 from Jan 2016 to Dec 2020 and investigate 27 world-leading ports with 138 container terminals. The container ports are selected according to Lloyd's List One Hundred Ports list in 2019. We further use Lloyd's List Ship database to extract vessel operator information and match it with AIS to identify each vessel's operating shipping line.

Utilizing these multiple databases, we apply data processing algorithms to construct the following key variables for the empirical study, namely waiting time for berthing (waiting time), market concentration (HHI), degree of berthing priority provision (priority share) and the final dataset is an unbalanced panel dataset at the vessel-terminal-month level. Since priority is often provided at the terminal level instead of the port level, to examine the impact of priority on berth congestion and internalization behaviors of shipping lines, we fine-tune waiting time and market concentration measures at the terminal level. Additionally, both

the waiting time and berthing priority calculations require the exact locations of berth and anchorage areas at each terminal, we therefore rely on the satellite map and an automatic berth and anchorage area identification method proposed by Bai et al. (2023a) to construct a dataset containing terminal berth and anchorage areas information.

Waiting time The berth area congestion at each terminal can cause berthing waiting time. If a ship arrives at a container terminal and all the berths are occupied for loading or unloading containers, it must queue up at an anchoring area and wait for its time to berth. The waiting time for berthing is broadly accepted as a congestion measure (Talley and Ng, 2016). The waiting time of each vessel is not publicly available, therefore, we leverage AIS data to construct a unique dataset that tracks each vessel's waiting time in anchorage areas at each terminal. Since the congestion time cannot be directly extracted from AIS, we refer to a tailored algorithm developed by Bai et al. (2023a) to calculate each vessel's waiting time at the terminal. An example of the identification results of berth and anchorage areas is provided in Figure A.1 of the Appendix A. The final waiting times are obtained at the vessel-terminal call level, measured in hours. Figure 2.2 summarizes the average waiting time for the terminals of different ports examined in this study. Tanjung Priok port in Indonesia suffers from the highest waiting times, followed by Ningbo and Yangshan in China, where vessels need to wait around 11-16 hours on average before berthing. To validate our waiting time data, we presented the monthly average ship waiting hours in Figure A.2 of the Appendix A and compared the data with reported events.

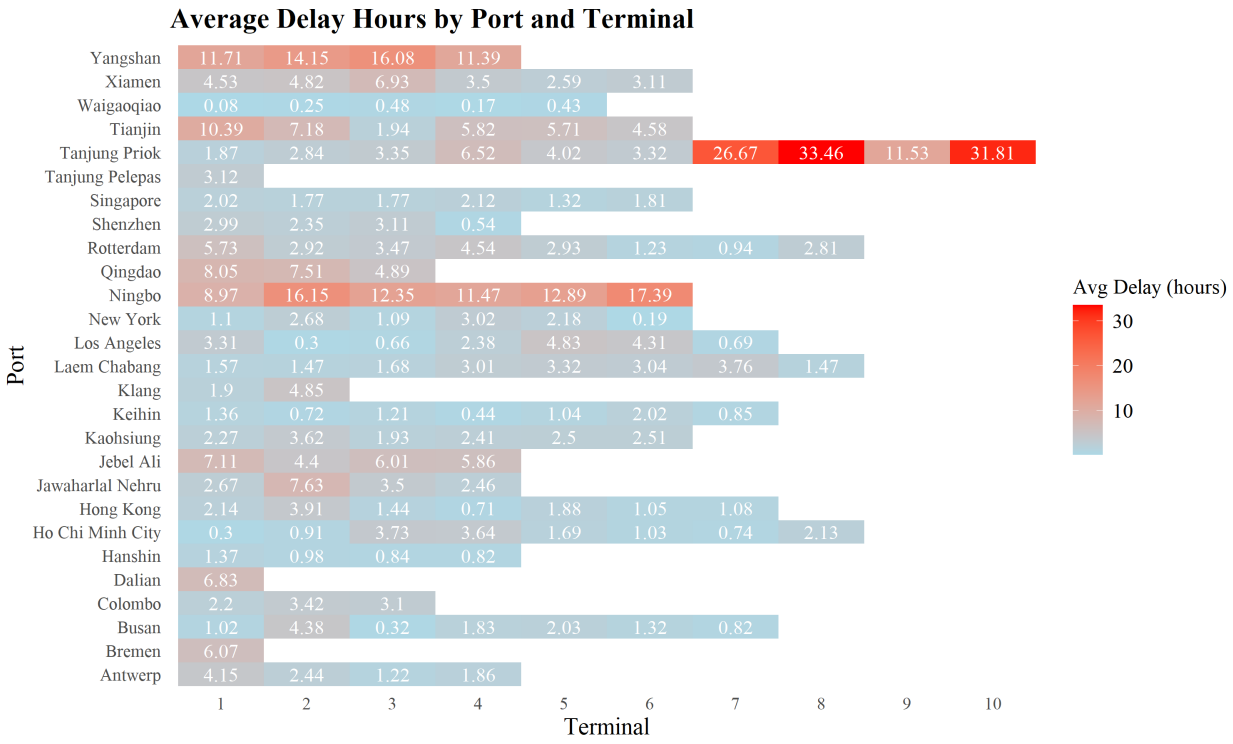

Figure 2.2: Average terminal delays

Terminal Level HHI As a measure of terminal concentration, we compute the Herfindahl-Hirschman index (HHI) at the shipping line level. It is calculated by taking the summation of the squared traffic volume of each shipping line in the terminal for a given month. A higher HHI often indicates a more concentrated market.

Queue Length To compute the queue length for berthing when a port call is made, we count the real-time length for berthing at each terminal. Specifically, the length for berthing is initialized as 0. The length then increases by 1 when a vessel arrives at anchorage and decreases by 1 when a vessel at anchorage leaves for berthing.

Priority Share The degree of priority provision of a terminal is measured by the total market share of shipping lines with priority at this terminal. We define priority as being permitted to jump the queue for berthing when the terminal is congested (that is, there is at least one vessel in the queue, and we assume there is a single queue for all berths in each terminal). Notice that the prioritized vessel only jumps to the beginning of the queue, and it still needs to wait for vessels already in the berths to be handled if all berths are occupied upon arrival. This reflects a non-preemptive priority assumption, where the ongoing service of a vessel cannot be interrupted by the arrival of a higher-priority vessel. Specifically, we record the queue length when a vessel arrives at the terminal. If the length of the queue is larger than zero, we label the state of the terminal at the vessel's arrival as congested. If

the terminal is labeled as congested upon the vessel's arrival, we check whether the vessel waits at the anchorage or berths earlier than others that arrive earlier than this vessel. If the vessel berthed earlier, we consider this a sign of priority, showing that the terminal gives the vessel permission to jump the queue for berthing. It should be noticed that situations where vessels from the same shipping line jump ahead of each other are not considered cases of berthing priority, because this is more likely an operation decision of the carrier rather than a sign of priority, and we cannot tell whether the carrier has priority by the jumping behaviors among its own vessels. The algorithm for identifying ship priority is presented in Figure 2.3.

To ensure the accuracy and reliability of our data analysis, we removed certain outlier cases from the queuing process. Some vessels may experience unreasonable long waiting times and are jumped by an unusually large number of vessels from other carriers, due to special circumstances, such as vessel layups or avoiding early arrival to its next destination (Port of NY & NJ, 2022). Therefore, we removed outliers with the following conditions: (1) vessels with waiting time exceeding 24.65 hours (the 95th percentile of vessel waiting time); (2) vessels that were jumped by more than 11 vessels (the 99th percentile of the number of vessels jumping the queue after subtracting the cases of self-queuing); (3) vessels that were jumped by vessels from more than three different companies (the 99th percentile for the number of different companies jumping the queue after subtracting the cases of self-queuing firms). After removing the outlier port calls, for each shipping line, we count its number of vessel calls that jumped the queue and the number of vessel calls when the terminal is congested throughout each sampling year. The ratio of these two counts tells whether a shipping line's vessel can jump the queue whenever there is a queue upon arrival. If the ratio reaches 100% and the shipping line has no fewer than 20 port calls per annum at the terminal, the shipping line will be identified as being granted priority by the terminal. This is to ensure that only shipping lines with a significant presence at the terminal are considered to have priority, and this criterion is derived by consulting the staff from the port authority of Singapore. Then, we sum up the market shares of identified priority shipping lines to approximate the degree of priority at the terminal. The methodology flowchart for identifying key variables of our model is shown in Figure 2.4.

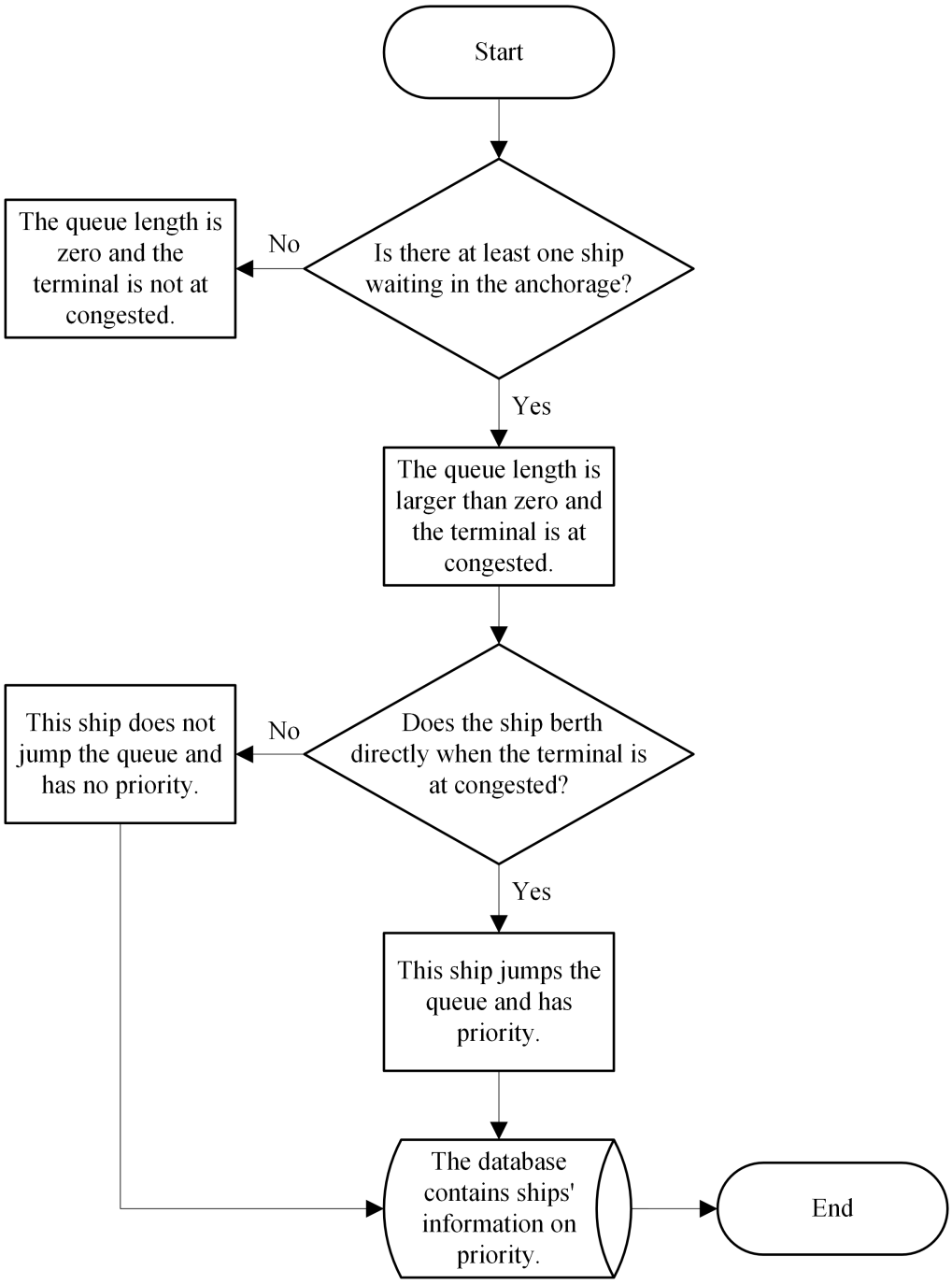

Figure 2.3: Ship priority identification

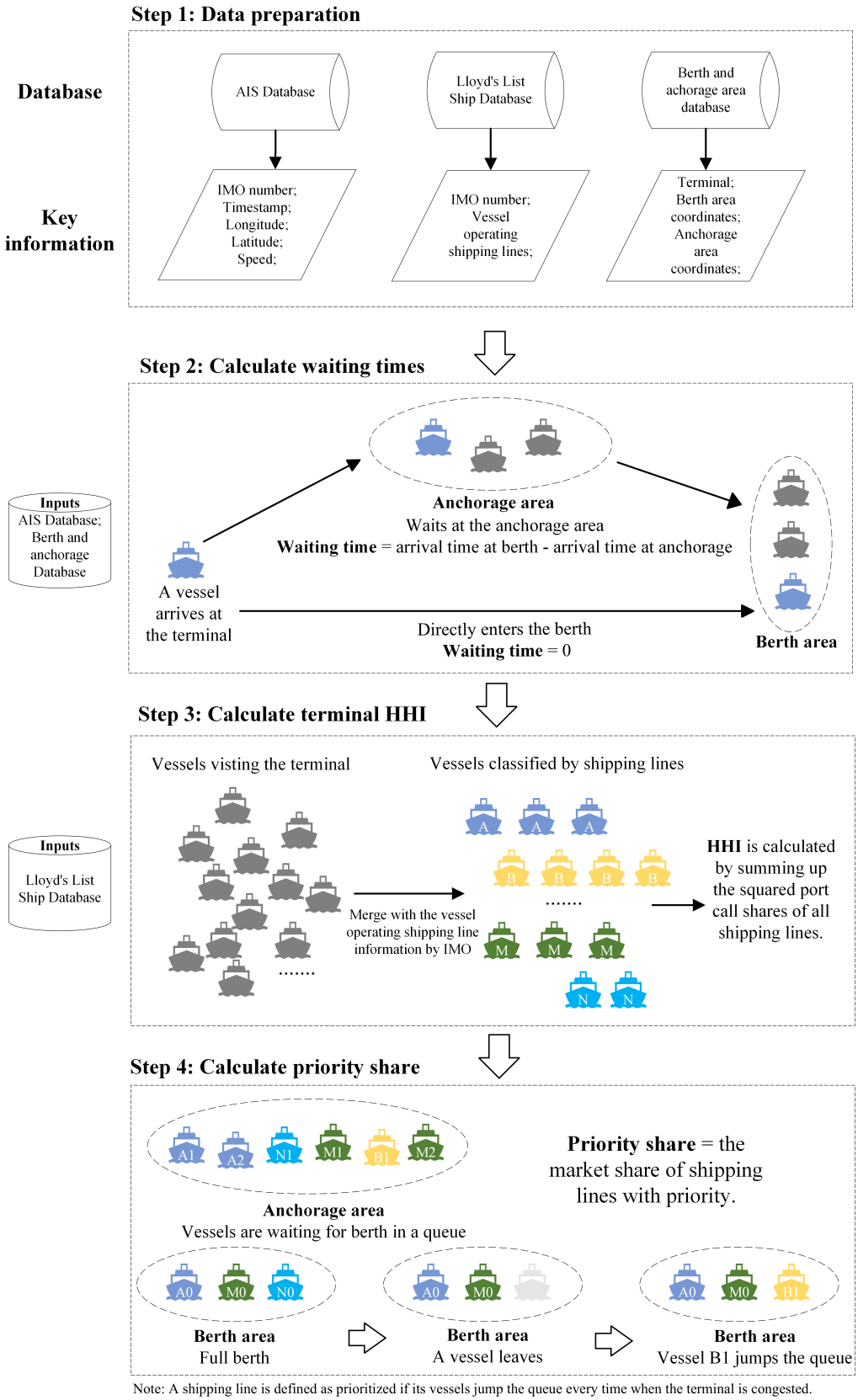

Note: A shipping line is defined as prioritized if its vessels jump the queue every time when the terminal is congested.

Figure 2.4: Methodology flowchart for identifying key variables

The summary statistics for the key variables in our data are presented in Table 2.1. On average, a vessel waits around 1.267 hours when calling at a terminal, with a standard deviation of 4.154. The average HHI across all terminals is around 0.076 with a standard deviation of 0.053. The average priority share is 0.130 across all terminals with a standard deviation of 0.104. A newly arrived vessel faces a relatively low probability (0.684) of encountering a queue length greater than one, although the variation is large, with the maximum queue length reaching 27.

Table 2.1: Summary statistics of key variables

Variable	**N**	**Mean**	**SD**	**Min**	**Max**
Waiting Time (Hour)	593,987	1.267	4.154	0	24.649
HHI	593,987	0.076	0.053	0.020	0.634
PriorityShare	593,987	0.130	0.104	0	0.632
Daily Portcall	593,987	5.990	3.768	1	28
DWT (Deadweight Tonnage)	593,987	56,398.507	46,763.319	1,438	232,606
Vessel Priority	593,987	0.076	0.265	0	1
Queue Length	593,987	0.684	1.256	0	27

Note: Terminals with twenty or fewer monthly vessel visits were excluded as outliers.

2.3.2 Statistical models

Model specification To test these hypotheses, we propose the following base empirical specification to examine the relationship between the delays, HHI, and priority share.

$$WaitingTime_{ijk} = \alpha_0 + \alpha_1 HHI_{jt} + \alpha_2 PriorityShare_{jT} + \boldsymbol{\beta}\mathbf{Controls}_{ijk} + \delta_j + \gamma_t + \tau_s + \epsilon_{ijk} \tag{2.1}$$

The dependent variable $WaitingTime_{ijk}$ is the waiting time of ship i's kth port call at terminal j. The independent variables of interest include the monthly terminal level HHI_{jt} and the share of ships with priority $PriorityShare_{jT}$ at terminal j in year T. We control the factors that may affect the waiting time of ships, including ship size in logarithm format, whether a ship has priority to jump the queue at congestion, and the daily terminal visits. The algorithm for port call identification can be found in Bai et al. (2023a). δ_j, γ_t, and τ_s are fixed effects of terminal, month, and shipping line, respectively. ϵ_{ijk} stands for the error term.

Instrumental variables (IV) approach In our OLS estimation, potential endogeneity issues may arise, particularly due to reverse causality. For example, if a terminal frequently experiences congestion with extended waiting times for berthing, shipping lines may opt to switch to alternative terminals to minimize the costs associated with extra waiting times. Consequently, longer waiting times at a terminal could result in fewer shipping lines choosing to call at that terminal, thereby reducing the market concentration level (measured by HHI). This reverse causality between waiting time and HHI can lead to biased estimates of the effect of HHI on waiting time. Similarly, reverse causality may also bias the estimation results when analyzing the relationship between priority share and waiting time. Less congested terminals may offer priority to attract shipping lines and improve berth utilization, while more congested ones are less inclined to do so due to sufficient traffic.

Thus, we conduct an IV/2SLS estimation using instrumental variables to address endogeneity. A valid instrument variable should be correlated with the potential endogenous variable (HHI or $PriorityShare$) but not be correlated with the dependent variable ($WaitingTime$). In our model, the instrument variable of HHI is a proxy market concentration calculated by the global share of shipping lines, denoted as $HHIGlobalShare$. A shipping line's global share is defined as its total port calls at all the sampled terminals over the sum of port calls across all shipping lines and terminals in month t. $HHIGlobalShare$ is computed by replacing the market shares of individual shipping lines visiting terminal j in month t with their global shares in the same month. Large shipping lines are likely to maintain or extend their dominance at specific terminals, thus leading to a higher market share in both global and local terminal-specific contexts. This observation hints at a positive association between HHI and $HHIGlobalShare$. That is, terminals mainly serving shipping lines with global dominance are likely to have a high HHI. Furthermore, $HHIGlobalShare$ is not directly related to the congestion at the terminal, as one single terminal's efficiency is not likely to drive a shipping line's global market share.

To address the reverse causality between priority share and waiting time, we use the annual priority propensity of all shipping lines that visited the terminal, which is denoted as $AvgLinerPriority$, as the instrument of priority share. The calculation and rationale for this instrument variable are detailed in the Appendix A. We assume that this index is unrelated to waiting time at terminals, as it measures the probability of shipping lines enjoying priority at all other terminals, excluding the terminal being measured, and whether other terminals providing priority to shipping lines should have no effects on waiting times at the given terminal. We further test the validity and endogeneity of our instrument variables in the next section.

2.4 Empirical results

This section examines the hypotheses proposed in 2.2.3 regarding the impact of internalization of congestion and berth priority on delays.

2.4.1 OLS estimation results

Table 2.2 presents the OLS estimation of the baseline model provided in 2.3.2. We run regressions separately with the full sample, which includes all observations in our dataset, and the restricted sample that excludes observations from those terminals with unstable priority share over the five-year period. In both cases, HHI has a significantly negative relationship with the waiting time, indicating that congestion reduces in terminal concentration, which is in line with **Hypothesis 1**. The coefficients of *PriorityShare* are also negative, indicating that the congestion reduces in the degree of priority provision, which is inconsistent with **Hypothesis 2**. Note that the OLS method is likely to generate biased estimates since market concentration and priority share may not be exogenous. Therefore, in the following sections, we opt for an instrumental variable approach.

Table 2.2: OLS estimation results

	(1) Full sample *WaitingTime*	(2) Restricted sample *WaitingTime*
HHI	-0.894***	-3.025***
	(0.270)	(0.644)
PriorityShare	-1.130***	-1.182***
	(0.080)	(0.139)
Log (Number of Portcall)	0.401***	0.466***
	(0.019)	(0.035)
Log (DWT)	-0.348***	-0.322***
	(0.013)	(0.023)
Vessel Priority	-2.068***	-2.959***
	(0.016)	(0.029)
Constant	4.881***	5.064***
	(0.164)	(0.295)
Observations	593,987	218,831
R^2	0.125	0.174
F-statistic	165.435	170.726
Fixed Effects	Terminal / Month / Shipping line	

Note: Standard errors are clustered by terminal-month-shipping line category. * $p < 0.1$, ** $p < 0.05$, *** $p < 0.01$.

2.4.2 IV estimation results

Table 2.3 presents the results using IV/2SLS method with the instrumental variables constructed in Section 2.3.1. In the first-stage regression results, the large F-statistic and the significant coefficients of the IVs, $HHIGloablShare$ and $AvgLinerPriority$, validate their relevance to the endogenous variables HHI and $Priority$. The positive relationship between $HHIGloablShare$ and HHI reflects our conjecture that terminals visited by shipping lines with large global presence tend to have high market concentration. Additionally, the positive relationship between $AvgLinerPriority$ and $PriorityShare$ is consistent with our assumption that the average propensity of shipping lines at the terminal to seek priority is positively correlated with their likelihood of seeking priority at this specific terminal. Further, we employ Lagrange-Multiplier (LM) test and Wald F test based on the Kleibergen–Paap rk statistic (Kleibergen and Paap, 2006) to check underidentification and weak identification, respectively. Our models pass the above two tests, and the F-statistics of all the first-stage regressions are large (Table 2.3), indicating that the chosen instruments are valid and strong. Moreover, unlike the OLS estimators, the 2SLS estimators are in line with both **Hypotheses 1 & 2**, and the changes are consistent with our expectation (see detailed discussion below). Therefore, we believe the OLS regression results can be biased due to endogeneity, and the 2SLS estimators are more credible.

Table 2.3: Instrument variable regression results

	(1)	(2)	(3)	(4)	(5)	(6)
	Full sample			Restricted sample		
	2SLS	First-stage		2SLS	First-stage	
	WaitingTime	*HHI*	*PriorityShare*	*WaitingTime*	*HHI*	*PriorityShare*
HHI	-1.308**			-3.942***		
	(0.576)			(1.234)		
PriorityShare	0.217			6.942***		
	(1.667)			(2.424)		
HHIGlobalShare		0.042***	-0.003**		0.038***	0.002
		(0.001)	(0.001)		(0.002)	(0.002)
AvgLinerPriority		0.004***	0.011***		0.003***	0.014***
		(0.000)	(0.001)		(0.000)	(0.001)
Constant	4.352***	0.110***	0.153***	3.452***	0.108***	0.141***
	(0.321)	(0.002)	(0.004)	(0.477)	(0.002)	(0.006)
Controls	Y	Y	Y	Y	Y	Y
Observations	593,987	593,987	593,987	218,831	218,831	218,831
R^2	0.124	0.825	0.615	0.166	0.818	0.828
F-statistic	3171.164	2274.305	2432.455	405.888	1183.424	1477.457
Kleibergen-Paap LM stat.	187.295			145.090		
	(0.000)			(0.000)		
Kleibergen-Paap Wald F	95.828			68.947		
Fixed Effects	Terminal / Month / Shipping line					

Note: Standard errors are clustered by terminal-month-shipping line category. * $p < 0.1$, ** $p < 0.05$, *** $p < 0.01$. The model is estimated using the 2SLS method. P-values of Kleibergen-Paap LM statistics are in parentheses. For the Kleibergen-Paap Wald F statistics, the corresponding Stock-Yogo critical value for 10% maximal IV size is 7.03.

The 2SLS estimators of our variables of interest differ from the OLS estimators. Although the estimated HHI coefficients in Tables 2 and 3 are both significant and negative, the 2SLS estimators are larger in magnitude ($\beta_1 = -1.308$ with full sample; $\beta_1 = -3.025$ with restricted sample) than the OLS estimators ($\beta_1 = -0.894$ with full sample; $\beta_1 = -3.942$ with restricted sample). This marked difference confirms our concern about the endogeneity issue. The larger magnitude of the 2SLS estimator of HHI meets our expectation, as we conjecture that the endogeneity is attributed to the impact of expected berth waiting time on market concentration. In the case of long expected berth waiting time, small shipping lines, which are often less equipped to absorb the cost associated with waiting times, may opt for rerouting to alternative terminals. Conversely, large shipping lines are likely to keep using the busy terminals due to the benefit from economies of scale, which means they can operate at a lower cost per unit as their cargo throughput increases at the terminal, and this benefit might outweigh the additional cost incurred from waiting. As a result, long waiting times could cause a terminal's traffic to be highly dominated by large shipping lines and hence raise HHI. Therefore, in addition to the negative impact of HHI on waiting time, there might be a positive correlation between waiting time and HHI due to reverse causality. When we employ IV to effectively remove the positive correlation due to reverse causality, the coefficient of HHI is expected to be more negative. In sum, based on the 2SLS regression without outliers, we predict that an increase in HHI by 0.01 unit may lead to an average decrease of approximately 1.308 hours in the waiting time, holding other variables constant.

The coefficients of *PriorityShare* are negative in OLS estimation but positive in 2SLS. In column (1) of Table 2.3, the coefficient of Priority is statistically insignificant, while the coefficient is significant when we restrict the sample to terminals with a fixed priority policy. This result may align with Ouyang et al. (2022), who proposed that a fixed deterministic priority policy without considering the state of customers may increase the waiting cost. The discrepancy in the coefficient for *PriorityShare* between OLS (-1.128) and 2SLS (6.942) methods is also in line with our expectation. In congested terminals, the incentive for terminal operators to offer priority is diminished due to sufficient shipping demand, whereas in less congested settings, priority offerings serve as a strategy to attract shipping lines since these terminals have relatively lower utilization. This results in a negative correlation between congestion and priority share. By excluding the negative impact of waiting time on priority share, it is expected that the coefficient of Priority should become positive in 2SLS. It is revealed that if the priority share increases by 0.01 unit, the waiting time may rise by around 6.942 hours on average. This is consistent with our **Hypothesis 2** that berthing priority aggravates the congestion at terminals.

2.4.3 Mechanism test

So far, we find that market concentration, as measured by HHI, is negatively associated with the average waiting time of ships at anchorage. To further investigate the underlying mechanism, we follow Barkley and Mcleod (2022) and use the queue length at anchorage when a new ship arrives as a proxy. The idea is that waiting times can be reduced if shipping lines consciously adjust vessel arrival schedules in response to terminal congestion. Although it is difficult to directly observe such scheduling decisions, a shorter queue length, especially under congested conditions, can serve as an indirect indicator of such coordination. Therefore, we hypothesize that shipping lines internalize congestion by managing the length of vessel queues at anchorage. We test this mechanism using Eq. 2.2 below:

$$\ln(Queue_{ijk}+1) = \alpha_0 + \alpha_1 HHI_{jt} + \alpha_2 PriorityShare_{jT} + \boldsymbol{\beta}\mathbf{Controls}_{ijk} + \delta_j + \gamma_t + \tau_s + \varepsilon_{ijk} \tag{2.2}$$

The dependent variable $\ln(\text{Queue}_{ijk}+1)$ denotes the logarithm of one plus the queue length at terminal j when vessel i arrives for its kth port call. The independent variables, control variables, and fixed effects are as defined in section 2.3.2. This specification tests whether market concentration influences queue length at a given terminal. Accordingly, we expect that terminals with higher levels of concentration will exhibit shorter average queue lengths on average.

Table 2.4 presents the estimation results. The coefficients of HHI are negative and statistically significant at the 1% level, indicating that a 1% increase in HHI is associated with a 0.585% reduction in average queue length at the terminal. This effect becomes stronger, reaching a 1.207% reduction, when terminals with large variations in priority provision are excluded. These findings suggest that terminals with higher market concentration levels tend to have shorter queues, implying that shipping lines internalize congestion by coordinating the arrival times of their vessels. In contrast, the coefficients of the Priority variable are not statistically significant in either specification, suggesting that priority provision may not have a significant effect on queue length at anchorage.

Table 2.4: Effects on queue length

	(1) Full sample *Ln(Queue+1)*	(2) Restricted sample *Ln(Queue+1)*
HHI	-0.585***	-1.207***
	(0.055)	(0.138)
PriorityShare	0.094	-0.172
	(0.197)	(0.280)
Constant	0.459***	0.523***
	(0.038)	(0.053)
Controls	Y	Y
Observations	593,987	218,831
R^2	0.369	0.400
F-statistic	2887.174	375.992
Kleibergen-Paap LM stat.	187.295	145.090
	(0.000)	(0.000)
Kleibergen-Paap Wald F	95.828	68.947
Fixed Effects	Terminal / Month / Shipping Line	

Note: Standard errors are clustered by terminal-month-shipping line category. * $p < 0.1$, ** $p < 0.05$, *** $p < 0.01$. Model is estimated using the 2SLS method. P-values of Kleibergen-Paap LM statistics are in parentheses. The Stock-Yogo critical value for 10% maximal IV size is 7.03.

2.4.4 Heterogeneity analysis

In this section, we explicitly test **Hypothesis 3**, that whether HHI and $PriorityShare$ have heterogeneous impacts on the waiting time by categorizing terminals based on their priority share over a five-year span (from 2016 to 2020). As presented by Table A.1 in the Appendix, terminals display different characteristics of waiting times and priority provision in different groups classified by priority share. Thus, we run regressions separately in two distinct terminal groups: those with a priority share consistently above and those with a priority share consistently below the 50th percentile. The findings from 2SLS regressions are presented in Table 2.5.

The results indicate that the impact of HHI on waiting times is negative and statistically significant for terminals with a priority share below the $50th$ percentile over the specified period, while for terminals with a priority share above the median, the impact remains insignificant. This suggests that high market concentration leads to lower waiting times, and such an effect is dampened by priority provision, consistent with **Hypothesis 3**. It indicates that the priority policy reduces the incentive of shipping lines with priority to internalize congestion and exerts higher internalization pressure for shipping lines without priority.

The Priority coefficient in Table 2.5, significant in column (1) and insignificant in column (2), illustrates the differential impacts of priority across subsamples. Notably, terminals with higher priority shares experience increased congestion with priority implementation, resulting in significant marginal effects. In contrast, terminals with low priority shares exhibit almost no impact from priority. This observation of the varying impacts of Priority on the waiting time across different terminal groups, categorized by their priority share, aligns with the findings in Ouyang et al. (2022). They noted that a fixed priority policy is worse than FCFS when the prioritized customer type accounts for a larger proportion. The first-stage results of the 2SLS analysis are shown in Table A.2 of the Appendix, and the F-statistic values indicate a strong association between instruments and endogenous explanatory variables, which exceed the commonly recommended threshold of 10. The significance of F-statistic value confirms the validity and robustness of our instrument variables.

Table 2.5: Heterogeneity analysis using IV/2SLS estimation

	(1) $PriorityShare > 50th$ $WaitingTime$	(2) $PriorityShare < 50th$ $WaitingTime$
HHI	2.689	-7.289***
	(2.051)	(1.587)
PriorityShare	12.721*	-8.313
	(6.860)	(8.408)
Constant	-0.277	6.667***
	(1.024)	(0.631)
Controls	Y	Y
Observations	103,347	115,484
R^2	-0.065	0.149
F-statistic	41,634.454	71.181
Kleibergen-Paap LM stat.	14.697	139.248
	(0.000)	(0.000)
Kleibergen-Paap Wald F	7.090	56.567
Fixed Effects	Terminal / Month / Shipping line	

Note: Standard errors are clustered by terminal-month-shipping line category. * $p < 0.1$, ** $p < 0.05$, *** $p < 0.01$. Model is estimated using the 2SLS method. P-values of Kleibergen-Paap LM statistics are in parentheses. The Stock-Yogo weak instrument critical value for 10% maximal IV size is 7.03. The negative R^2 in column (1) reflects the nature of the 2SLS estimator. Unlike OLS, 2SLS focuses on correcting for endogeneity and may yield a negative R^2, which does not affect inference validity.

2.4.5 Robustness test

As a robustness check, following Brueckner (2002), we use the market share of the largest shipping line at the terminal, denoted as $MaxShare$, as an alternative measure to capture congestion internalization, as shipping lines with higher market shares are supposed to internalize more congestion externalities. Additionally, as $PriorityShare$ is calculated based on traffic shares, we can also use the share of shipping lines with priority status at the terminal in each year as an alternative measure of the degree of priority, denoted as $PriorityN$. The robustness regression results in Table A.3 of the Appendix are similar to those from 2SLS estimates in Table 2.3, proving the robustness of the results.

2.5 Conclusion and Implications

2.5.1 Conclusion and discussion

Our research contributes to the literature on the impact of priority provision on operational efficiency in maritime transportation, as well as other service sectors with non-atomistic customers. We provide an in-depth understanding of how shipping lines internalize congestion as market concentration increases, and its effects on terminal efficiency. Additionally, we examine how terminal operators' berth prioritization policies directly influence congestion and the incentives for shipping lines to internalize congestion externalities. Empirically, we documented that the negative relationship between market concentration and waiting times also holds at terminals, and carriers internalize congestion by shortening the queue lengths, which serves as a generalization of the airline congestion literature. As mentioned in the literature review, it remains an ongoing debate regarding whether the large carrier would internalize congestion in the airline literature. Nevertheless, in the shipping industry, the evidence for the internalization of congestion by carriers is much clearer, as shipping carriers have additional incentives compared to airlines to internalize congestion by slow steaming. By slowing down, carriers could both save massive fuel costs and alleviate congestion. Priority provision has been a common operational strategy to attract targeted customers in service operations, for example, healthcare, amusement parks, and financial services (Gavirneni and Kulkarni, 2016). In this study, we empirically test the effect of priority on congestion and the dampening effect of priority on congestion internalization, supplementing previous operation management literature with the effect of priority on operation efficiency where customers are non-atomistic. Besides, the heterogeneity analysis provides rich implications. First, the strategy of offering berthing priority in less congested terminals aims to attract a guaranteed number of ship visits, which, on the surface, seems beneficial for

both terminals and shipping lines. However, the analysis reveals that while designed to enhance efficiency and attract business, berthing priority provision can exacerbate congestion. The marginal effect here refers to the additional congestion caused by prioritizing certain vessels over others. This occurs because priority provision, while ensuring access for some, can cause non-priority vessels to wait, thereby causing substantial imbalances in shipping flow patterns. Such imbalances in shipping flows result in an overall increase in time costs for all carriers (Lin et al., 2024). Thus, terminal operators need to balance the benefits of attracting vessels through priority access against the potential for increased congestion, especially in terminals where capacity is not yet a significant issue. Second, in terminals experiencing higher waiting times, the incentive for offering priority decreases. This is because such terminals are likely operating at or near full capacity; their berths are well-utilized, and the demand exceeds the available space. In this context, offering priority does little to enhance terminal efficiency and may generate substantial costs for carriers. Instead, it fosters a highly competitive environment where shipping lines compete for the limited priority slots available. This competition can lead to strategic behavior among shipping lines, where they may choose to avoid direct competition for priority berths in the same terminal with each other. This competitive environment underscores the complex dynamics at play in priority allocation. While berthing priority can be a powerful tool for attracting business, its effectiveness is contingent on the specific operational context of each terminal. Especially in less congested terminals, the focus might better shift towards optimizing scheduling and throughput, rather than allocating priority berths, which could decrease operational efficiency. This study offers new insights into the dynamics of competition behaviors of shipping lines and terminal operators on terminal efficiency, along with the relationship between priority provision and congestion internalization at congested infrastructure. The results have significant implications for the management of scarce resources or facilities where priority is offered by the resource provider.

2.5.2 Managerial implications

The findings from this study also contain rich managerial implications. First and foremost, the results have significant implications for optimal congestion pricing for social planners. Considering carriers' congestion internalization behavior, Brueckner (2002) concluded that imposing a congestion toll corresponding to the uninternalized portion of congestion could help improve traffic allocation. He further suggested that the optimal toll should be marginal congestion cost times one minus the market share of a carrier. However, simply extrapolating this result from the airline literature to the maritime setting could be prob-

lematic due to the provision of priority by terminal operators. Under the priority scheme, the amount of internalization is determined by the priority share, and carriers with (without) priority internalize less (more) the proportion they impose on themselves, the optimal toll shall also take this into account. Second, the findings carry significant managerial suggestions for terminal operators regarding priority provision. Although the priority scheme brings stable and guaranteed container volume to the terminal, it is important for terminals to recognize the negative congestion externality the priority scheme introduces, especially in less congested ones. The dampening effect of priority intensity on congestion internalization suggests that terminal operators should be cautious about whether and how much priority shall be offered to carriers, considering the tradeoffs between higher berth utilization and lower operation efficiency. Third, shipping lines are encouraged to closely analyze how berthing priority schemes affect their operations. Those with priority might face less waiting time, but this could result in an unfair cost burden on those without priority. Particularly in less congested terminals, an increase in the priority share may lead to longer overall waiting times. Shipping lines need to assess whether the benefit of obtaining or maintaining priority (e.g., faster loading and unloading times) outweighs the cost associated with trade flow distortions caused by more priority provisions. Additionally, our analysis of three terminal groups, classified by the priority share median value, reveals that more congested terminals are less likely to offer berthing priority. Furthermore, our first-stage regression result of the heterogeneity test indicates that shipping lines tend to avoid competition with others in terminals with longer waiting times and limited priority slots. Therefore, shipping lines in these terminals with less priority provided could consider collaborating and sharing strategy information regarding priority preferences to maximize operational efficiency.

Chapter 3

Port Vulnerability to Natural Disasters: An Integrated View from Hinterland to Seaside

3.1 Introduction

Ocean freight shipping serves as a fundamental pillar of global trade and economic activity (UNCTAD, 2021a; Verschuur et al., 2020). Meanwhile, ports are vulnerable to unexpected events, including natural disasters, e.g., earthquakes, hurricanes, and tsunamis, along with human-related incidents, e.g., labor strikes, geopolitical tensions, and pandemics. These disruptions can severely impact the global supply chains, leading to vessel delays, increased transportation costs, and shortages of essential commodities. For example, Hurricane Ida in 2021 forced the closure of major U.S. ports along the Gulf and Atlantic Coasts, leading to substantial shipment delays and creating ripple effects that spread through global supply chains, resulting in shortages of various commodities, from grains to computer chips (The New York Times, 2021).

Therefore, port vulnerability to external shocks, which represents the degree of disruptions each port experiences before restoring its normal activities, is critical to trade resilience and economic stability worldwide. Recent progress in technology, especially the application of Automatic Identification System (AIS), has facilitated detailed analysis of port disruptions. Several studies have used high-frequency vessel-level data to quantify port vulnerability to external disruptions using case studies (Farhadi et al., 2016; Touzinsky et al., 2018). For instance, Verschuur et al. (2020) has utilized the AIS data to analyze 141 incidences of port disruptions due to natural disasters. More recently, Verschuur et al. (2023) estimated the

physical damages to port infrastructure and trade losses caused by the global port shutdown. They further underlined that port resilience is a function of a range of port characteristics, including engineering standards, reconstruction costs, and critical infrastructure assets.

While valuable, existing literature that focuses on the physical attributes of ports per se often overlooks their role as transportation interfaces, linking hinterland industrial activities to the global shipping network. Port performance is shaped not only by its inherent characteristics but also by the production capabilities of nearby firms and its strategic position within the global shipping network (Robinson, 1998). These factors can either constrain or boost a port's recovery following natural disasters. This lack of understanding seriously limits our comprehension of the mechanisms underlying port resilience or vulnerability.

Global economic development also exhibits significant geographical disparities, and the spatial distribution of ports is highly uneven. Ports in economically developed areas boast comprehensive hinterland industrial systems and higher shipping network connectivity. In contrast, less developed regions have more limited local industries and lower importance within the maritime network. These geo-economic differences are bound to influence ports' ability to recover from external disruptions, yet limited studies have delved into this aspect.

To fill the research gap, combining daily shipping traffic data at 735 container ports and coordinates data of 1,768 natural disasters occurring between 2015 and 2019, we first construct a port vulnerability index by dividing the number of days each port takes to return to its pre-disaster level of port calls by the number of days the port closes or reduces its activity. Next, going beyond existing literature emphasizing port characteristics to explain port resilience, we extend the analytical framework by examining how hinterland industrial diversity and port network centrality facilitate more rapid recovery from natural disasters for container ports. We address the endogeneity concern through an instrument variable (IV) approach, confirming the robustness of our results. We discover that ports with enhanced infrastructure, a diversified manufacturing structure within their hinterland, and stronger network connectivity within the global liner shipping network are less vulnerable to natural disasters. We further perform heterogeneity tests by categorizing observations by the median level of GDP per capita, the type of natural disasters (i.e., hydrological disasters and meteorological disasters), respectively.

The contribution of this paper is three-fold: Firstly, this study advances existing literature by proposing an integrated framework for analyzing the vulnerability of container ports through the lens of the port interface, hinterland, and the global liner shipping network. Unlike bulk ports that primarily serve mining production and are used in port-to-port shipping routes, container ports act as critical interfaces connecting hinterland industries with the global shipping network (Stopford, 2008). Previous studies have often not fully accounted

for the unique characteristics of container ports, particularly in terms of the influences of hinterland industrial diversity and network connectivity. Our research addresses this gap by examining the interplay between hinterland industries, network connectivity, and port vulnerability to external disruptions, thus providing a deeper insight into the mechanisms underlying vulnerability. Moreover, methodologically, this study enriches existing literature by employing an econometric model to simultaneously analyze determinants of port vulnerability. Finally, we have explored how the effects of hinterland industrial diversity, port infrastructure, and network connectivity on port vulnerability may vary based on the economic development levels of the hinterland and types of natural disasters. The nuanced estimation results from our study enable us to provide more targeted policy recommendations that address the unique challenges faced by ports in varying contexts, especially when resources are limited.

This paper is organized as follows: Section 2 provides a review of the related literature; Section 3 details the data and methodology; Section 4 provides the economic analysis along with a discussion of our main findings; Section 5 concludes.

3.2 Literature review

This section explores the literature on "resilience", including the concept of resilience, the measurement for quantifying and evaluating it, and factors influencing resilience.

3.2.1 Resilience in Maritime Transportation System

The term "resilience", originating from the Latin to mean "bounce back", was first proposed in the field of ecology by Holling (1973). Since then, it has been broadly adapted across diverse disciplines, including economics, psychology, supply chain, and transportation (Hosseini and Barker, 2016; Zhou et al., 2019; Gu and Liu, 2024). In maritime literature, "resilience" has been employed to evaluate various systems, covering ports (Omer et al., 2012; Pant et al., 2014; Hossain et al., 2019; Notteboom et al., 2021), inland waterway transportation (Campo et al., 2012; Baroud et al., 2014), global shipping network (Bai et al., 2023b), maritime supply chain Liu et al. (2023a); Gu and Liu (2023), and port-hinterland transportation network (Chen et al., 2017, 2018).

Despite its widespread use, a standardized definition of resilience remains unsettled in existing literature. In the context of maritime systems, Omer et al. (2012) defined resilience as the system's capacity to withstand disruptions and rebound to its regular service state or close to it. Similarly, Pant et al. (2014) emphasized restoring stability after disruption.

Hossain et al. (2019) interpreted it as the ability of port infrastructure to return to desired functionality within a reasonable period post-disruption. Nonetheless, the core principle consistently recognized across studies is a system's ability to recover to its normal functionality following a disruptive event.

Our study falls into the strand of literature quantifying system resilience with metrics. Henry and Ramirez-Marquez (2012) developed a time-dependent metric to assess a system's resilience, defined as the ratio of "recovery to loss". In this metric, resilience is calculated as the ratio of the recovery performance to possible maximum service losses due to disruptions. This metric has been foundational for many maritime studies analyzing resilience (Baker et al., 2012; Pant et al., 2014).

In particular, the utilization of the "recovery to loss" metric, in conjunction with high-frequency and detailed vessel data from the AIS database, has enabled more advanced empirical analyses on port resilience based on vessel activities at ports on a daily basis. Key performance parameters like vessel dwell time and net vessel counts, extracted from the AIS database, have been instrumental in assessing the resilience of port systems during major disruptive events. For instance, Farhadi et al. (2016) and Touzinsky et al. (2018) examined the resilience of the U.S. ports under both man-made and natural disruptions, demonstrating the potential and benefits of using AIS data in quantitative methods. Verschuur et al. (2020) measured port resilience by computing the total duration of affected days due to natural disasters. They also used AIS data, providing empirical evidence covering 74 ports and 27 disasters. They defined the disruption duration as the total number of affected days, including reduction days, closure days, and recovery days, and evaluated port recovery ability by dividing the sum of reduction and closure days by recovery days. Additionally, Gu et al. (2024) employed the daily port congestion index from the Shipping Intelligence Network (SIN) by Clarksons Research as a proxy for port resilience based on AIS data, while their analysis only covers nine global ports.

The broader application of the AIS database significantly enriches the existing literature on port resilience by enabling analyses at a daily frequency, compared to the typically coarser weekly or quarterly public disclosure data. However, most prior studies have been limited in scope, focusing on a few ports and disruptive events without distinguishing container ports from other types of ports. This study addresses this limitation by examining a comprehensive sample of 735 container ports from 2015 to 2019, providing a more representative and granular understanding of port vulnerability and resilience across the global maritime transportation network.

3.2.2 Factors Influencing Port Resilience

Existing maritime literature has developed various methods to evaluate resilience, for example, case studies (Omer et al., 2012), empirical analysis (Gou and Lam, 2019; Notteboom et al., 2021), game theory (Chen et al., 2018; Li et al., 2022), optimization models (Dui et al., 2021), simulation models (Pant et al., 2014; Chen et al., 2017; Wei et al., 2022), Bayesian networks (Hosseini and Barker, 2016; Hossain et al., 2019; Wang et al., 2023), and graph theory (Liu et al., 2023b). Our study closely relates to the studies on empirical analysis and Bayesian networks, which focus on identifying factors affecting port resilience.

Among existing literature, port characteristics, especially factors relating to port infrastructure, have been extensively examined, and many found evidence of the crucial role of infrastructure on port resilience (Hossain et al., 2019; León-Mateos et al., 2021; Gu and Liu, 2023). For example, Hossain et al. (2019) utilized a Bayesian network method, which pinpointed maintenance, alternative routing, and manpower recovery as crucial components of port resilience with a case study on a U.S. inland deep-water port. In this context, maintenance refers to activities such as crane upkeep and channel repairs, which emphasizes the significance of infrastructure reliability during disruptions. Similarly, León-Mateos et al. (2021) and Gu and Liu (2023) both identified port infrastructure as one of the key elements in developing a framework for port resilience analysis.

Additionally, a few resilience studies have considered spatial characteristics of ports. Xu et al. (2023) analyzed spatial correlations among global ports, revealing significant agglomeration effects and positive spatial spillovers in port resilience in late 2021, indicating that ports in countries with resilient neighboring ports were less affected during the COVID-19 pandemic, while their data is at the quarterly level. From a network perspective, Qin et al. (2023)constructed a port resilience index assessing ports' importance in the liner shipping network, while their study is limited to Chinese ports. Indeed, ports with higher network centrality typically have more direct shipping connections with other ports, which means they have more alternative routes and transshipment options available in the event of a disaster, allowing for a rapid reorganization of shipping lanes and logistics. Due to their frequent handling of high volumes and complex logistics, these ports may also possess richer experience in emergency management and higher operational capabilities, enabling them to recover more quickly during disasters. Yet, there is little systematic analysis at the global scale to evaluate the effect of network structure on port resilience.

Lastly, the hinterland industrial structure has rarely been considered in examining determinants of port resilience. However, ports are essential in bridging hinterland industries to the global market, and the structure of hinterland industries (such as diversified or concentrated) can potentially affect a port's recovery ability under disruptions. In classic economics

literature, studies have found that industrial diversity fosters economic system resilience and is inversely related to unemployment rates during economic downturns (Malizia and Ke, 1993; Izraeli and Murphy, 2003; Mizuno et al., 2006; Brown and Greenbaum, 2017; Wang and Wei, 2021) or natural disasters (Xiao and Drucker, 2013), since industrial diversification inherently increases a region's adaptive capacity (Eraydin, 2016). Hence, we anticipate that ports with a more diversified hinterland industrial structure are more resilient than ports with a more concentrated one, since a diversified industrial structure can distribute risks across different sub-sectors. These ports are, therefore, more likely to continue operating or recover more quickly from natural disasters, as unaffected sectors can compensate for disrupted ones.

Building upon previous literature, this study examines a comprehensive sample of 735 container ports, the largest dataset in existing literature. We firstly provide an integrated vulnerability analytical framework, especially considering the role of container ports as interfaces linking the hinterland industries and the global liner shipping network, expanding existing literature focusing on factors related to port characteristics. Methodologically, this study enriches existing literature by employing an econometric model to analyze determinants of port vulnerability. In particular, we address the endogeneity problem arising from reverse causality between industrial diversity and port vulnerability, and between port connectivity and port vulnerability, respectively, using an instrumental variable (IV) approach.

3.3 Data and Methodology

This section introduces the dataset, the "port vulnerability index", and the econometric model to estimate the effects of port infrastructure, hinterland industrial diversity, and port connectivity on port vulnerability.

3.3.1 Data

Our initial dataset is the daily port calls of 735 container ports worldwide from 2015 to 2019. However, due to the outbreak of COVID-19, we excluded data after 2019, as the pandemic and its related restrictions could confound our port vulnerability measure.

The accuracy and precision of port locations are crucial for retrieving data on vessel visits, which is essential for analyzing vessel traffic at ports under natural disasters and further assessing port vulnerability. We first leverage the AIS database and global container port coordinates from Lloyd's List database to refine port berth coordinates. The process begins by filtering out vessels with speeds less than one knot to focus on those in berth and

anchorage areas. We then identify all mooring points for each port according to the port coordinates from Lloyd's List. Next, we apply the Iterative Multi-Attribute Density-Based Spatial Clustering of Applications with Noise (IMA-DBSCAN) technique (Bai et al., 2023a) to determine the appropriate radius and the minimum number of vessels in each cluster based on variances in mooring point clusters across ports. Vessel headings further help differentiate berth areas from anchorage areas within the mooring point clusters. In berths, vessels are aligned in the same or directly opposite directions, while in anchorages, headings are more irregular. Finally, we designated the stabilized berth areas resulting from the previous step as the official port berth locations and updated the Lloyd's List database accordingly.

Port call data is then constructed by matching vessel location coordinates from the AIS database with the updated port berth coordinates based on the Lloyd's list. Vessels are filtered based on two criteria: a vessel must have a speed of less than one knot, and its location must be within a 10 km radius of a port. A port call is recorded when a vessel meets these conditions, indicating it is moored at the port berth (Bai et al., 2023a).

Next, we merge the port call data with location data of 1,768 natural disasters worldwide from the Emergency Events Database (EM-DAT), including earthquakes, volcanic activities, wildfires, floods, storms, and extreme temperatures. A port is considered to be potentially affected by a disaster if the disaster occurs within a radius of 300km from the port [1]. To rule out cases of port closures unrelated to disasters, we only include the ports with average daily port calls exceeding three during the period starting 30 days before any disaster. These procedures result in 919 port-disaster pairs in our sample.

Figure 3.1 displays the annual and geographic distribution of natural disasters in our sample, showing an uneven distribution by disaster types and locations. Storms are the most common disaster affecting ports, occurring in more than 30 instances annually from 2016 to 2019, peaking in 2016 with 45 instances worldwide. Floods, which mostly happened in 2017 with around 40 instances, are the second most common disaster affecting ports.

The left-side maps in Figure 3.1 display the geographic distribution of disasters from 2015 to 2019. Storms frequently occur along the east coasts of Asia and North America, while floods usually happen in East Asia and Southeast Asia. Ports in Japan faced extreme temperatures most severely in 2015 and 2016. Western and southern Europe experienced more instances of extreme temperatures, particularly in 2017 and 2019. Although extreme temperatures dropped from 2016 to 2018 worldwide, they surged to 11 instances in 2019, affecting Western Europe and Japan again. Wildfires typically occurred along the west coast

[1] Many studies on the impact of natural disasters including floods, storms, volcanic activities and wildfires have used the radius of 300 km, and the multiple references regarding the impact range of different natural disasters are summarized in Table B.1 in the Appendix. Based on previous studies, we selected a radius of 300 km from the port as the threshold for determining whether a port could be affected by a natural disaster.

of North America and occasionally near Mediterranean ports in 2016 and 2018. The occurrences of landslides remained almost stable during the time, and Southeast Asian ports mostly faced threats from landslides. Ports in East Asia were the most susceptible to earthquakes, experiencing 7 out of 17 incidents from 2015 to 2019, followed by Southeast Asia with 4 incidents. Volcanic activity was the least-happened disaster, with only two instances in 2018, one in Indonesia and one in southern Italy.

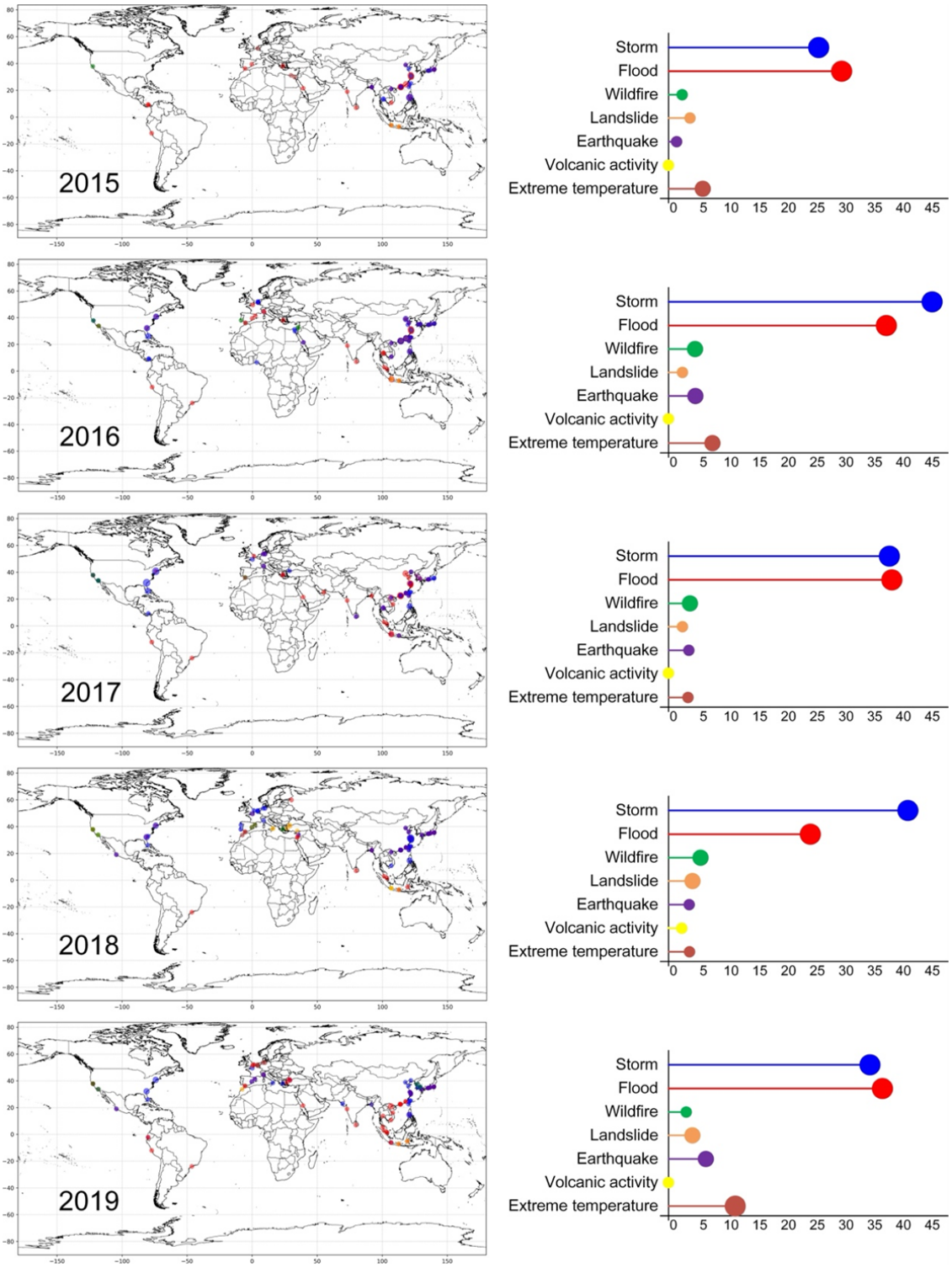

Figure 3.1: Annual disaster distribution near global container ports

3.3.2 Constructing the port vulnerability index

To calculate the port vulnerability index [2], we need to precisely identify when a port experiences vessel visits decline or closes due to natural disasters, as well as when port vessel visit picks up again. The date that a disaster starts is retrieved from the international natural disaster database, EM-DAT, and the minimum vessel visit day and the port shutdown day are generated from the daily vessel visit data. However, the decreased start day and the recovery day (i.e., the days it takes to restore pre-disaster traffic) are not straightforward from the vessel visits, since it can be hard to distinguish significant changes from normal seasonal variations, especially when the vessel visits have a high daily variation. Therefore, following Farhadi et al. (2016) and Touzinsky et al. (2018), we apply a Bayesian change-point detection algorithm called BEAST (A Bayesian Estimator of Abrupt change, Seasonal change, and Trend), proposed by Zhao et al. (2019), to detect the changepoints in the vessel visits time series data. The BCP algorithm uses probabilistic modeling to determine the likelihood of a changepoint at each point in time by analyzing the data distribution and detecting where the statistical properties, such as mean or variance, change significantly. This approach can more accurately identify sudden changes in vessel visits that differ from regular daily fluctuations caused by seasonal patterns.

In Appendix B, we present two algorithms developed to detect significant changes in vessel visit patterns at ports under disasters using BEAST. Both algorithms start by determining the decrease start day by analyzing daily vessel visit changes, anchored to a pre-disaster baseline represented by a three-day rolling average of vessel visits at each port. Algorithm 1 focuses on ports that completely shut down post-disaster, while Algorithm 2 focuses on ports that remain open but experience reduced operations. For both methodologies, decrease days are calculated from the start of the decline in vessel visits to the first closure day or the day with minimum vessel visits, and recovery days extend from the first-day vessel visits the port following a closure or the day of minimum activity, until normal operations are resumed. This structured approach effectively quantifies the decrease days, recovery days and closure days, providing a robust framework for assessing disaster impacts on port operations. The methodology flowchart is shown in Figure 3.2.

[2]In this study, we chose to frame our index around port vulnerability by following the view describing vulnerability as the opposite of resilience (Gallopín, 2006; Duncan McIntosh and Becker, 2017), which allows us to clearly identify ports that are particularly susceptible to natural disasters. By concentrating on vulnerability, we aim to provide targeted recommendations for ports at higher risk, offering a more direct pathway to addressing specific weaknesses and improving overall resilience.

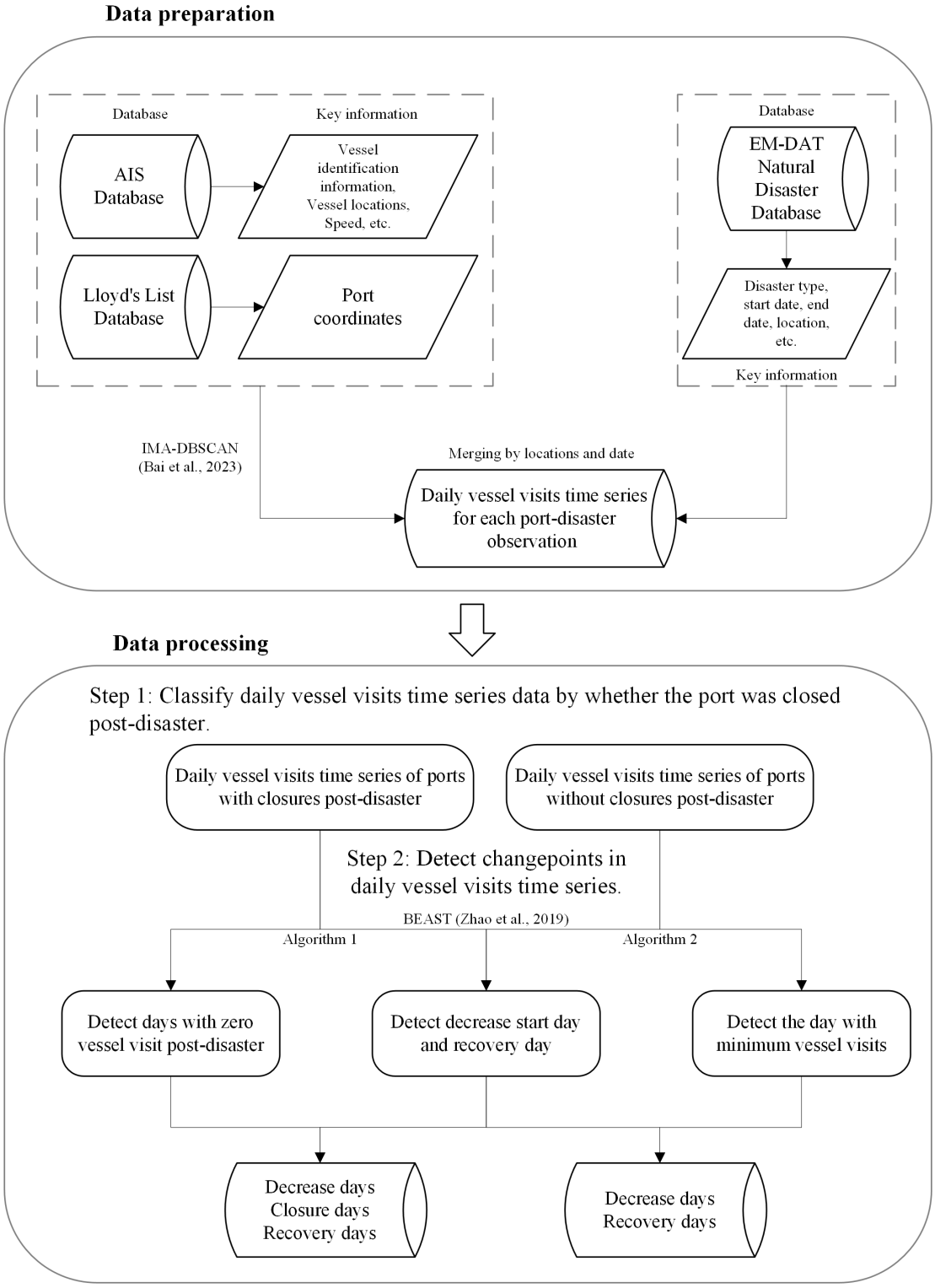

Figure 3.2: Methodological flowchart

The vulnerability index, adapted from the resilience metric proposed by Henry and Ramirez-Marquez (2012), measures the time-dependent ratio of 'recovery to loss'. It is calculated by dividing the days a port takes to recover from disruptions by the time it experiences losses in vessel visits. Ports experiencing higher losses but with shorter recovery times are regarded to perform better than those with similar losses but longer recovery times (Linkov et al., 2014; Verschuur et al., 2020). A higher recovery-to-loss ratio indicates poorer port performance during disruptions, thus identifying the port as more vulnerable.

To calculate the index, we first merge daily port call data with information on natural disasters. Port vessel traffic is quantified by the number of daily vessel visits to the port, employing a three-day rolling average to account for potential seasonal variations in port calls due to weather conditions or economic activities (the absolute number of vessel visits or a seven-day rolling average are also considered in robustness tests). For ports that remain operational despite natural disasters, or where vessel visits do not decrease to below 35% of the pre-disaster levels, the vulnerability index is set as zero. Furthermore, if a port's closure or the day with the minimum vessel visits is recorded more than a week after the disaster ends or more than two weeks after the onset of a disaster for cases where the disaster end date is missing (given that the average of disaster duration is around 6.4 days), it suggests that the closure or reduction in traffic is not disaster-related, and thus, the vulnerability index remains zero.

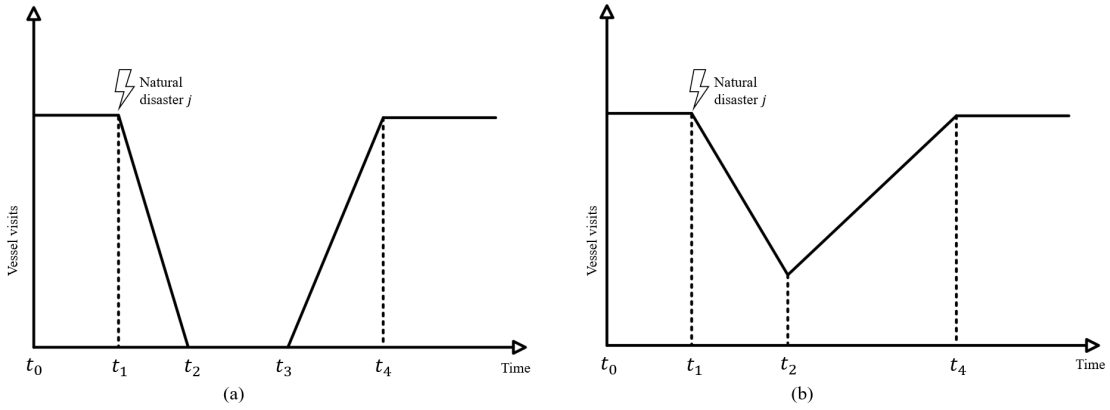

Figure 3.3: Changes in vessel visits at port i during natural disaster j

Figure 3.3 illustrates variations in daily vessel visits at a port i during a natural disaster j. Figure 3.3a depicts a scenario where the port shuts down due to natural disaster j, and Figure 3.3b presents the scenario where the port experiences a decrease in vessel visits post-disaster. In both scenarios, t_0 denotes the origin date when port performance is at the pre-disaster level, $t1$ denotes the date when the vessel visits start to decrease, $t2$ denotes the date when the port either shut down (Figure 3.3a) or its vessel visits reach to the minimum

value post-disaster (Figure 3.3b). In Figure 3.3a, $t3$ denotes the date when the port reopened after its initial shutdown. In both scenarios, $t4$ denotes the date when the port resumed to its pre-disaster level.

The calculation formula of the port vulnerability index under natural disaster j for port i is shown in Equation 3.1. For ports that closed post-disaster, the index is calculated as the ratio of recovery days to decrease days plus the ratio of recovery days to closure days. For ports that did not close post-disaster, the index is the ratio of recovery days to decrease days. In previous literature, the sum of decrease days and closure days was used in the denominator of the index to represent the loss of a port post-disruption (Verschuur et al., 2020) without distinguishing between ports that were completely closed and those that were only partially affected. Recognizing that port closure or decrease in operations is likely to exert differential impacts, we have refined the denominator to account for these distinct scenarios. Our index in Equation 3.1 more accurately captures the difference in port resilience by accounting for the severity of the disruption, recognizing that a complete shutdown indicates a lower level of resilience compared to a decrease in vessel visits.

$$\textit{The Vulnerability Index}_{i,j} = \begin{cases} \dfrac{\textit{Recovery days}_{t_3,t_4}}{\textit{Decrease days}_{t_1,t_2}} + \dfrac{\textit{Recovery days}_{t_3,t_4}}{\textit{Closure days}_{t_2,t_3}}, \\ \qquad \text{if the port closed post-disaster} \\ \dfrac{\textit{Recovery days}_{t_2,t_4}}{\textit{Decrease days}_{t_1,t_2}}, \\ \qquad \text{if the port did not close post-disaster} \end{cases} \tag{3.1}$$

$Decreasedays_{t_1,t_2}$ denotes the total number of days with a decrease in daily vessel visits for port i from time $t1$ to $t2$, and $Closuredays_{t_2,t_3}$ includes the shutdown days from time $t2$ to $t3$. Closure days would be set as zero if the port did not close during the disaster, meaning that t_2 is the minimum vessel visit day. $Recoverydays_{t_3,t_4}$ refers to the total number of days from $t3$ to $t4$ for ports that shut down post-disaster, and $Recoverydays_{t_2,t_4}$ refers to the total number of days from $t2$ to $t4$ for ports that did not close post-disaster. Expanding upon previous studies that aggregate the days of decreased activity with closure days when assessing port vulnerability, our methodology offers a more nuanced distinction between scenarios of port closure and reduced port operations.

For example, Figure 3.4 displays the time series of port calls (i.e., daily vessel visits) of Port Chiwan from one month before to two months after the start date of Typhoon Hato in 2017. According to the data, the typhoon struck on August 24, 2017, leading to a cessation of vessel visits from August 26 to August 27, and the port minimum visit day is August 27,

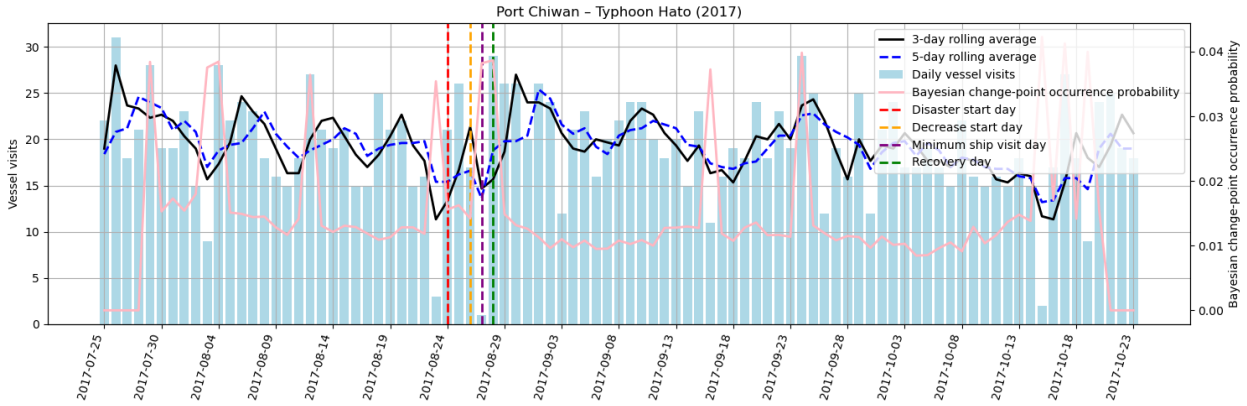

Figure 3.4: Port calls of Port Chiwan during Typhoon Hato in 2017

with only one vessel visiting. We use the BEAST algorithm to detect that August 28 is the recovery day with a positive trend slope and daily change in vessel visits, noting that Chiwan regained its pre-disaster activity level by August 28. Thus, the total number of decrease days is two, and the recovery day is one; the vulnerability index is calculated as 1/2.

Similarly, Figure 3.5 presents the Port Kaohsiung, which shut down during Typhoon Nesat & Haitang in 2017. It took two days for Port Kaohsiung to resume to its pre-disaster level. Thus, the duration of recovery is two days, from July 31 to August 1, with the port experiencing vessel visits declining for one day at the disaster start day on July 29 and being closed for a single day on July 30. Consequently, the vulnerability index calculated for this event is 4.

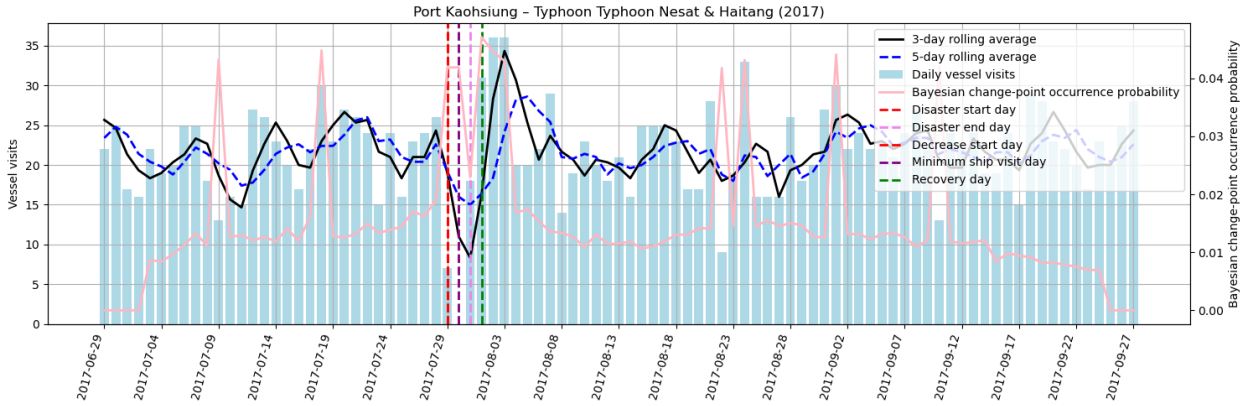

Figure 3.5: Port calls of Port Kaohsiung during Typhoon Nesat & Haitang in 2017

3.3.3 Determinants of port vulnerability

Existing literature has primarily focused on identifying internal factors integral to port construction or operation for analyzing port resilience (Hossain et al., 2019; León-Mateos et al., 2021; Verschuur et al., 2023; Gu and Liu, 2023). Yet, the hinterland environment and the transportation network where the port is embedded can also affect how quickly it recovers from external shocks. To test these predictions, we employ econometric regressions to test the effects of hinterland industrial diversity, port size (as a proxy for port infrastructure), and port centrality in the global liner network on port vulnerability.

In the regressions, hinterland industrial diversity is measured using the inverse of an Herfindahl-Hirschman index (HHI) (Glaeser et al., 1992; Baptista and Swann, 1998) of manufacturing firms within a radius of 300km of the port, based on data from Bureau van Dijk (BVD) Orbis, a comprehensive global database offering detailed information on public and private companies [3]. This index quantifies market concentration by summing up the squares of each manufacturing subsector's market share, as classified under the 4-digit North American Industry Classification System (NAICS) 2017 codes. The formula for HHI is shown in Equation 3.2,

$$HinterlandHHI_{i,T} = \sum_{n=1}^{N_{i,T}} \left(\frac{f_{n,i,T}}{F_{i,T}} \right)^2 \tag{3.2}$$

where $HinterlandHHI_{i,T}$ denotes the market concentration in the hinterland of port i in year T, $f_{n,i,T}$ represents the number of firms in the n-th subsector, $F_{i,T}$ is the total number of firms in all subsectors within the hinterland, and $N_{i,T}$ is the total number of subsectors. A higher HHI indicates greater market concentration and, thus, lower diversity. Thus, the inverse of HHI, i.e., $1/HinterlandHHI_{i,T}$, is used to measure the hinterland industrial diversity, where a higher value indicates greater diversity.

To measure a port's position in the global network, we have adopted a port connectivity indicator, named closeness centrality from Bai et al. (2022). Closeness centrality, derived from graph theory (Freeman et al., 2002; Latora et al., 2017), quantifies the convenience with which goods can be transported from one port to all others in the network. It is calculated by dividing the number of the shortest paths from the given port to every other port by the total number of intermediary ports along these paths. Essentially, the more centrally located a port is within this network, the more efficiently it can connect to other ports. Port size is defined as the maximum deadweight tonnage (DWT) of vessels visiting the port each year,

[3] We select manufacturing firms in the hinterland of container ports for our study, as these ports mainly serve international trade of finished manufacturing products, while bulk/breakbulk and oil ports often handle the trade of raw materials and commodities (Stopford, 2008).

assuming a port's ability to accommodate larger ships reflects better port infrastructure.

We also accounted for other factors, such as control variables, that may influence port vulnerability. We have controlled port activity levels using annual port calls. We also controlled the minimum distance between the port and the disaster locations, as the severity of disaster impact generally decreases with the distance. At the hinterland level, we have controlled regional climate conditions, including monthly maximum wind speed, monthly average precipitation, and temperature. To control for the influence of regional economic conditions on port vulnerability, we have included regional per capita GDP, trade openness, and unemployment rate in the regressions. Table 3.1 below displays the summary statistics of key variables and a detailed description of all variables is available in Table B.3 of the Appendix.

Table 3.1: Summary statistics of key variables

Variable	**N**	**Mean**	**SD**	**Min**	**Max**
Port vulnerability index	919	3.82	7.90	0	82
Hinterland industrial diversity	919	28.9	9.8	3.92	195
Port size	919	158,113	56,585	24,157	228,149
Network centrality (%)	919	45.9	4.18	34.7	57.7
Annual vessel visits	919	3,520	2,555	497	12,853
Hinterland GDP per capita	919	31,166	18,731	1,236	85,178
Hinterland trade openness (%)	919	63.7	67.7	8.57	389
Hinterland unemployment rate (%)	919	4.45	3.63	0.597	31.7
Distance (km)	919	139	84.6	1.72	299
Max wind speed	919	1.68	0.975	0.044	6.69
Total precipitation	919	6.7	4.97	0.002	34.4
2m temperature	919	23.1	6.44	-5.45	31.7

3.3.4 Statistical models

Baseline model Equation 3.3 below shows the baseline specification for examining the determinants of port vulnerability. $Vulnerability_{i,j,t}$ denotes the port vulnerability index for port i in month t during the natural disaster j, and $Hinterland\ industrial\ diversity_{i,T}$ denotes the industrial diversity in the hinterland of port i in year T. $Port\ size_{i,T}$ denotes the maximum deadweight tonnage (DWT) of ships visiting the port in year T, and $Network\ centrality_{i,T}$ includes the closeness centrality of port i in year T. $Controls_{i,j,t}$ denotes the control variables. γ_i, θ_j, and τ_t denote the port, disaster, and month fixed effects, respectively, and $\epsilon_{i,j,t}$ denotes the error term.

$$Log(Vulnerability_{i,j,t}+1) = \alpha_0 + \alpha_1 \cdot Hinterland\ industrial\ diversity_{i,T} + \alpha_2 \cdot Port\ size_{i,T} + \alpha_3 \cdot Network\ centrality_{i,T} + \boldsymbol{\delta}\mathbf{Controls}_{i,j,t} + \gamma_i + \theta_j + \tau_t + \epsilon_{i,j,t} \tag{3.3}$$

Instrumental variables (IV) approach We notice the potential endogeneity issue in our model, particularly stemming from the relationships between the hinterland industrial diversity (independent variable) and port vulnerability (dependent variable), as well as between port network centrality (independent variable) and port vulnerability (dependent variable). For the variable measuring industrial diversity, port vulnerability may influence the industrial structure in the hinterland, thus causing a reverse causality problem. Similarly, the absorbance and recovery ability of a port following disruptive events might influence its connections to other ports. Intuitively, a port with higher resilience might assume a more strategic position in the network, thereby complicating causality inference. Additionally, we assume the port infrastructure factor, measured by the maximum DWT of vessels arriving at the port, as exogenous due to its stability over short periods. This factor, closely related to port size and the depth and width of berths and channels, remains almost unchanged within the five-year scope of our dataset and is thus unaffected by port vulnerability.

We use the IV approach to mitigate the endogeneity problem in our estimations. A valid IV must satisfy two assumptions: 1) relevance assumption: the IV must be correlated with the potentially endogenous variable; 2) exclusion assumption: the IV must be exogenous, meaning that it affects the dependent variable only through the independent variable and not directly. Based on these two assumptions, we carefully select IVs for the endogenous variables. Firstly, we use the number of operational coal mines within a radius of 300km of the port and the average distance from the port to coal mines each year within the same region as instruments for the hinterland industrial diversity. The data regarding the location and opening year of these mines are sourced from the Global Coal Mine Tracker database. We hypothesize that these IVs should be correlated to the development of a diversified manufacturing industry in the hinterland. Existing studies have found positive spillover effects from the resources extraction industry on the upstream and downstream linked-manufacturing industries (Allcott and Keniston, 2018). Additionally, the increase in local income can boost consumer demand for goods, thereby fostering the growth and diversity of manufacturing industries (Black et al., 2005; Feyrer et al., 2017; Cavalcanti et al., 2019). Consequently, we suppose that the presence of mineral resources should correlate with the manufacturing diversity in the port hinterlands. We also consider such an IV as exogenous because the mine-richness of a region is geologically determined and by itself is unrelated to port operation and performance, including resilience.

As for the network centrality variable, we construct an instrument by averaging the monthly network centrality of all other ports within the same region for the given port. We anticipate that this regional average of network centrality will correlate with the annual network centrality of the specific port but remain uncorrelated with the recovery ability of

the port under disruptions. This method follows Fisman and Svensson (2007), which employs location-industry average as an instrument to investigate the effect of bribes and taxation rates on firm growth.

3.4 Results and Discussions

In this section, we report and discuss the estimations of the port vulnerability index and the empirical findings on the determinants of port vulnerability.

3.4.1 Vulnerability index of major global container ports

Table 3.2 illustrates the average vulnerability index of container ports in our sample. Port of Leixoes in Portugal exhibits the highest vulnerability index of 34, followed by Butterworth (Malaysia), with an index of 17, and Yingkou (China), with an index of 15.54. Six ports from East Asia are in the top 20 most vulnerable container ports, followed by three ports each from Southeast Asia, Middle East-southeast Asia, Middle East, and North America, and two ports each from Southern Europe and South Asia. The list also includes one port from West Africa. Within East Asia, Mainland China has four ports on the list: Yingkou, Suzhou, Zhangzhou, and Qingdao. South Korea and the U.S. each have two ports on the list, Incheon and Ulsan, as well as Los Angeles and Long Beach.

According to Figure 3.6 and Table 3.2, nearly half of the 20 ports are located in areas frequently impacted by storms and floods, specifically in the coastal areas of East Asia. Storms pose the greatest threat to global port resilience, occurring much more frequently in these areas than other disasters, such as wildfires and landslides, as illustrated in Figure 1.

Table 3.2: Top 20 container ports with the highest vulnerability index

Port	**Country or Region**	**Average Port Vulnerability Index**
Leixoes	Portugal	34.00
Butterworth	Malaysia	17.00
Yingkou	Mainland China	15.54
Los Angeles	U.S.A.	15.00
Makassar	Indonesia	14.71
Suzhou	Mainland China	12.07
Haifa	Israel	11.55
Gioia Tauro	Italy	11.05
Beirut	Lebanon	11.00
Da Nang	Vietnam	10.75
Incheon	South Korea	10.55
Ulsan	South Korea	9.75
Ras Misalla	Egypt	9.63
Manzanillo	Mexico	9.53
Mundra	India	9.50
Lagos	Nigeria	9.00
Long Beach	U.S.A.	8.44
Jawaharlal Nehru	India	7.54
Zhangzhou	Mainland China	7.44
Qingdao	Mainland China	7.35

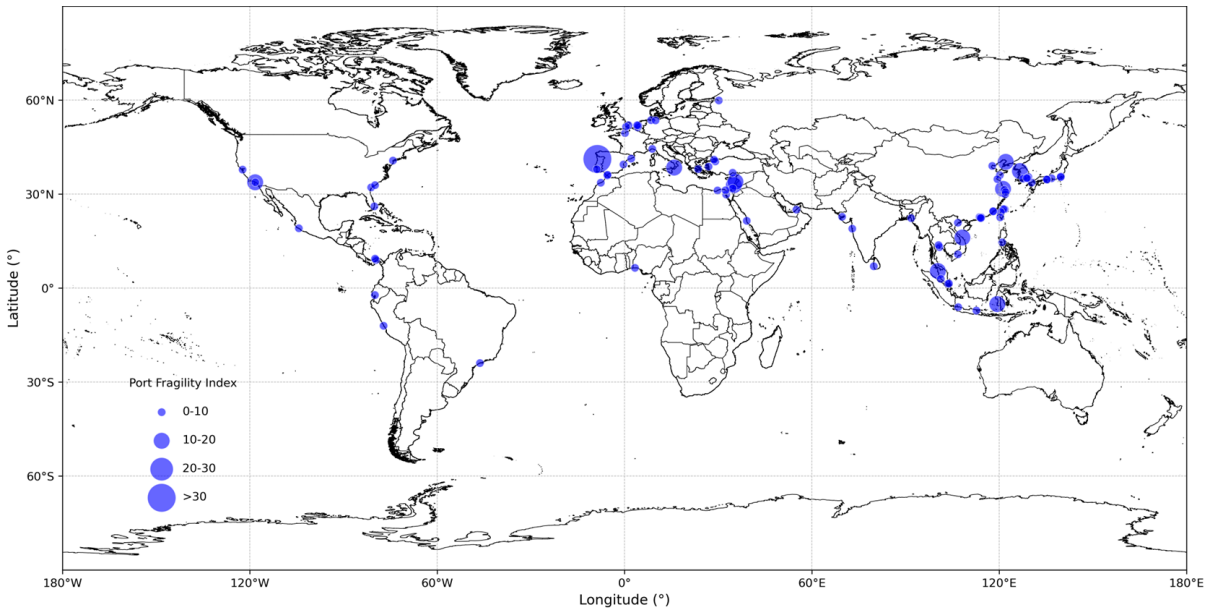

Figure 3.6: Vulnerability of major global container ports

3.4.2 Causality analysis of port vulnerability

The results in this section show that port vulnerability is inversely correlated to port size, hinterland industrial diversity, and port connectivity in the global shipping network.

Table 3.3 reports our regression results in OLS estimates. The coefficient of hinterland industrial diversity is -0.204 in column (1) and significant at 1% level, indicating ports located in a hinterland with a more diversified manufacturing structure exhibit less vulnerability to natural disasters, compared to those in hinterlands dominated by a few industries. Results from columns (2) and (3) demonstrate the robustness of our hinterland industrial diversity estimates after considering other potential determinants of port vulnerability. This result yields a novel insight from the maritime side: a diversified manufacturing structure in the hinterland can bolster port resilience, likely by distributing risks across various industries. It aligns with prior research in regional economics, which has proved that industrial diversification can mitigate the adverse effects of unforeseen events and foster economic stability (Brown and Greenbaum, 2017; Wang and Wei, 2021). For a port with a diversified industrial structure, while certain industries may be significantly affected by specific natural disasters, others might experience less impact and thus offset the losses. Consequently, local ports can expedite recovery by resuming the transportation of goods from less affected industries.

The coefficient for hinterland industrial diversity decreases in magnitude when factors such as port size and connectivity are considered, suggesting these elements also contribute to reducing port vulnerability. Specifically, a coefficient of -0.243 for port size means that a

1% increase in the maximum DWT of vessels visiting at the port is correlated with around 21.5% [4] decrease in port vulnerability index under natural disasters. This indicates that a port with better infrastructure is more resilient or less vulnerable, confirming previous research where investment in port infrastructure and facilities restoration, and maintenance have been found can improve port resilience (Hossain et al., 2019; Wang et al., 2023; Gu et al., 2024). For example, the current U.S. government has invested over $653 million in the port infrastructure improvement program across 41 ports aimed at enhancing port resilience and strengthening supply chains (Bloomberg, 2023). Our results contribute to this strand of literature by providing empirical evidence for the importance of port infrastructure in facing natural disasters.

The coefficient of network centrality is -0.058 in column (3), significant at the 5% level, underscores the role of convenience in a port's connectivity with others, suggesting that higher network centrality aids ports in adapting to and recovering from disruptions. The significance of port's location in the global shipping network for measuring port resilience has been noted by Qin et al. (2023), and our study qualitatively assesses how the port's network connectivity can reduce port vulnerability. This could be because higher connectivity allows ports to more effectively reconfigure their shipping lanes in response to natural disasters, and these ports may also benefit from more extensive experience in emergency management and superior operational capabilities.

[4] This impact of port size on the vulnerability index is calculated using $exp(-0.243) - 1 \approx 21.5\%$, since the dependent variable is in logarithmic format, i.e., $Log(Vulnerability + 1)$.

Table 3.3: Determinants of port vulnerability

	(1) *Log(Vulnerability+1)*	(2) *Log(Vulnerability+1)*	(3) *Log(Vulnerability+1)*
Hinterland industrial diversity	-0.204***	-0.202***	-0.168**
	(0.069)	(0.070)	(0.068)
Port size		-0.246*	-0.243*
		(0.145)	(0.132)
Network centrality			-0.058**
			(0.027)
Log (Annual vessel visits)	-0.602***	-0.587***	-0.669***
	(0.164)	(0.156)	(0.130)
Log (Hinterland GDP per capita)	-0.850	-0.805	-1.461*
	(0.667)	(0.681)	(0.767)
Hinterland trade openness	-0.909	-0.854	-1.151
	(0.878)	(0.861)	(0.967)
Hinterland unemployment rate	0.048	0.048	0.063**
	(0.033)	(0.033)	(0.026)
Distance (km)	-0.066	-0.066	-0.078*
	(0.043)	(0.043)	(0.043)
Max wind speed	0.097***	0.096***	0.092***
	(0.035)	(0.034)	(0.033)
Total precipitation	0.004	0.004	0.002
	(0.007)	(0.007)	(0.007)
2m temperature	0.010	0.011	0.010
	(0.019)	(0.019)	(0.018)
Constant	22.817***	24.898***	34.930***
	(7.910)	(7.801)	(10.386)
Observations	919	919	919
R^2	0.296	0.296	0.301
F-statistic	17.247	15.896	17.963
Fixed Effects		Port / Month / Disaster	

Note: Standard errors in parentheses are clustered at the natural disaster-region level. * $p < 0.10$, ** $p < 0.05$, *** $p < 0.01$.

3.4.3 IV regression results

Table 3.4 displays the IV regression results. The instrument variable approach in our model passes the Wald F statistic and LM statistic based on the Kleibergen–Paap rk statistic (Kleibergen and Paap, 2006) for weak identification and underidentification, respectively. Additionally, the Sargan Hansen J statistic test has a p-value larger than 0.1, supporting the null hypothesis that all instruments are valid instruments (Hansen, 1982).

The IV results confirm that hinterland industrial diversity and network centrality can mitigate port vulnerability, with coefficients significant at the 10% level. A comparison of coefficients reveals that the OLS estimates are biased downwards for the coefficient of endogenous variables: the coefficient for hinterland industrial diversity is -0.168 in the OLS regression versus -0.382 in the IV approach, and for network centrality, it is -0.058 in OLS versus -0.077 in IV. These differences suggest potential reverse causality between port resilience and these two endogenous variables, as well as possible measurement errors, exist.

Table 3.4: 2SLS regression results using IVs

	(1)	(2)	(3)
	2SLS	First-stage	
	Log(Vulnerability+1)	*Industrial Diversity*	*Network Centrality (%)*
Hinterland industrial diversity	-0.382*		
	(0.225)		
Network centrality	-0.077*		
	(0.046)		
IV: Log(Count mines within 300km)		0.495***	-2.050***
		(0.169)	(0.715)
IV: Log(Avg. distance from mines)		-20.064***	-57.385***
		(5.100)	(19.844)
IV: Regional avg. network centrality		0.144***	1.364***
		(0.047)	(0.170)
Port size	-0.223*	0.154	0.215
	(0.125)	(0.097)	(0.459)
Controls	Y	Y	Y
Observations	919	919	919
R^2	0.056	0.999	0.937
F-statistic	13.764	62.303	414.791
Kleibergen-Paap rk LM stat.	5.483		
Chi^2 P-value	0.064		
Kleibergen-Paap rk Wald F stat.	16.583		
Hansen J stat.	2.190		
Hansen J p-value	0.139		
Fixed Effects		Port / Month / Disaster	

Note: Standard errors in parentheses are clustered at the natural disaster-region level. * $p < 0.10$, ** $p < 0.05$, *** $p < 0.01$. Control variables are included but omitted from the table for brevity. The Kleibergen-Paap rk Wald F statistic (16.583) exceeds the Stock-Yogo critical value (13.43), rejecting the null hypothesis of weak instruments.

3.4.4 Heterogeneous test results

The first heterogeneity test, as reported in Table 3.5, is conducted by splitting ports into two groups: those located in the hinterlands with above- or below-median per capita GDP. The regression result reveals that in groups where the per capita GDP is relatively lower, industrial diversity negatively impacts port vulnerability (-0.315) with a significance level of 5%, while the port size does not have a notable effect. Conversely, in groups where the per capita GDP exceeds the median value, port size has a negative effect (-0.673) at the 10% significance level, whereas industrial diversity does not exert a significant impact. The connectivity of ports has significant effects on vulnerability in both groups.

A plausible explanation for these results is that in ports located in regions with lower economic development or lower per capita GDP, industrial diversity plays a more crucial role in aiding recovery from disasters or in enhancing disaster resistance. This is because these ports depend more heavily on local industries and are primarily engaged in import and export activities. Since the late 1990s, trade liberalization has driven many corporations to relocate their manufacturing bases to less developed regions with low labor costs, such as China, Vietnam, and Malaysia (Alfaro and Chor, 2023). As a result, these regions have become crucial components in the global supply chain for handling substantial manufacturing processes (Nicita et al., 2013), which heavily relies on ports to export their manufacturing goods. This close tie between ports and hinterland manufacturing industries indicates that industrial diversity is vital to a port's capacity in enduring and recovering from disruptive events. However, in economically more developed regions, the primary function of ports as transit hubs means that infrastructure has a greater impact on maintaining normal operations or on recovery post-disaster. For example, Hong Kong and Singapore, two of the busiest transshipment ports globally, illustrate this point. Singapore alone manages about 20% of the world's transshipment activities and is equipped with advanced infrastructure, including 52 berths and more than 200 quay cranes and gantry cranes capable of servicing large container ships (CBRE, 2022).

Table 3.5: Sub-group regression by GDP per capita

	(1) *Log(Vulnerability+1)* *Below-median per capita GDP Group*	(2) *Log(Vulnerability+1)* *Above-median per capita GDP Group*
Hinterland industrial diversity	-0.315**	-0.039
	(0.126)	(0.086)
Port size	0.206	-0.673*
	(0.199)	(0.349)
Network centrality	-0.064*	-0.074*
	(0.032)	(0.037)
Constant	51.025***	1.277
	(18.492)	(16.123)
Controls	Y	Y
Observations	460	459
R^2	0.357	0.292
F-statistic	186.779	11.865
Fixed Effects	Port / Month / Disaster	

Note: Standard errors in parentheses are clustered at the natural disaster-region level. * $p < 0.10$, ** $p < 0.05$, *** $p < 0.01$.

The second heterogeneity test shown by Table 3.6 classified four types of disasters with significant impacts on ports into two categories: hydrological disasters (floods and landslides) and meteorological disasters (storms and extreme weather). In the hydrological disaster group, industrial diversity significantly decreases port vulnerability (-0.212) with a significant level of 10%, whereas port size and network connectivity do not have a noticeable impact. For the meteorological disaster group, port network connectivity has a significantly negative effect (-0.061) on vulnerability with a significant level of 10%, but industrial diversity and port infrastructure or size do not.

This variation in results above can be attributed to the differing natures of the disasters. Hydrological disasters, such as floods and landslides, typically occur on the landside and mainly affect the connections between ports and their hinterlands. This emphasizes the role of industrial diversity in mitigating risks in port hinterlands. For instance, Xiao and Drucker (2013) used the 1993 Midwest flood in the United States as a quasi-experiment to demonstrate that regions with industrial diversity exhibited better economic resilience, measured by employment rates and income levels, post-disaster. This suggests that diverse industries can better support hinterland recovery after disasters, thereby aiding the restoration of port operations. On the other hand, meteorological disasters, such as storms and extreme temperatures, have a broader impact area, mainly affecting ports' connections on the seaside. These disasters challenge the ports' ability to maintain sea-bound logistical operations due to risks of navigational hazards and disrupted maritime routes caused by meteorological disasters. The network connectivity facilitates the flexible rerouting and management of vessels during adverse conditions, which are crucial for reducing losses and rapid recovery. This observation

is supported by Mou et al. (2024), who explored the impact of typhoon disasters on Chinese ports, underscoring the importance of network connectivity to resist typhoon-induced risks.

Table 3.6: Sub-group regression by disaster type

	(1) *Log(Vulnerability+1) Hydrological disasters*	(2) *Log(Vulnerability+1) Meteorological disasters*
Hinterland industrial diversity	-0.212*	-0.145
	(0.119)	(0.107)
Port size	0.224	-0.613
	(0.321)	(0.410)
Network centrality	-0.005	-0.061*
	(0.042)	(0.035)
Constant	33.475**	39.490**
	(13.214)	(16.465)
Controls	Y	Y
Observations	384	466
R^2	0.479	0.308
F-statistic	4.381	3.752
Fixed Effects	Port / Month / Disaster	

Note: Standard errors are in parentheses and clustered at the port level. * $p < 0.10$, ** $p < 0.05$, *** $p < 0.01$.

3.4.5 Robustness tests

To validate the robustness of the findings above on determinants of port vulnerability, we conducted six robustness tests, each reinforcing the results from our main regression analyses.

First, we explored the sensitivity of our results to variances in the criteria used to identify decrease days, recovery days, and closure days post-disaster. By substituting the three-day rolling average of vessel visits before the disaster with the total vessel visits and a seven-day average of vessel visits on the day before the disaster to represent the pre-disaster level of port operation, we recalculated the key changepoints in vessel visits for all potentially affected ports. These modifications did not alter the outcome, as shown in Table B.6 of the Appendix B.

Second, we adjusted the threshold for determining the minimum vessel visits day from 35% to 30% and 40% of the pre-disaster ship visit average. This test aimed to assess if varying this threshold would potentially impact the classification of ports without closure

but being affected by disaster. The result, presented in Table B.7 of the Appendix B, also confirms the robustness of our initial findings.

Third, we addressed the challenge of accurately defining port hinterlands, which are dynamic and influenced by variables such as cargo types, market competition, and geographic proximity (Notteboom, 2008; Notteboom and Rodrigue, 2017). We varied the hinterland radius used to calculate industrial diversity from 300km to 400km and 500km to examine the influence on our regression outcomes. This adjustment consistently yielded significant and negative coefficients for our key independent variables, underscoring the robustness of our results, as displayed in Table B.8 of the Appendix B.

Fourth, considering that closure days likely have more severe consequences compared to decrease days, and this distinction may affect our results, we introduced a weighted average ratio in Equation (1) to compute a new resilience index. Specifically, we assigned a weight of 0.6 and 0.55 to the fraction of recovery days to closure days and a weight of 0.4 and 0.45 to the fraction of recovery days to decrease days. The results of the regression analysis remained robust, as shown in Table B.9 of the Appendix B, indicating that our conclusions hold even after considering the different impacts of closure days versus decrease days.

Fifth, we included control variables to account for the effects of the severity of natural disasters and regional conflicts to evaluate the robustness of our results. To represent the severity of natural disasters, we used the total number of affected people in natural disasters as a proxy, obtained from the EM-DAT natural disaster database. To control for the effects of regional conflicts, we constructed two variables: (1) Conflicts, a dummy variable that equals 1 if the port is located in a country or region involved in any armed conflict in the year, sourced from UCPD/PRIO Armed Conflict Dataset [5]; 2) Deaths in conflicts, which is the logarithm of the total number of deaths in armed conflicts plus one in the country or region where the port is located in the year, retrieved from the UCDP Battle-related Deaths Dataset [6], serving as a proxy for the severity of regional conflicts. The corresponding results are displayed in Table B.10 of the Appendix B, where the coefficients of key variables (i.e., industrial diversity index, port size, and closeness centrality) remain statistically significant and negative, confirming the robustness of our findings. These tests collectively affirm the reliability of our analytical framework in assessing the determinants of port vulnerability.

Finally, considering the function of container ports (i.e., whether ports mainly handle

[5]The UCPD/PRIO Armed Conflict Dataset is a joint project between Uppsala Conflict Data Program (UCPD) at Uppsala University and the Centre for the Study of Civil War at the International Peace Research Institute in Oslo (PRIO), which provides information on armed conflicts from 1946 to 2023, where at least one party is a state government (Gleditsch et al., 2002).

[6]The UCDP Battle-related Deaths Dataset provides information on the number of deaths in armed conflicts from 1989 to 2023. This dataset includes annual data on both direct and indirect deaths resulting from armed conflicts involving at least one state government (Gleditsch et al., 2002).

transshipment cargo flows) may affect the determinants of port vulnerability, we conducted an extra heterogeneity test. Following Ducruet and Notteboom (2012), we used closeness centrality as a proxy for the transshipment share of container ports. This measure captures the convenience with which goods can be transported from one port to all others in the network. Ports with higher convenience centrality compared to other ports are more likely to function as transshipment hubs. We then segmented our data based on the median of port closeness centrality and performed subsample regressions for each group. The results are displayed in Table B.11 of the Appendix B. Port infrastructure plays an important role in enhancing the resilience of transshipment ports, whereas for non-transshipment ports, network connectivity is more crucial for resilience. These results are consistent with expectations, as transshipment ports may rely heavily on port infrastructure, such as the size and adequacy of berths and yards (Notteboom et al., 2023). However, for non-transshipment ports, increased connectivity allows them to establish more alternative routes for cargo imports and exports, which significantly reduces their dependency on a limited number of shipping paths. This added flexibility can better equip the ports to handle unexpected disruptions, including natural disasters, thus enhancing their overall resilience.

3.5 Conclusion and Policy Implication

Expanding on prior research examining the effects of natural disasters on port operations (Cao and Lam, 2019; Verschuur et al., 2020, 2023), this study utilizes high-frequency vessel tracking data coupled with a comprehensive natural disaster database to calculate a vulnerability index for global container ports. We further apply an econometric model to explore the underlying factors influencing port vulnerability, considering factors from the hinterland, port interface, and maritime network levels. This study discovers that port resilience is positively affected by port infrastructure, hinterland industrial diversity, and connectivity within the global liner shipping network. The heterogeneity tests show that hinterland industrial diversity significantly influences port vulnerability in less-developed regions, whereas port infrastructure plays a more critical role in more-developed regions. Additionally, industrial diversity markedly reduces port vulnerability during hydrological disasters, while port connectivity is the key factor instead during meteorological disasters.

This study offers valuable insights for policymakers and port authorities, highlighting through our heterogeneity tests that port resilience planning requires tailored approaches rather than a "one-size-fits-all" solution. More specifically, strategies are supposed to be customized to accommodate specific regional characteristics and the nature of prevalent disasters. Furthermore, while all three key determinants are essential for enhancing port re-

silience, resource limitations can constrain policymakers and port authorities when designing policies or strategies. This finding complements the conventional application of a uniform resilience analysis framework across ports with differing economic and geographical characteristics, serving as an empirical basis for future studies developing resilience frameworks tailored to different ports.

To further illustrate how policy recommendations could be derived from our results, we consider Makassar Port in Indonesia and Haiphong Port in Vietnam as case examples. Makassar Port is the second-largest port in Indonesia and ranks as the fifth most vulnerable port from our analysis, with a vulnerability index of around 14. Haiphong Port in Vietnam shares many similar characteristics with Makassar Port, such as both ports are mostly threatened by hydrological disasters and are located in less developed countries. However, Haiphong Port has a much lower vulnerability index of around 3, and higher levels of port network connectivity and hinterland industrial diversity. Therefore, based on our findings, we recommend that policymakers and the port authority at Makassar Port focus on enhancing both network connectivity and hinterland industrial diversity to improve port resilience. Improving network connectivity could involve establishing collaborative platforms with multiple stakeholders to share information and resources, as well as working with international shipping lines to design and introduce new routes and services, linking domestic and international shipping services (UNCTAD, 2017). Hinterland industrial diversity is also crucial for reducing port vulnerability, though it may be beyond the direct control of port authorities. Local government policymakers have a more significant role in this regard, with effective measures including reducing trade barriers, opening markets to foreign investments, and lowering corporate taxes (Brenton et al., 2019; UNCTAD, 2021b). These endeavors may help Makassar Port to enhance its resilience to future disruptions from natural disasters. However, transforming industrial structure may take time, for a more realistic consideration, policymakers can consider strategically developing key container ports in areas with greater industrial diversity. This approach would help create a more resilient port system and strengthen regional trade resilience against natural disasters.

While robust, the findings of this study should be approached with caution given the limitations. Firstly, our research is confined to global container ports from 2015 to 2019, omitting port activities after the COVID-19 pandemic. Secondly, our heterogeneity tests applied a relatively simple classification. Future studies could expand upon our study by further classifying ports based on their unique characteristics and investigating the factors influencing port resilience more deeply. For instance, the second heterogeneity test classified disasters into hydrological and meteorological categories. This basic categorization could be refined to account for different disaster compositions, recognizing that ports often face

multiple concurrent disasters. According to Verschuur et al. (2023), nearly half of global ports are threatened by four or five natural disasters. This insight underscores the need for a more comprehensive classification system that can capture the complex interplay of different disaster types affecting a port. Such an approach would allow for a more nuanced analysis of port resilience, tailoring strategies to better withstand and recover from the diverse challenges posed by multiple disasters. Thirdly, we focused on natural disasters, while port vulnerability or resilience can also be affected by human-related disruptions, such as labor strikes and pandemics. Future research should consider a wider spectrum of disruptions and expand the vessel tracking dataset to explore determinants of port vulnerability. Such an approach will facilitate a more holistic analysis of port operations and resilience when confronted with natural and anthropogenic challenges.

Chapter 4

The Impact of Geopolitical Risks on Port Carbon Emissions

4.1 Introduction

In recent years, geopolitical risks have emerged as a critical source of disruptions in global trade and transportation systems (Roscoe et al., 2022). Events such as armed conflicts, political instability, international sanctions, and deteriorating diplomatic relations have not only reshaped global supply chains but also posed significant challenges to maritime logistics and port operations (Notteboom et al., 2022). The maritime sector, which carries over 80% of global trade by volume (UNCTAD, 2024), is particularly vulnerable to such shocks due to its reliance on stable trade routes, predictable vessel schedules, and international cooperation. Ports, as key nodes in the global shipping network, are directly affected by these disruptions through changes in shipping demand, vessel rerouting, and operational inefficiencies.

While a growing body of research has investigated the economic and operational implications of geopolitical risks on trade flows, freight rates, and maritime supply chain reliability, less attention has been paid to their environmental consequences for ports. This is important, as although the majority of maritime CO_2 emissions (75–90% depending on ship type) still occur when vessels are at sea, a substantial amount of emissions (10–25%) arises when vessels are manoeuvring, anchoring, or berthing near the port (IMO, 2020). Therefore, understanding the impact of geopolitical risks (GPR) on port-level carbon emissions matters, as geopolitical tensions can undermine regional or global commitments to coordinated carbon mitigation targets or effective climate policies (Paramati et al., 2025) and weaken the incentives or capacity of port operators to enforce emission reduction strategies, potentially allowing carbon emissions to increase.

One potential mechanism underlying the impact of GPR on port carbon emission is that in response to volatile geopolitical environments, shipping companies may alter vessel schedules or deviate from established routes. For instance, due to the Red Sea Crisis since October 2023, many vessels have begun bypassing the Suez Canal and instead taking the longer route around the Cape of Good Hope. By mid-February 2024, a total of 586 container vessels had been rerouted, and container tonnage through the canal dropped by 82% (UNCTAD, 2024). Yang et al. (2025) further documented that the Red Sea Crisis led to a noticeable deterioration in schedule reliability among major shipping alliances. These irregularities in vessel arrivals make it more difficult to efficiently allocate berth resources and handle cargos, ultimately increasing carbon emissions from ships at berth.

It is worth noting that, the heterogeneity of port characteristics may play a critical role in the relationship between GPR and port carbon emissions. First, the average ship size calling at a port reflects its role in the global shipping network. Larger ships are more likely to operate on long-haul international routes (Meng and Wang, 2011), and therefore more exposed to geopolitical shocks. Second, the relationship between geopolitical disruptions and port emissions might be impacted by the level of competition for a port. Evidence from the air transport industry (Brueckner, 2002; Mayer and Sinai, 2003) has highlighted that higher airport market concentration is usually associated with less delays, as dominant airlines have the capacity and incentives to internalize congestion by smoothing arrival patterns. As the shipping and port industry share a similar structure than the airline industry, with the four largest carriers accounting for over half of the global market in 2022 and with the generalization of dedicated terminals in ports (UNCTAD, 2022; Haralambides et al., 2002; Sys, 2009), we will investigate if ports where a limited number of carriers control most calls exhibit more stable schedules and are therefore less impacted by geopolitical disruptions. Therefore, to contribute to these underexplored areas, this paper focuses on three key research questions:

(1) To what extent do geopolitical risks (GPR) affect carbon emissions from ships at berth across global container ports?

(2) How do port characteristics, specifically average vessel size and market concentration level, moderate the impact of GPR on port emissions?

(3) What are the implications of these findings for designing effective port-level carbon abatement policies?

To address these questions, we construct a balanced panel dataset covering monthly port-level emissions and shipping activity at 269 container ports across 40 countries and regions from January 2016 to December 2023. We use a newspaper-based and country-specific geopolitical risk (GPR) index developed by Caldara and Iacoviello (2022) as the

main explanatory variable. To estimate the dynamic relationship between geopolitical risks and port emissions while addressing potential endogeneity concerns, we employ a system generalized method of moments (SYS-GMM) estimator.

This study makes several contributions to the existing literature. First, it enriches the emerging strand of research on the environmental consequences of geopolitical tensions by providing causal, port-level empirical evidence on how GPR affects carbon emissions, a dimension that has received limited attention in prior work. Second, this study uncovers the mechanism of ship arrival variations through which geopolitical risk propagates. This perspective advances our understanding of how global political disruptions translate into environmental inefficiencies in maritime logistics. Ultimately, the study provides practical policy recommendations for enhancing the resilience and sustainability of port operations in the face of geopolitical uncertainty. These include integrating geopolitical risk considerations into environmental policy frameworks and proposing port-specific carbon mitigation strategies that account for heterogeneity (i.e., average vessel size and market concentration level) in port structure.

This study is organized as follows: section 2 briefly introduces related literature; section 3 presents the data and methodology; section 4 reports the results; section 5 discusses the findings and provides policy implications; section 6 concludes.

4.2 Literature review

Our study builds on four streams of literature: (1) the introduction of geopolitical risk (GPR); (2) the environmental consequences of GPR; (3) the impact of GPR on maritime transportation; (4) operational determinants of port emissions. Building on prior literature, we propose two channels through which GPR influences port carbon emissions.

4.2.1 Geopolitical risk index

Historically, the concept of geopolitical risk (GPR) is rooted in the traditional understanding of geopolitics, which refers to the practices of states controlling and competing for territory, often associated with war, empire, and diplomacy (Flint, 2021). In modern international relations, however, geopolitics has expanded to include power struggles that occur without the presence of war or armed conflict, such as trade disputes, economic sanctions, and visa restrictions (Yang et al., 2025). Caldara and Iacoviello (2022) defines GPR as the threat, realization, and escalation of adverse events associated with war, terrorism, and tensions among states or political actors that disrupt the peaceful conduct of interna-

tional affairs. To quantify this concept, they construct newspaper-based indices of GPR at both daily and monthly frequencies, using the relative frequency of articles that contain pre-defined keywords related to geopolitical tensions in major international newspapers. The indices are available in both global and country-specific formats and are designed to be consistent and comparable over time. A growing body of research has examined the economic and logistical consequences of GPR. For example, geopolitical tensions have been shown to affect firm-level decisions such as cash holdings (Lee and Wang, 2021) and investment (Wang et al., 2024b), increase volatility in financial markets (Phan et al., 2022; **?**), and set off a chain reaction effect through global value chains, such as strategic responses including manufacturing locations (Moradlou et al., 2021), sourcing behaviours (Huq et al., 2021), and buyer-supplier relationships (Fan et al., 2024).

4.2.2 The environmental consequences of GPR

One stream of research empirically examines how geopolitical risk (GPR) affects carbon emissions through two channels (Anser et al., 2021; Syed et al., 2022). The escalation channel suggests that higher GPR dampens research and development, slows technological progress and clean innovation, thereby increasing emissions. Consistent with this view, country-level panel evidence showed that GPR impedes renewable-energy investment (Flouros et al., 2022). Using a cross-sectionally autoregressive distributed lag (CS-ARDL) model for 21 countries from 2000 to 2021, Hunjra et al. (2024) also reported a positive association between GPR and environmental degradation, while showing that green energy may mitigate this effect. Extending the escalation perspective, Chen et al. (2024) found that GPR exacerbated emissions inequality, measured by per-capita emissions within the top 10% income group, because lower-income economies face tighter constraints in adopting sustainable products under instability and uncertainty, while high-income groups tend to increase fuel consumption to secure positions and assets. Paramati et al. (2025) further argued that GPR weakens multilateral cooperation and undermines progress toward net-zero targets, reinforcing escalation effects. The mitigation channel points out the other way: heightened uncertainty can depress economic activity and energy use or accelerate the energy transition under supportive conditions, thereby reducing emissions. Wang et al. (2023) employed a quantile regression model using data from China and showed that GPR indirectly lowers emissions by suppressing investment and industrial output. Using panel data for 38 countries from 2002 to 2020, Li et al. (2024a) reported that GPR can reduce emissions through adverse effects on economic development and energy supply. In OECD economies, Wang et al. (2024a) found that instability in energy-supplying countries (e.g., the Russia–Ukraine conflict) may accel-

erate energy transitions in energy-importing countries, which is vital to achieving carbon neutrality. This effect is particularly pronounced where green innovation and environmental regulation are stronger. Overall, existing studies provide mixed evidence on the impact of GPR on carbon emissions. While most evidence is at the national level, far less is known at finer spatial scales. To fill this gap, our study examines per-call CO_2 emissions from ships at berth, capturing the operational consequences of geopolitical uncertainty at ports, an important yet understudied component of trade-related emissions.

4.2.3 The impact of GPR on maritime transportation

In maritime transportation, geopolitical shocks can significantly disrupt port operations and the global shipping network. A growing literature examines how specific disruptive events affect maritime trade flows, port activity, and network connectivity. Studies have, for example, analyzed the Suez Canal closure (1967–1975) (Feyrer, 2021), the 9/11 attack (Rousset and Ducruet, 2020), the Red Sea crisis (Yap and Yang, 2024; Yang et al., 2025), and the Russia–Ukraine conflict (Xiao et al., 2024; Zhang and Wang, 2024; Lyu et al., 2025). Feyrer (2021) used the Suez Canal's closure as a natural experiment to evaluate its impact on trade at the country level. Rousset and Ducruet (2020), using Lloyd's List Intelligence ship data, analyzed how the 9/11 attack affected port traffic and extended the analysis to how such shocks undermine ports' positions within shipping network systems. With the wider use of AIS data, analyses of GPR effects can be pinpointed to the level of shipping alliances, lines, and even individual vessels. Yap and Yang (2024) adopted a Structure–Conduct–Performance (SCP) paradigm to examine changes in weekly port calls and shipping capacity along Asia–Europe and Asia–Mediterranean routes at the alliance level, documenting declines in both indicators after the onset of the Red Sea crisis. Building on this, Yang et al. (2025) used ship on-time rates to show that schedule reliability declined for several major carriers and identified port skipping as a key strategy in response to the disruption. Together, these studies provide high-frequency evidence that carriers adjust schedules, reroute, and skip ports under geopolitical threats. Environmental implications remain less explored. Peng et al. (2024) showed, using causal analysis, that rerouting via the Cape of Good Hope during the Red Sea crisis increased voyage distances and led to carbon leakage. By contrast, Lyu et al. (2025) reported that global carbon emissions from crude-oil shipping declined by about 5.8% in the year following the Russia–Ukraine conflict.

Our study contributes to this emerging literature by providing causal, port-level evidence on how GPR affects per-visit CO2 emissions using real-time vessel activity data from the AIS database. By focusing on emissions from ships at berth, our analysis captures the op-

erational consequences of geopolitical uncertainty, such as vessel arrival irregularities and increased coordination costs, that are often overlooked in national or port-level emission assessments. This port-level perspective offers novel insights into how global political tensions can propagate through maritime operations to affect environmental outcomes, thereby filling an important gap in both the geopolitical and environmental economics literature, and highlighting the importance of incorporating geopolitical considerations into policy frameworks for environmental abatement in the shipping sector.

4.2.4 Operational determinants of port-call emissions

At the micro level, port-call emissions are typically measured by combining AIS trajectories with ship technical specifications, which also depends on different operational modes, including berthing, anchoring, maneuvering, and sailing. This bottom-up approach enables per-call estimates that vary with call duration, ship characteristics, and navigation status (e.g., IMO (2020)). While emissions also depend on fuel type and vessel design, our review focuses on port operations. One stream of literature examines how operational efficiency shapes emissions. Efficient port operation shortens time in port and auxiliary-engine hours, which lowers emissions per call, a critical factor for port-level emission reduction (Moon and Woo, 2014). At a global scope, Ducruet et al. (2014) documented cross-port time efficiency, measured by ship turnaround time (the average time a vessel stays in port) in 1996, 2006, and 2011, and relates it to traffic volume, vessel size, and ports' positions in liner networks. Using a unique Norwegian dataset for 2014, Rødseth et al. (2018) analyzed determinants of ship working time and associated air emissions, showing that vessel size, operation type (loading vs. unloading), and container status (empty vs. laden) materially affect time in port. A second strand of literature highlights the importance of arrival uncertainty and coordination for port operational efficiency. Wang and Guo (2018) Wang and Guo (2018) first incorporated uncertainty in ship arrivals into port efficiency analysis by using a berth allocation and quay crane assignment (BA-QCA) optimization model. Such uncertainty in ship arrivals combined with the first-come, first-served (FCFS) scheme may lead to inefficient berth allocation. When vessels must wait at port for available services, they often keep auxiliary engines and boilers running, thus contributing to additional emissions (Zhang et al., 2024). To address this, the just-in-time (JIT) arrival scheme has been proven to reduce unnecessary waiting and associated emissions through communicating about the berth availability between shipping lines and port operators (Jia et al., 2017; Grigoriadis et al., 2024). Furthermore, Rhodes et al. (2025), using a bottom-up emission model combining AIS data and vessel specifications, evaluated the new queuing system at the Ports of Los Angeles

and Long Beach, where berthing positions are pre-assigned before ships depart their previous ports, and found a 16% to 24% reduction in per-voyage emissions after implementation.

Taken together, these studies point to a potential pathway through which uncertainty in ship arrivals imposes coordination costs on port operations and leads to increased carbon emissions. Building on this insight, our study constructs a measure of ship arrival time variation, defined as the coefficient of variation in inter-arrival times within a month at each port, to capture schedule reliability on the waterside. We then examine whether GPR, as an upstream shock to vessel arrival regularity, is associated with higher per-call CO2 emissions at ports.

4.2.5 Conceptual framework

This study considers that geopolitical risk (GPR) may influence port-level carbon emissions through two theoretically grounded channels: a direct policy channel and an indirect operational channel.

First, the direct policy channel. Environmental quality is widely recognized as a public good (Siebert, 1998), and carbon mitigation constitutes a transboundary public-goods problem. To address this, countries negotiate international environmental agreements (IEAs). These agreements must be self-enforcing, meaning that participation and compliance must be individually rational and incentive-compatible, given the absence of supranational enforcement mechanisms (Barrett, 1994). However, heightened geopolitical tensions may undermine trust among nations, reduce the credibility of enforcement mechanisms, or shift domestic political incentives away from international cooperation. Geopolitical tensions might also impact the willingness of ports to comply with new regulations and lead them to reallocate fiscal and administrative resources from social and environmental programs to national security (Bove et al., 2017). As a result, climate mitigation efforts may be crowded out or deprioritized, leading to reduced regulatory enforcement and environmental degradation.

Second, the indirect operational channel. At the micro level, geopolitical risks introduce uncertainty that disrupts firm-level decision-making. According to the theory of investment under uncertainty, greater uncertainty increases the value of waiting and reduces investment, particularly when capital expenditures are irreversible and outcomes depend on future information (Pindyck, 1990; Dixit and Pindyck, 1994; Bloom et al., 2007). In liner shipping, we assume that this could lead shipping firms to delay, reschedule, or cancel operational decisions, particularly regarding ship arrivals at ports located in geopolitically risky regions, which may result in irregular vessel arrivals and greater arrival-time variation. From an operation management perspective, greater variability in arrivals to queuing systems with limited

capacity increases waiting and system time and lowers operational performance (Wolff, 1977). Applied to ports, irregular and unpredictable arrivals may complicate berth allocation and cargo-handling processes, thereby reducing port efficiency (Wang and Guo, 2018). These inefficiencies prolong waiting and handling times, increasing fuel consumption and ultimately raising port-related carbon emissions (Rødseth et al., 2018; Wang et al., 2022).

4.3 Data and Methodology

4.3.1 Data and variable description

We construct a port-month panel data spanning from Jan 2016 to Dec 2023, including 269 ports across 40 countries and regions. Our data sample includes two major data resources. The first dataset is the country-level Geopolitical risk index developed by Caldara and Iacoviello (2022) [1]. The second dataset is the ship-level activity data sourced from the Automatic Identification System (AIS) Database. The AIS Database provides dynamic information on container ships, including ship location, speed, direction, etc., together with port location information, ship identification information, and ship technical information from Lloyd's List, we calculated the average CO_2 emission during the time when ship berthing at ports.

Geopolitical risk (GPR) Index. The geopolitical risk index is measured by adverse geopolitical events and its associated risks based on text-search of ten newspapers: Chicago Tribune, the Daily Telegraph, Financial Times, The Globe and Mail, The Guardian, the Los Angeles Times, The New York Times, USA Today, The Wall Street Journal, and The Washington Post. The index is calculated as the share of articles related to adverse geopolitical events together with the name of the country, its capital, or major cities (Caldara et al., 2024). This index measures the exposure of the country to geopolitical risk and concerns.

Port CO_2 emission calculation. We calculated the CO_2 emission of ships using a bottom-up evaluation model. First, we identify ship visits at ports using AIS data and port location coordinates. A ship is considered to be berthed at a port if it remains within a 10km radius of that port and its speed is below 1 knot. Second, we calculated the CO_2 emission for each ship using the Ship Traffic Emission Assessment Model (STEAM) (Johansson et al., 2017; Li et al., 2024c). The emission from engine type ρ under navigational status τ is calculated as:

$$E_{\rho,\tau} = P_\rho * EF_{\rho,\tau} * LF_t * A_{LF,t} * \delta T_t \tag{4.1}$$

[1]Data downloaded from `https://www.matteoiacoviello.com/gpr.htm` on April 10th, 2025.

$$LF_t = (\frac{v_t}{v_{ds}})^3 \tag{4.2}$$

$E_{\rho,\tau}$ is the CO_2 emission from engine type ρ (main engine, auxiliary engine, or boiler) under navigation status τ. P_ρ refers to the engine power for type ρ. The navigational status τ including berthing, anchoring, maneuvering and sailing, determined by ship speed and distance from the port (Liu et al., 2016; Olmer et al., 2017). $EF_{\rho,\tau}$ is the CO_2 emission factor, which is referred from the fourth IMO GHG emission report (IMO, 2020). LF_t is the loading factor at time t, $A_{LF,t}$ is the emission adjustment factor when loading factor is lower than 20%, δT_t is the time interval between consecutive speed records. The load factor is the ratio of the actual speed v_t divided by the maximum designed speed v_{ds} of the ship and we set the speed ratio exponent as 3 [2]. Finally, we aggregate the CO_2 emissions for each ship while berthed at port for each port call, then compute the monthly average CO_2 emission per ship at each port. This value serves as the dependent variable in our analysis.

Mechanism variable. To capture the potential mechanism through which geopolitical risk influences port emissions, we construct a proxy for ship schedule reliability based on the coefficient of variation (CV) of the time difference between consecutive ship arrivals at a port, which is the *Arrival Time Variation*. Specifically, the *Arrival Time Variation* is calculated as the standard deviation divided by the mean of inter-arrival times within each month at each port. A higher *Arrival Time Variation* indicates greater variability in ship arrivals, reflecting lower schedule stability and more irregular vessel traffic patterns. This approach is motivated by the notion that heightened geopolitical risk, such as regional conflicts, sanctions, or disruptions in trade policy, may lead to increased uncertainty in global supply chains, causing shipping lines to adjust or delay their schedules (UNCTAD, 2024; Yap and Yang, 2024; Yang et al., 2025). Such irregularities can increase the unpredictability of port operations, leading to higher coordination cost, inefficient berth allocation, long berthing durations, and ultimately higher emissions at port. Therefore, by linking geopolitical risk to changes in the CV of ship arrival intervals, we identify a plausible operational mechanism through which external shocks may affect port-level emissions.

Control variables. Port carbon emissions are also influenced by a variety of port-level and macroeconomic factors. Following previous studies on the factors of port emissions, we include a set of control variables. For port-level characteristics, AIS data are used to construct monthly indicators related to port activities. Port container throughput is widely used as a proxy for the development level of ports (Li et al., 2024b), and we include the number of port calls to reflect the frequency of vessel movements. The average deadweight

[2]When engine loads fall below 20%, emission factors rise due to lower combustion efficiency, so a low load adjustment factor of 1 is applied for CO_2 estimation (IMO, 2020).

tonnage (DWT) of visiting ships is also included, as larger vessels tend to require longer berthing time and energy use (Rødseth et al., 2018). In addition, we control for the number of shipping lines calling at the port to capture the effects of market structure which may influence port emissions (Irannezhad et al., 2018). We also include port handling efficiency, which has been shown to impact emissions through affecting ship turnaround time (Rødseth et al., 2020). To account for differences in national or regional development, we include macroeconomic variables from the Global Macro Database (Müller et al., 2025), including GDP per capita, population size, unemployment rate, and trade openness (measured by the sum of export and import shares). These variables have been widely applied in empirical studies examining the drivers of carbon emissions (Paramati et al., 2025).

The detailed description of variables is presented in Table 4.1 and summary statistics are shown as Table 4.2.

Table 4.1: Variable descriptions

Variable	**Description**
Avg CO_2 (kg)	The monthly average CO_2 emissions (in kilograms) generated per ship during berthing at the port.
GPR index	GPR index is the news-based monthly index from Caldara and Iacoviello (2022), measuring a country's exposure to geopolitical risk as the share of news articles mentioning adverse geopolitical events together with the country's name, capital, or major cities.
Avg DWT	The average deadweight tonnage (DWT) of all ships that called at the port within a given month.
No Shipping Lines	The number of distinct shipping lines whose ships called at the port in a given month.
Port Calls	The total number of ship arrivals at the port during the month.
Handling Efficiency	Calculated as the monthly average of ship-level handling efficiency, where a ship's efficiency is defined as its DWT divided by its total berthing time at the port (Yang et al., 2023).
GDP per capita ($)	The gross domestic product per capita (in U.S. dollars) at the national level.
Population (Million)	The total population of the country where the port is located.
Unemployment Rate (%)	The national unemployment rate.
Openness (%)	The degree of trade openness, measured as the sum of exports and imports divided by the country's total GDP.
Arrival Time Variation	The coefficient of variation (CV) of ship arrival times at a port within a given month, calculated as the standard deviation divided by the mean of the time intervals between consecutive ship arrivals.

Table 4.2: Summary statistics

Variable	N	Mean	SD	p10	p90
Avg CO_2 Emission (kg)	25,555	28,613.178	21,483.402	8,826.102	51,478.035
GPR index	25,555	0.562	0.860	0.019	1.918
Avg DWT	25,555	44,533.859	29,026.226	11,246.034	86,134.492
No Shipping Lines	25,555	22.315	23.565	3	56
Port Calls	25,555	69.984	105.956	7	194
Handling Efficiency	25,555	2,631.535	2,366.912	687.171	4,976.081
GDP per capita ($USD)	25,531	30,189.207	22,846.711	3,855.751	65,110.535
Population (Million)	25,555	286.428	443.779	17.232	1,389.030
Unemployment Rate (%)	25,266	6.648	4.313	3.235	12.109
Openness (%)	25,532	57.577	35.969	27.040	94.051
Arrival Time Variation	25,239	0.863	0.272	0.553	1.144

4.3.2 Model

Baseline model. This paper uses the system generalized method of moments (SYS-GMM) estimator developed by Blundell and Bond (1998) to examine the effect of geopolitical risk on port emissions. Compared to fixed-effects and random-effects estimators, the GMM approach is better suited for addressing endogeneity by using lagged values of the dependent variable and other potentially endogenous regressors as instruments (Arellano and Bond, 1991). In particular, the system GMM combines moment conditions in both first-differences and levels, significantly improving estimation efficiency and reducing the bias associated with weak instruments (Roodman, 2009), especially in the presence of highly persistent variables such as port emissions. This method is particularly appropriate given the structure of our panel dataset, which features a relatively short time dimension (small T) and a large number of cross-sectional units (large N). The system-GMM model is as follow[3]:

$$LnAvgCO_{2i,t} = \alpha_0 + \alpha_1 LnAvgCO_{2i,t-1} + \alpha_2 GPR_{i,t-1} + \boldsymbol{\beta}\mathbf{Controls}_{i,t} + \delta_t + \epsilon_{i,t} \quad (4.3)$$

$LnAvgCO_{2i,t}$ denotes the average CO_2 emissions of container ships berthing at port i in month t, $LnAvgCO_{2i,t-1}$ is the first-order lag term of the dependent variable. $GPR_{i,t-1}$ is the Geopolitical risk index in the country of port i in month $t-1$. We use one-month lag term of GPR index to account for the certain time lag exist in the economic and social impacts of GPR. Control variables include average ship DWT visiting the port, number of

[3]The individual fixed effects are differenced out in the GMM framework and thus are not explicitly included in the estimation. To account for potential time-specific shocks, we include time fixed effects (Roodman, 2009).

shipping lines, monthly port calls at the month- and port-level, handling efficiency, GDP per capita, unemployment rate, openness rate (export and import shares of total GDP), total population at year- and country-level. δ_t denotes the month fixed effect and $\epsilon_{i,t}$ is the error term.

Mediation effect model. We conduct a mediation analysis to examine whether variable Arrival time variation mediates the relationship between GPR index and Port CO_2 emissions. The specific regression models are as follows:

$$\begin{aligned} ArrivalTimeVariation_{i,t} = \alpha_0 + \alpha_1 ArrivalTimeVariation_{i,t-1} + \alpha_2 GPR_{i,t-1} \\ + \boldsymbol{\beta}\mathbf{Controls}_{i,t} + \delta_t + \epsilon_{i,t} \end{aligned} \tag{4.4}$$

$$\begin{aligned} LnAvgCO_{2i,t} = \alpha_0 + \alpha_1 LnAvgCO_{2i,t-1} + \alpha_2 GPR_{i,t-1} + \alpha_3 ArrivalTimeVariation_{i,t} \\ + \boldsymbol{\beta}\mathbf{Controls}_{i,t} + \delta_t + \epsilon_{i,t} \end{aligned} \tag{4.5}$$

$ArrivalTimeVariation_{i,t}$ is the mediating variable, which denotes the coefficient variation of ship arrival times at port i in month t. The control variables and fixed effects are the same as Eq.4.3. Eq.4.4 examines the effect of geopolitical risks on ship arrival time variation, and Eq.4.5 is the baseline model that includes arrival time variation as a potential mediator. If the coefficient of GPR in Eq.4.4 and that of arrival time variation in Eq.4.5 are both significant, it suggests that part of the effect of geopolitical risks on emissions is transmitted through increased volatility in ship arrivals, that is, the existence of arrival time variation as the mediator.

4.4 Results

This section begins by presenting the temporal and spatial distributions of the GPR index and port-level carbon emissions. Next, we answer the first research question: *To what extent do GPR affects carbon emissions from ships at berth across global container ports?* and explore the second research question by examining *how port characteristics, specifically average vessel size and market concentration level, moderate the impact of GPR on port emissions?* Finally, we present the robustness checks to validate the main findings.

4.4.1 Spatial distributions of GPR and port carbon emissions

We select four time points from our sample data to analyze the spatial distribution of our key variables: the main independent variable, average port-level carbon emissions, and the dependent variable, the GPR index. Figures 4.1 to 4.4 display country-level GPR, shown as a shaded background where darker colors indicate higher geopolitical tensions, along with the average port-level CO_2 emissions, represented by circles. The size of each circle reflects the monthly average CO_2 emissions per vessel calling at that port. Among the sampled countries, the United States, China, and Russia exhibit higher GPR levels. Notably, China's GPR index increased significantly in 2018 compared to 2016, likely due to the escalation of the US–China trade war. Similarly, Russia's GPR index spiked in 2022, as the outbreak of the Russia–Ukraine war led to a visible shift in map color from orange in 2020 to dark blue in 2022. These patterns indicate a gradual intensification of global geopolitical tensions over time. Port-level average emissions appear more stable across years. While no clear temporal trend is observed, certain ports, such as Los Angeles and Long Beach in the United States, and Durban and Cape Town in South Africa, report higher average carbon emissions per vessel. The annual level data in the remaining years and the country/region-port reference table can be found in the Appendix C.

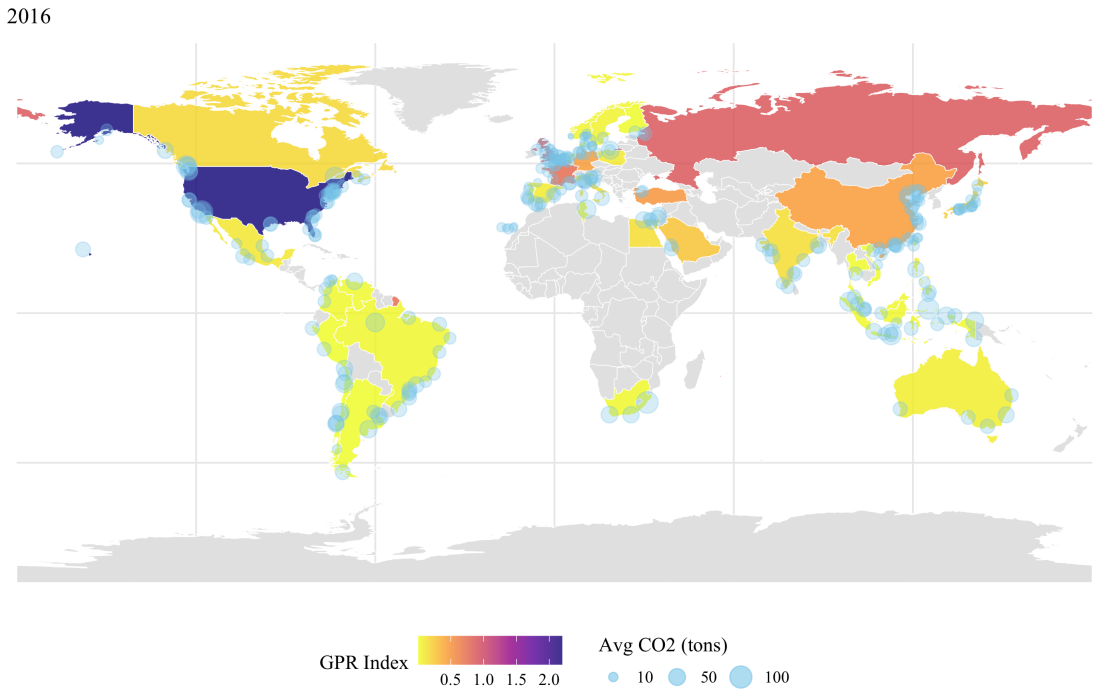

Figure 4.1: Geopolitical risks and average port CO_2 emissions in 2016

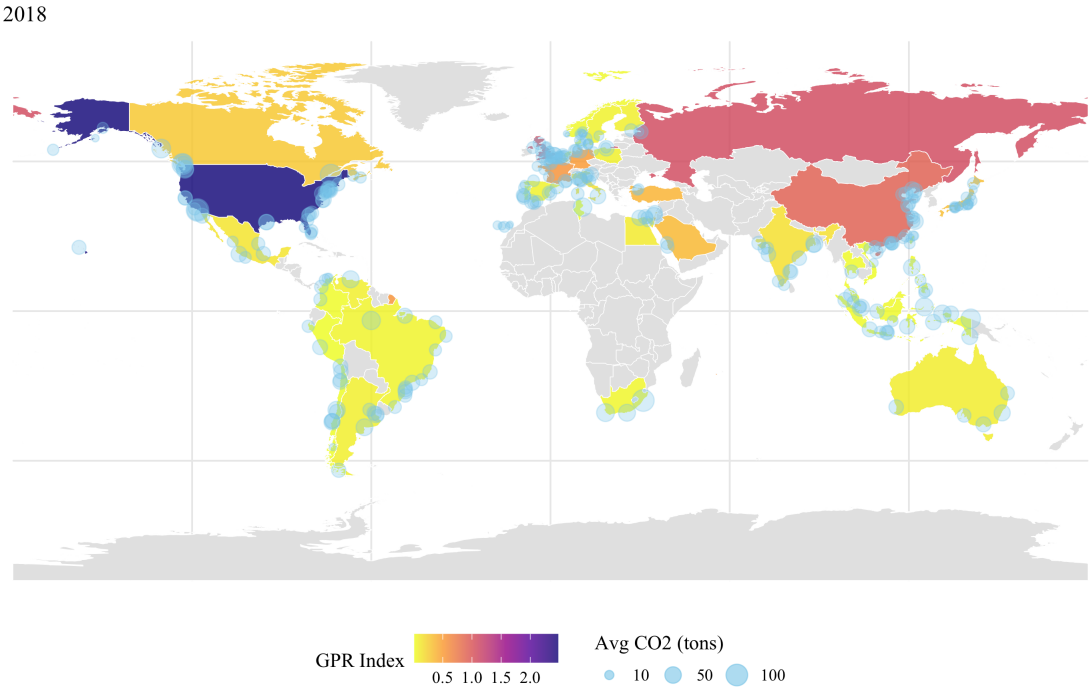

Figure 4.2: Geopolitical risks and average port CO_2 emissions in 2018

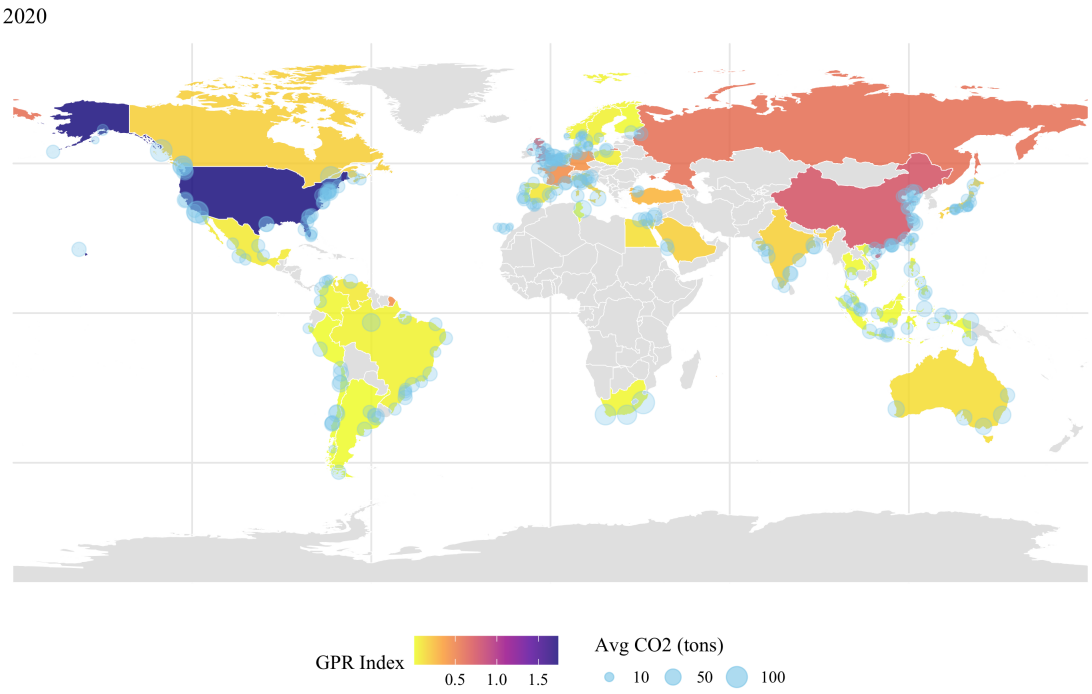

Figure 4.3: Geopolitical risks and average port CO_2 emissions in 2020

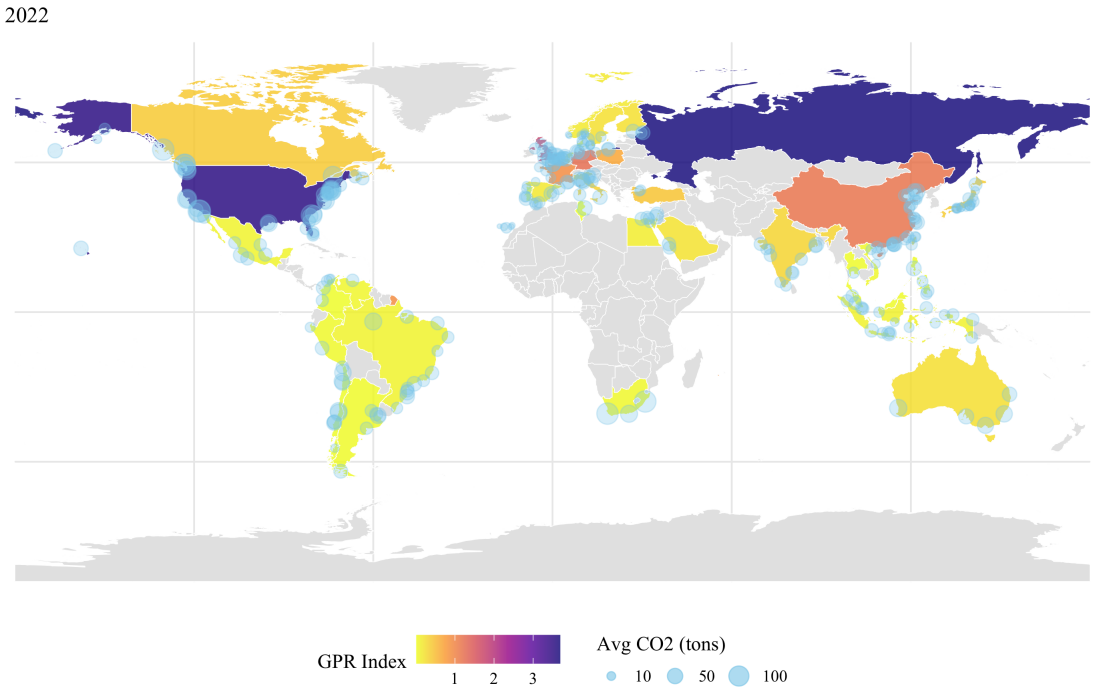

Figure 4.4: Geopolitical risks and average port CO_2 emissions in 2022

4.4.2 Baseline regression results

Table 4.3 presents the results of system GMM models. In Column (2), we include more country- or region- level control variables (Population, unemployment rate and openness), and the coefficients of $GPR_{i,t-1}$ are both positive and statistically significant at 1% level. These results indicate that the unstable geopolitical status or adverse geopolitical events may exacerbate the emissions level at ports. 1% increase in GPR index may lead to approximately 2.7% increase in the average port carbon emission level. The significant and positive coefficient of one-month lag term of average port carbon emission displays a potential cumulative growth effect of port emission level. This suggests that the prior emission level may have a continuous effect on the emission level of next month. Table 3 also presents the results of Arellano-Bond test for autocorrelation and Hansen test for over identification. The p-values of first-order difference, AR(1) is 0, and of the second-order difference, AR(2) is 0.280 in Column (2), showing that the residuals have first-order correlation but no second-order correlation, which is valid for using system GMM estimation (Roodman, 2009). Additionally, the p-value of Hansen test is 0.189, larger than 0.1, showing that the instrument variables have no over identification problem.

Table 4.3: The impact of geopolitical risk on port emissions

	(1)	(2)
	$LnAvgCO_2$	
L.LnAvgCO_2	0.077***	0.078***
	(0.016)	(0.016)
L.GPR	0.025**	0.027**
	(0.011)	(0.012)
LnAvgDWT	1.121***	1.117***
	(0.024)	(0.025)
Ln(NoShippingLines+1)	0.181***	0.185***
	(0.029)	(0.029)
Ln(PortCalls+1)	-0.146***	-0.150***
	(0.023)	(0.024)
LnHandlingEfficiency	-0.808***	-0.807***
	(0.021)	(0.022)
LnGDPpercapita	-0.029***	-0.028***
	(0.008)	(0.011)
LnPopulation		0.008
		(0.009)
Unemployment Rate		0.002
		(0.002)
Openness		0.017
		(0.014)
Constant	9.481	9.146
	(8.512)	(9.298)
Observations	25,531	25,243
AR(1) p-value	0.000	0.000
AR(2) p-value	0.259	0.280
Hansen test	5.835	6.145
Hansen p-value	0.212	0.189
Time FE	Y	Y

Note: Robust standard errors in parentheses. * $p < 0.10$, ** $p < 0.05$, *** $p < 0.01$.

4.4.3 Mechanism test

Table 4.4 presents the results of the mediation effect model. In Column (1), the effect of GPR index on ship arrival time variation is 0.017, which is statistically significant at 10% level, suggesting that the increased geopolitical risks can lead to higher volatility of ship arrival schedules. The coefficient of Arrival Time Variation is positive and significant at 5% level, and the coefficient of the lag term of GPR becomes lower (from 0.027 to 0.022) and the significant level decreases from 5% to 10%, suggesting the mediating effect of ship arrival time variation on the impact of geopolitical risk on port emissions.

Table 4.4: The impact of geopolitical risk on ship schedules

	(1) *Arrival Time Variation*	(2) *LnAvgCO₂*
L.GPR	0.017*	0.022*
	(0.010)	(0.012)
L.LnAvgCO$_2$		0.086***
		(0.014)
Arrival Time Variation		0.176**
		(0.078)
L.Arrival Time Variation	0.062***	
	(0.018)	
Constant	121.523***	15.272
	(42.289)	(10.735)
Controls	Y	Y
Observations	24,733	24,933
AR(1) p-value	0.000	0.000
AR(2) p-value	0.808	0.382
Hansen test	1.633	11.462
Hansen p-value	0.201	0.245
Time FE	Y	Y

Note: Robust standard errors in parentheses. * $p < 0.10$, ** $p < 0.05$, *** $p < 0.01$.

In both columns, the p-values of the AR(1) tests are 0, and those of the AR(2) tests are above 0.1, indicating no second-order autocorrelations. The p-values of the Hansen test are also above 0.1, supporting the validity of the overidentifying restrictions.

4.4.4 Heterogeneity test

So far, we have examined the impact of geopolitical risk on port CO_2 emissions and tested the mediation variable, ship arrival time variation. Our findings indicate that the unstable geopolitical status results in a higher port emission on average, and one of the channels is that the geopolitical tension affects the decision of shipping lines and may adjust and cancel ship arrivals, leading to high volatility of ship schedules. Therefore, the increased operational cost of the port operator leads to lower efficiency, increasing the port emissions.

Next, we will investigate what characteristics of ports will affect the relationship between GPR index and port emissions. First, the average ship size that ports serve may play a role in the impact of GPR index on port emissions. This is motivated by that larger ships typically operate on long-haul international routes (Meng and Wang, 2011) and are thus more exposed to global geopolitical events. In contrast, smaller ships tend to serve regional or short-haul routes, which may be less sensitive to geopolitical risks. Hence, we suppose that ports that primarily serve larger vessels are more likely to be affected by geopolitical risks compared to ports mainly serving smaller ships in terms of carbon emissions. Second, the level of market concentration may influence how geopolitical risk affects port emissions. The global container shipping market is dominated by a small number of large shipping lines, with the top few carriers accounting for a substantial share of total vessel calls (Sys, 2009). These dominant carriers are generally more capable of responding to geopolitical disruptions by adjusting their operations, for example, by smoothing vessel arrivals to maintain port handling efficiency. Since prolonged waiting times and lower operational efficiency can also adversely affect their own fleets (Jiang et al., 2017), such firms have strong incentives to internalize the impact of GPR shocks. Therefore, we hypothesize that ports with higher market concentration, typically dominated by a few major shipping lines, are better equipped to absorb or mitigate the negative effects of geopolitical risk on emissions than more fragmented ports. To empirically test this hypothesis, we calculate the monthly Herfindahl-Hirschman Index (HHI) for each port, based on the market share of shipping lines calling at the port, as a proxy for port-level market concentration.

To capture heterogeneity related to port characteristics, we divide the sample into different groups according to the median of average ship DWT and market concentration ($PortHHI$) and perform subgroup regressions, respectively. The results are presented in Tables 4.5 and 4.6.

From Table 4.5, it can be seen that the coefficient of GPR in the group with a lower average ship DWT is insignificant, and that of GPR in the group with a higher average ship DWT is positive and significant at 5% level. This result suggests that geopolitical uncertainty may have a stronger effect for larger fleet sailing along international routes, while ports

that mainly accommodate smaller, regionally operating ships exhibit no significant emission response to changes in GPR, possibly due to lower exposure to international disruptions.

Table 4.6 demonstrates the sub-group regression results based on the median value of $PortHHI$. In Column (1), the coefficient of $PortHHI$ is negative and statistically significant at 1% level, indicating that a higher market concentration level may lower the average emission levels through more organized arrival schedules and increase the port efficiency. Columns (2) and (3) demonstrate that GPR has a stronger and more significant effect on average port emission in the group with a $PortHHI$ below the median level compared to that in the group with a $PortHHI$ above the median level. This finding supports our hypothesis that dominant carriers at concentrated ports are more responsive to geopolitical uncertainties. These carriers may proactively adjust their ship schedules or redistribute port calls to mitigate operational disruptions, which in turn leads to a lower increase in emissions.

Table 4.5: Heterogeneity test: the impact of ship DWT

	(1)	(2)
	$LnAvgCO_2$	
	$AvgDWT < 50th$	$AvgDWT > 50th$
L.LnAvgCO_2	0.065***	0.104***
	(0.020)	(0.022)
L.GPR	0.024	0.032**
	(0.017)	(0.015)
LnAvgDWT	1.131***	1.055***
	(0.034)	(0.051)
Constant	4.490	10.171
	(23.247)	(21.434)
Controls	Y	Y
Observations	12,633	12,610
AR(1) p-value	0.000	0.000
AR(2) p-value	0.465	0.704
Hansen test	2.917	5.533
Hansen p-value	0.572	0.237
Time FE	Y	Y

Note: Robust standard errors in parentheses. * $p < 0.10$, ** $p < 0.05$, *** $p < 0.01$.
The median value of average ship DWT visiting the port in a month is 37,528 tonnes.

Table 4.6: Heterogeneity test: the impact of market concentration level

	(1)	(2)	(3)
		$LnAvgCO_2$	
		$PortHHI <$ 50th	$PortHHI >$ 50th
L.LnAvgCO_2	0.077***	0.114***	0.070***
	(0.015)	(0.022)	(0.017)
L.GPR	0.024**	0.031**	0.026*
	(0.012)	(0.015)	(0.015)
PortHHI	-0.498***	-0.414	-0.476***
	(0.070)	(1.708)	(0.090)
Constant	8.654	-18.655	38.131*
	(9.210)	(28.058)	(20.739))
Controls	Y	Y	Y
Observations	25,243	12,677	12,566
AR(1) p-value	0.000	0.000	0.000
AR(2) p-value	0.419	0.302	0.584
Hansen test	6.322	1.591	5.495
Hansen p-value	0.176	0.810	0.240
Time FE	Y	Y	Y

Note: Robust standard errors in parentheses. * $p < 0.10$, ** $p < 0.05$, *** $p < 0.01$.

The median value of monthly HHI at the port is approximately 0.042. Column (1) presents the results with $PortHHI$ as a control variable; Columns (2) and (3) show sub-group regressions for low and high concentration ports, respectively.

4.4.5 Robustness test

To test the robustness of our baseline results, we re-estimate the model using a fixed effects specification and aggregate the data to the country or regional level. The corresponding results are reported in Table 4.7. Column (1) shows the results using the fixed effect model, and Column (2) shows the results at the country- or region- level. Both the coefficients of GPR are positive and statistically significant, which is in line with the baseline model, indicating the robustness of our initial findings.

Table 4.7: Robustness test

	(1)	(2)
		$LnAvgCO_2$
	FE Model	Country/Region Level
L.LnAvgCO_2	0.205***	0.099***
	(0.008)	(0.024)
L.GPR	0.015***	0.081*
	(0.003)	(0.043)
Constant	8.084***	-19.423
	(0.564)	(94.710)
Controls	Y	Y
Observations	25,243	1,775
AR(1) p-value		0.000
AR(2) p-value		0.131
Hansen test		1.306
Hansen p-value		0.860
Port FE	Y	
Time FE	Y	Y

Note: Robust standard errors are in parentheses. * $p < 0.10$, ** $p < 0.05$, *** $p < 0.01$.

4.5 Discussion and policy implications

This section first discusses the main findings, followed by an analysis of the policy implications.

4.5.1 Discussions

First, our baseline regression results indicate that GPR significantly increases carbon emissions at ports. This finding is consistent with previous studies on the environmental im-

plications of geopolitical instability. For instance, Paramati et al. (2025) found that GPR is positively associated with country-level carbon emissions. This direct effect can be explained by the fact that geopolitical tensions often undermine international relationships (Caldara and Iacoviello, 2022), which is essential for achieving climate goals. When the global political environment deteriorates, countries may reduce investments in environmental protection or delay the implementation of climate-related initiatives. In such contexts, environmental regulations may be deprioritized or weakened, crowding out effective climate action (Paramati et al., 2025). At the port level, environmental management also depends on stable international trade relations and institutional coordination. The uncertainty and insecurity induced by GPR can disrupt these mechanisms, making it more difficult for port authorities to maintain or enforce green operational standards. This may further explain the observed increase in port-level emissions during periods of heightened geopolitical tensions.

Second, the mechanism test further provides evidence of an indirect effect of GPR on port-level carbon emissions through its disruption of ship arrival schedules. We use variation in ship arrival times as a proxy for schedule stability and find that higher levels of GPR are associated with greater variability, indicating increased schedule instability. For instance, Yang et al. (2025) examined the resilience of global shipping alliances during the Red Sea crisis and found that, post-crisis, schedule reliability declined for the three major alliances (2M, Ocean Alliance, and THE Alliance) and ten representative carriers. In their study, schedule reliability was measured by the average on-time arrival rate of vessels. The uncertainty in arrival times, driven by rerouting, cancellations, and rescheduling in response to heightened GPR, can compromise the efficiency of berth allocation and extend service times at port (Wang and Guo, 2018). These disruptions reduce the efficiency of cargo loading and unloading, prolong the duration of vessel stays, and ultimately increase port-level carbon emissions (Rødseth et al., 2018; Wang et al., 2022).

Furthermore, we conducted two heterogeneous tests by examining how average ship DWT and market concentration level moderate the impact of GPR on port carbon emissions. First, we identified that emissions in ports serving larger container ships are more affected by geopolitical tensions. This is likely because large vessels typically operate on long-haul, international trade routes that travel through politically sensitive chokepoints, such as the Suez Canal. This finding carries important policy implications for port authorities. Ports that predominantly serve large container vessels on long-haul routes should proactively adjust their environmental management strategies in response to GPR. For example, resilience planning, such as increasing buffer capacity in yard operations and deploying low-emission auxiliary equipment during high-uncertainty periods, could help mitigate carbon emission surges associated with ship congestion or rescheduling caused by geopolitical events. Ad-

ditionally, we find that a higher market concentration level can mitigate the adverse effect of geopolitical risk on port carbon emissions. This result is likely driven by the internalization behaviour of dominant shipping lines (Jiang et al., 2017). Similar patterns have been documented in the aviation industry, where a higher market concentration leads to fewer delays, as major carriers coordinate flight schedules to reduce congestion (Brueckner, 2002; Mayer and Sinai, 2003). Applying this logic to ports, dominant shipping lines may voluntarily adjust their fleet arrival schedules to minimize operational disruptions and reduce berthing time, which in turn lowers carbon emissions. Our findings suggest that the market structure at the port level plays a critical role in buffering the environmental consequences of geopolitical uncertainties.

4.5.2 Policy implications

In this sub-section, we aim to answer our last research question: *what are the implications of these findings for designing effective port-level carbon abatement policies?* First, our main results highlight the adverse impact of heightened GPR on port-level carbon emissions, which underscores the need for international organizations, such as the International Maritime Organization (IMO), to incorporate geopolitical instability into the design of emission reduction policies. Traditional decarbonization frameworks often assume stable global shipping networks, however, our findings suggest that environmental policy resilience under external shocks must be explicitly considered as it can lead to significant changes in emissions.

Second, building on our heterogeneity tests, we further develop a $2 * 2$ matrix dividing ports into different categories based on their features that may affect the impact of GPR on carbon emissions, which is presented in Figure 4.5. These characteristics shape the extent to which operational decisions are potentially dominated by shipping lines, coordinated by port authorities, or require joint efforts, and they lay the groundwork for understanding ports' heterogeneous responses to the GPR index. It considers that port characteristics influence the adoption and effectiveness of emission reduction measures (Sornn-Friese et al., 2021), and that accounting for such structural factors is essential for designing effective mitigation policies.

Short-sea ports refer to ports with higher market concentration and smaller average vessel sizes, typically dominated by a few carriers serving frequent regional or short-haul routes. These ports are generally less affected by GPR, as major carriers with substantial market shares can internalize external shocks by adjusting vessel schedules directly. The impact of GPR on port carbon emissions is therefore easier to abate, given the relatively low coordi-

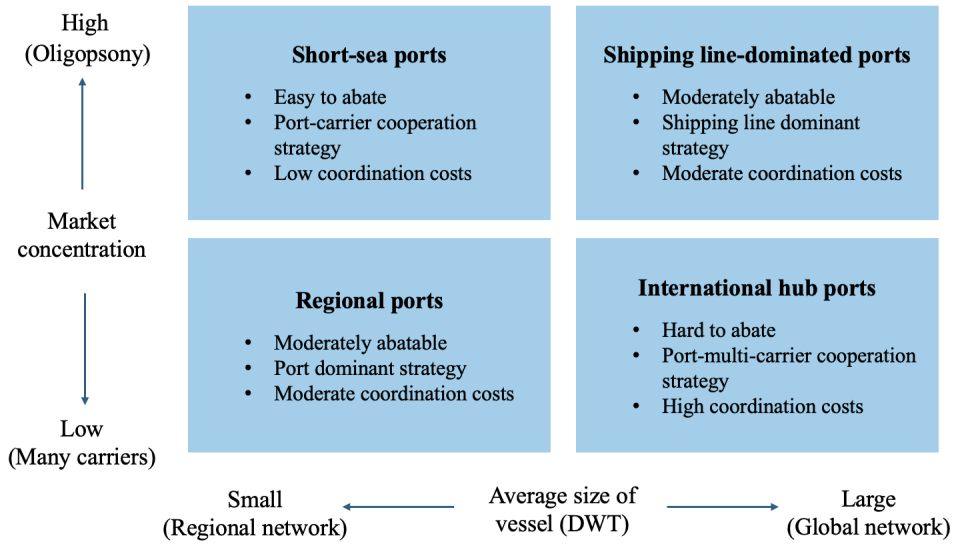

Figure 4.5: Port classification by average vessel size and market concentration

nation costs between multi-stakeholders. To further mitigate the carbon impact of GPR, it is recommended that port authorities and dominant carriers establish joint monitoring mechanisms for geopolitical disruptions and proactively adjust berthing windows or sailing speeds. Taking advantage of the low coordination costs to reduce emissions arising from arrival uncertainty.

Regional ports typically serve short-haul routes with smaller vessels and exhibit low market concentration. Due to their fragmented market structure and limited administrative capacity, these ports can struggle to effectively absorb disruptions caused by GPR. The presence of many small-scale shipping lines also makes coordinated response efforts more challenging. Therefore, port authorities should take a leading role in managing vessel scheduling and infrastructure planning. Specific measures include investing in green and smart infrastructure, such as smart queuing systems, and alternative fuelling capacity (e.g., shore power), and strengthening institutional capacity to govern diverse users.

Shipping line-dominated hubs are ports that serve large vessels and exhibit high market concentration, often controlled operationally by a few major carriers. These ports are sensitive to geopolitical risks, as their role in global mainline services means that any disruption, such as rerouting or delay, can propagate across a tightly scheduled network. Although the limited number of carriers enables some level of coordination, the operational complexity due to vessel size and long-haul planning increases the risk of irregular schedules and associated emissions. In this context, dominant shipping lines should take primary responsibility for mitigating GPR-induced emissions, including by adjusting sailing speeds, sequencing arrivals, and coordinating arrival windows. Port authorities can play a supporting role by

facilitating information exchange and providing flexible berth allocation.

International hub ports are globally connected ports that handle large vessels across a wide range of carriers. The low concentration of market power results in decentralized scheduling, which poses coordination challenges when GPR disrupts route reliability. These ports are particularly vulnerable to vessel arrival uncertainties, leading to lower operational efficiency and elevated emissions. Emission abatement at international hub ports can be particularly challenging due to the complexity of multi-carrier operations, and the irregularity of port calls (Styhre et al., 2017). We recommend a port–multi-carrier cooperation strategy, in which ports and carriers jointly establish cooperative scheduling platforms or information-sharing agreements. These tools should enable real-time data sharing on vessel schedules, berth availability, and port congestion, thereby supporting more responsive and adaptive scheduling under GPR-induced disruptions.

4.6 Conclusion

This study provides novel empirical evidence on the environmental consequences of geopolitical risk in the context of maritime logistics, a critical yet underexplored dimension in both environmental economics and maritime literature. By leveraging high-frequency vessel activity data and port-level carbon emission estimates, we find that geopolitical tensions significantly exacerbate emissions at ports. One potential mechanism is the disruption of vessel arrival schedules, which reduces handling efficiency and prolongs operational time at berth, thereby elevating port-level emissions. These findings reveal that geopolitical shocks not only disrupt global shipping networks but also create hidden environmental costs through operational inefficiencies at the port level. Our heterogeneity analyses further demonstrate that port characteristics play a pivotal role in moderating these effects. Ports serving larger ships are more susceptible to emission surges due to long international shipping distances are more exposure to geopolitical events, whereas concentrated markets, dominated by major carriers, exhibit greater resilience, likely due to better coordination of dominant shipping lines. These insights enrich the empirical understanding of how geopolitical uncertainty propagates through supply chains to influence local environmental outcomes. Going forward, policies aimed at maritime decarbonization must move beyond static emission targets and incorporate dynamic, risk-sensitive governance tools. This will be essential for building a more resilient and environmentally sustainable global shipping system in an increasingly uncertain world.

Last but not least, the findings of this study should be interpreted with caution due to several limitations. First, the emission data used in this study are restricted to CO_2

emissions from ship activities at berth, which may underestimate the total environmental footprint of port operations. Other emission sources, such as cargo handling equipment, yard trucks, and terminal power consumption, are not included due to data limitations. Second, the GPR index employed in this study is an aggregate measure that does not distinguish between different types of geopolitical events, such as armed conflict, trade sanctions, or diplomatic breakdowns. However, these events may influence port emissions through distinct mechanisms and magnitudes. Future research could address these limitations by integrating comprehensive port-level emission inventories and examining disaggregated geopolitical shocks to better capture their heterogeneous environmental impacts.

Chapter 5

Summary and Future Research

5.1 Summary

This dissertation investigates the vulnerability and sustainability of global container ports under three major types of disruptions: port congestion, natural disasters, and geopolitical tensions. By using high-frequency vessel movement data from the AIS Database, this study develops empirical frameworks to measure port performance under stress and identify the structural factors that shape port-level responses to disruptions.

The first chapter demonstrates that the higher market concentration is associated with lower waiting times at terminals due to internalization of dominant carriers, yet this effect is conditional on berthing priority provisions. The presence of berthing priority may dampen the internalization incentives of dominant carriers, potentially exacerbating terminal inefficiencies. The second chapter develops a vulnerability index to assess ports' ability to rebound from natural disaster-induced shocks, showing that port infrastructure, hinterland industrial diversity, and connectivity significantly enhance port resilience. The findings further indicate that resilience drivers differ by region and disaster type, suggesting the need for context-specific resilience strategies. The third chapter explores the environmental impacts of geopolitical disruptions, finding that rising geopolitical tensions increase port-level carbon emissions by disrupting vessel arrival schedules and prolonging time at berth. Ports serving larger vessels are particularly vulnerable to such shocks, while those with concentrated carrier markets show greater adaptive capacity due to more coordinated operations.

Together, these findings advance our understanding of port resilience from a multidimensional perspective, bridging research across maritime economics, disaster risk management, and environmental governance. The dissertation highlights the importance of structural port characteristics in shaping operational outcomes and calls for differentiated policy approaches tailored to regional capacities and specific disruption types. Importantly, it also uncovers a

previously underexplored link between geopolitical risk and port-level emissions, contributing new insights to the maritime decarbonization debate.

5.2 Future Research

Building on the findings of this dissertation, several promising directions for future research emerge. First, future research could assess the generality and adaptability of the analytical frameworks and models developed in this dissertation to other types of global and regional shocks that threaten maritime transport systems, such as the Suez Canal blockage or the Baltimore bridge collapse. Second, while this study examines disruptions individually, future work could investigate the interaction effects between different types of shocks, such as how extreme weather events may amplify congestion or how geopolitical tensions compound the effects of infrastructure failures. Integrated risk frameworks may offer valuable tools for capturing such compound disruptions. Third, given the interconnected nature of maritime logistics, it would be valuable to move beyond the port level and focus on port communities or clusters defined by shared shipping routes, shipping lines, or regional proximity. Understanding how disruptions at one port propagate through regional or global shipping networks would enhance our ability to model systemic risks and develop coordinated mitigation strategies. Finally, future studies could simulate the effects of targeted policy interventions, such as infrastructure investments, digitalization initiatives, improved coordination protocols, or carbon pricing mechanisms, on port performance under disruption scenarios. Such analyses would not only validate the empirical findings presented in this dissertation but also provide practical insights for policymakers aiming to build a more adaptive, resilient, and environmentally sustainable maritime transport system.

Bibliography

L. Alfaro and D. Chor. Global supply chains: The looming "great reallocation". Technical report, National Bureau of Economic Research, 2023.

H. Allcott and D. Keniston. Dutch disease or agglomeration? the local economic effects of natural resource booms in modern america. *The Review of Economic Studies*, 85(2): 695–731, 2018.

M. K. Anser, Q. R. Syed, and N. Apergis. Does geopolitical risk escalate co2 emissions? evidence from the brics countries. *Environmental Science and Pollution Research*, 28(35): 48011–48021, 2021.

M. Arellano and S. Bond. Some tests of specification for panel data: Monte carlo evidence and an application to employment equations. *The review of economic studies*, 58(2):277–297, 1991.

N. T. Argon and S. Ziya. Priority assignment under imperfect information on customer type identities. *Manufacturing & Service Operations Management*, 11(4):674–693, 2009.

I. Ater. Internalization of congestion at us hub airports. *Journal of Urban Economics*, 72 (2-3):196–209, 2012.

X. Bai, L. Cheng, D. Yang, and O. Cai. Does the traffic volume of a port determine connectivity? revisiting port connectivity measures with high-frequency satellite data. *Journal of Transport Geography*, 102:103385, 2022.

X. Bai, Z. Ma, Y. Hou, Y. Li, and D. Yang. A data-driven iterative multi-attribute clustering algorithm and its application in port congestion estimation. *IEEE Transactions on Intelligent Transportation Systems*, 2023a.

X. Bai, Z. Ma, and Y. Zhou. Data-driven static and dynamic resilience assessment of the global liner shipping network. *Transportation Research Part E: Logistics and Transportation Review*, 170:103016, 2023b.

C. Baker, R. Teasley, L. B. Davis, and X. Qu. A dynamic decision model for port hurricane preparation and shutdown. In *IIE Annual Conference. Proceedings*, page 1. Institute of Industrial and Systems Engineers (IISE), 2012.

R. Baptista and P. Swann. Do firms in clusters innovate more? *Research policy*, 27(5): 525–540, 1998. ISSN 0048-7333.

A. Barkley and K. Mcleod. Congestion and consolidation: An empirical study of a barge shipping merger. *Regional Science and Urban Economics*, 93:103725, 2022.

H. Baroud, K. Barker, J. E. Ramirez-Marquez, et al. Importance measures for inland waterway network resilience. *Transportation research part E: logistics and transportation review*, 62:55–67, 2014.

S. Barrett. Self-enforcing international environmental agreements. *Oxford economic papers*, 46(Supplement_1):878–894, 1994.

BBC. Canada wildfire: Evacuees flee yellowknife as fire nears northern city, 2023. URL `https://www.bbc.com/news/world-us-canada-66526554`. Accessed: 2025-07-18.

D. Black, T. McKinnish, and S. Sanders. The economic impact of the coal boom and bust. *The Economic Journal*, 115(503):449–476, 2005.

N. Bloom, S. Bond, and J. Van Reenen. Uncertainty and investment dynamics. *The review of economic studies*, 74(2):391–415, 2007.

Bloomberg. 41 us ports from new jersey to alaska win $653 million in funds. `https://www.bloomberg.com/news/articles/2023-11-03/41-us-ports-from-new-jersey-to-alaska-win-653-million-in-funds`, 2023. Accessed: 2025-07-19.

R. Blundell and S. Bond. Initial conditions and moment restrictions in dynamic panel data models. *Journal of econometrics*, 87(1):115–143, 1998.

V. Bove, G. Efthyvoulou, and A. Navas. Political cycles in public expenditure: Butter vs guns. *Journal of Comparative Economics*, 45(3):582–604, 2017.

P. Brenton, I. Gillson, and P. Sauvé. Economic diversification: Lessons from practice. In *Aid for Trade at a Glance 2019: Economic Diversification and Empowerment*, pages 135–160. World Trade Organization and OECD, Geneva, Switzerland, 2019.

L. Brown and R. T. Greenbaum. The role of industrial diversity in economic resilience: An empirical examination across 35 years. *Urban Studies*, 54(6):1347–1366, 2017. ISSN 0042-0980.

J. K. Brueckner. Airport congestion when carriers have market power. *American Economic Review*, 92(5):1357–1375, 2002.

J. K. Brueckner. Internalization of airport congestion: A network analysis. *International Journal of Industrial Organization*, 23(7-8):599–614, 2005.

J. K. Brueckner. Price vs. quantity-based approaches to airport congestion management. *Journal of Public Economics*, 93(5-6):681–690, 2009.

J. K. Brueckner and K. Van Dender. Atomistic congestion tolls at concentrated airports? seeking a unified view in the internalization debate. *Journal of Urban Economics*, 64(2): 288–295, 2008.

D. Caldara and M. Iacoviello. Measuring geopolitical risk. *American economic review*, 112 (4):1194–1225, 2022.

D. Caldara, S. Conlisk, M. Iacoviello, and M. Penn. Do geopolitical risks raise or lower inflation. *Federal Reserve Board of Governors*, 2024.

M. Campo, H. Mayer, and J. Rovito. Supporting secure and resilient inland waterways: evaluating off-loading capabilities at terminals during sudden catastrophic closures. *Transportation research record*, 2273(1):10–17, 2012.

X. Cao and J. S. L. Lam. Simulation-based severe weather-induced container terminal economic loss estimation. *Maritime Policy & Management*, 46(1):92–116, 2019.

T. Cavalcanti, D. Da Mata, and F. Toscani. Winning the oil lottery: The impact of natural resource extraction on growth. *Journal of Economic Growth*, 24(1):79–115, 2019.

CBRE. 2022 global seaport review: Singapore. `https://www.cbre.com/insights/local-response/2022-global-seaport-review-singapore`, 2022. Accessed: 2025-07-18.

H. Chen, K. Cullinane, and N. Liu. Developing a model for measuring the resilience of a port-hinterland container transportation network. *Transportation Research Part E: Logistics and Transportation Review*, 97:282–301, 2017.

H. Chen, J. S. L. Lam, and N. Liu. Strategic investment in enhancing port–hinterland container transportation network resilience: A network game theory approach. *Transportation Research Part B: Methodological*, 111:83–112, 2018.

L. Chen, G. Gozgor, C. K. M. Lau, M. K. Mahalik, K. N. Rather, and A. M. Soliman. The impact of geopolitical risk on co2 emissions inequality: Evidence from 38 developed and developing economies. *Journal of Environmental Management*, 349:119345, 2024.

CNN. What's wrong with America's supply chains. `https://amp.cnn.com/cnn/2021/10/25/business/supply-chain-ports-inflation`, 2021. Accessed: 2024-04-07.

A. Cobham. Priority assignment in waiting line problems. *Journal of the Operations Research Society of America*, 2(1):70–76, 1954.

D. R. Cox and W. L. Smith. *Queues*. Methuen & Co. Ltd., London, 1961.

J. I. Daniel. Congestion pricing and capacity of large hub airports: A bottleneck model with stochastic queues. *Econometrica: Journal of the Econometric Society*, pages 327–370, 1995.

J. I. Daniel and K. T. Harback. (when) do hub airlines internalize their self-imposed congestion delays? *Journal of Urban Economics*, 63(2):583–612, 2008.

Y. Ding, E. Park, M. Nagarajan, and E. Grafstein. Patient prioritization in emergency department triage systems: An empirical study of the canadian triage and acuity scale (ctas). *Manufacturing & Service Operations Management*, 21(4):723–741, 2019.

A. K. Dixit and R. S. Pindyck. *Investment under uncertainty*. Princeton university press, 1994.

C. Ducruet and T. Notteboom. The worldwide maritime network of container shipping: spatial structure and regional dynamics. *Global networks*, 12(3):395–423, 2012.

C. Ducruet, H. Itoh, and O. Merk. Time efficiency at world container ports. International Transport Forum Discussion Paper, 2014.

H. Dui, X. Zheng, and S. Wu. Resilience analysis of maritime transportation systems based on importance measures. *Reliability Engineering & System Safety*, 209:107461, 2021.

R. Duncan McIntosh and A. Becker. Seaport climate vulnerability assessment at the multi-port scale: A review of approaches. *Resilience and risk: Methods and application in environment, cyber and social domains*, pages 205–224, 2017.

A. Eraydin. Attributes and characteristics of regional resilience: Defining and measuring the resilience of turkish regions. *Regional Studies*, 50(4):600–614, 2016.

D. Fan, P. Ma, L. Cui, and D. W. Yiu. Locking in overseas buyers amid geopolitical conflicts. *Journal of Operations Management*, 70(5):756–792, 2024.

N. Farhadi, S. A. Parr, K. N. Mitchell, and B. Wolshon. Use of nationwide automatic identification system data to quantify resiliency of marine transportation systems. *Transportation Research Record*, 2549(1):9–18, 2016. ISSN 0361-1981.

J. Feyrer. Distance, trade, and income—the 1967 to 1975 closing of the suez canal as a natural experiment. *Journal of Development Economics*, 153:102708, 2021.

J. Feyrer, E. T. Mansur, and B. Sacerdote. Geographic dispersion of economic shocks: Evidence from the fracking revolution. *American Economic Review*, 107(4):1313–1334, 2017.

Financial Times. Record-breaking imports lead to congestion at the port of los angeles. `https://www.ft.com/content/eb21056b-5773-422a-ab78-92e59cddc1b5`, 2020. Accessed: 2025-07-18.

FinancialTimes. Ports face biggest crisis since start of container shipping. Retrieved from `https://www.ft.com/content/10e71eff-e59c-46fb-a9aa-a480bc86c093`, 2021. Accessed: 2025-01-02.

R. Fisman and J. Svensson. Are corruption and taxation really harmful to growth? firm level evidence. *Journal of development economics*, 83(1):63–75, 2007.

C. Flint. *Introduction to geopolitics*. Routledge, 2021.

F. Flouros, V. Pistikou, and V. Plakandaras. Geopolitical risk as a determinant of renewable energy investments. *Energies*, 15(4):1498, 2022.

L. C. Freeman et al. Centrality in social networks: Conceptual clarification. *Social network: critical concepts in sociology. Londres: Routledge*, 1:238–263, 2002.

G. C. Gallopín. Linkages between vulnerability, resilience, and adaptive capacity. *Global environmental change*, 16(3):293–303, 2006.

S. Gavirneni and V. G. Kulkarni. Self-selecting priority queues with burr distributed waiting costs. *Production and Operations Management*, 25(6):979–992, 2016.

E. L. Glaeser, H. D. Kallal, J. A. Scheinkman, and A. Shleifer. Growth in cities. *Journal of political economy*, 100(6):1126–1152, 1992.

N. P. Gleditsch, P. Wallensteen, M. Eriksson, M. Sollenberg, and H. Strand. Armed conflict 1946-2001: A new dataset. *Journal of peace research*, 39(5):615–637, 2002.

M. M. Golias, M. Boile, and S. Theofanis. Berth scheduling by customer service differentiation: A multi-objective approach. *Transportation Research Part E: Logistics and Transportation Review*, 45(6):878–892, 2009.

X. Gou and J. S. L. Lam. Risk analysis of marine cargoes and major port disruptions. *Maritime Economics & Logistics*, 21(4):497–523, 2019.

A. Grigoriadis, S. Mamarikas, and L. Ntziachristos. Quantitative impact of decarbonization options on air pollutants from different ship types. *Transportation Research Part D: Transport and Environment*, 133:104316, 2024.

B. Gu and J. Liu. Port resilience analysis based on the hhm-fcm approach under covid-19. *Ocean & Coastal Management*, 243:106741, 2023.

B. Gu and J. Liu. A systematic review of resilience in the maritime transport. *International Journal of Logistics Research and Applications*, pages 1–22, 2024.

B. Gu, J. Liu, X. Ye, Y. Gong, and J. Chen. Data-driven approach for port resilience evaluation. *Transportation Research Part E: Logistics and Transportation Review*, 186: 103570, 2024.

M. Guffanti, G. C. Mayberry, T. J. Casadevall, and R. Wunderman. Volcanic hazards to airports. *Natural Hazards*, 51:287–302, 2009.

H. Guo, C. Jiang, and Y. Wan. Can airfares tell? an alternative empirical strategy for airport congestion internalization. *Transportation Research Part A: Policy and Practice*, 118:648–661, 2018.

R. Haji and G. F. Newell. Optimal strategies for priority queues with nonlinear costs of delay. *SIAM Journal on Applied Mathematics*, 20(2):224–240, 1971.

L. P. Hansen. Large sample properties of generalized method of moments estimators. *Econometrica: Journal of the econometric society*, pages 1029–1054, 1982.

H. E. Haralambides, P. Cariou, and M. Benacchio. Costs, benefits and pricing of dedicated container terminals. *International Journal of Maritime Economics*, 4(1):21–34, 2002.

D. Henry and J. E. Ramirez-Marquez. Generic metrics and quantitative approaches for system resilience as a function of time. *Reliability Engineering System Safety*, 99:114–122, 2012. ISSN 0951-8320.

C. S. Holling. Resilience and stability of ecological systems. *Annual review of ecology and systematics*, 4(1):1–23, 1973.

N. U. I. Hossain, F. Nur, S. Hosseini, R. Jaradat, M. Marufuzzaman, and S. M. Puryear. A bayesian network based approach for modeling and assessing resilience: A case study of a full service deep water port. *Reliability Engineering & System Safety*, 189:378–396, 2019.

S. Hosseini and K. Barker. Modeling infrastructure resilience using bayesian networks: A case study of inland waterway ports. *Computers & Industrial Engineering*, 93:252–266, 2016.

A. I. Hunjra, M. Azam, P. Verhoeven, D. Taskin, and J. Dai. The impact of geopolitical risk, institutional governance and green finance on attaining net-zero carbon emission. *Journal of Environmental Management*, 359:120927, 2024.

F. Huq, K. S. Pawar, and N. Subramanian. Disturbances to the supply chains of high-value manufacturing firms: comparison of the perceptions of product managers and supply chain managers. *International Journal of Production Research*, 59(13):3916–3934, 2021.

A. Imai, E. Nishimura, and S. Papadimitriou. Berth allocation with service priority. *Transportation Research Part B: Methodological*, 37(5):437–457, 2003.

IMO. Fourth imo greenhouse gas study, 2020.

E. Irannezhad, C. G. Prato, and M. Hickman. The effect of cooperation among shipping lines on transport costs and pollutant emissions. *Transportation Research Part D: Transport and Environment*, 65:312–323, 2018.

C. Izaguirre, I. J. Losada, P. Camus, J. L. Vigh, and V. Stenek. Climate change risk to global port operations. *Nature Climate Change*, 11(1):14–20, 2021.

O. Izraeli and K. J. Murphy. The effect of industrial diversity on state unemployment rate and per capita income. *The Annals of Regional Science*, 37:1–14, 2003. ISSN 0570-1864.

H. Jia, R. Adland, V. Prakash, and T. Smith. Energy efficiency with the application of virtual arrival policy. *Transportation Research Part D: Transport and Environment*, 54: 50–60, 2017.

C. Jiang, Y. Wan, and A. Zhang. Internalization of port congestion: strategic effect behind shipping line delays and implications for terminal charges and investment. *Maritime Policy & Management*, 44(1):112–130, 2017.

L. Johansson, J.-P. Jalkanen, and J. Kukkonen. Global assessment of shipping emissions in 2015 on a high spatial and temporal resolution. *Atmospheric Environment*, 167:403–415, 2017.

F. Kleibergen and R. Paap. Generalized reduced rank tests using the singular value decomposition. *Journal of econometrics*, 133(1):97–126, 2006.

D. A. Kroodsma, J. Mayorga, T. Hochberg, N. A. Miller, K. Boerder, F. Ferretti, A. Wilson, B. Bergman, T. D. White, B. A. Block, et al. Tracking the global footprint of fisheries. *Science*, 359(6378):904–908, 2018.

V. Latora, V. Nicosia, and G. Russo. *Complex networks: principles, methods and applications*. Cambridge University Press, 2017.

C.-C. Lee and C.-W. Wang. Firms' cash reserve, financial constraint, and geopolitical risk. *Pacific-Basin Finance Journal*, 65:101480, 2021.

F. León-Mateos, A. Sartal, L. López-Manuel, and M. A. Quintas. Adapting our sea ports to the challenges of climate change: Development and validation of a port resilience index. *Marine Policy*, 130:104573, 2021.

R. Li, Q. Wang, and J. Guo. Revisiting the environmental kuznets curve (ekc) hypothesis of carbon emissions: exploring the impact of geopolitical risks, natural resource rents, corrupt governance, and energy intensity. *Journal of Environmental Management*, 351: 119663, 2024a.

S. Li, J. Wu, Y. Jiang, and X. Yang. Impacts of the sea-rail intermodal transport policy on carbon emission reduction: The china case study. *Transport Policy*, 158:211–223, 2024b.

W. Li, A. Asadabadi, and E. Miller-Hooks. Enhancing resilience through port coalitions in maritime freight networks. *Transportation Research Part A: Policy and Practice*, 157: 1–23, 2022.

X. Li, Y. Zhao, P. Cariou, and Z. Sun. The impact of port congestion on shipping emissions in chinese ports. *Transportation Research Part D: Transport and Environment*, 128:104091, 2024c.

Z. Li, Y. Zhang, and B. Wang. Prediction of port recovery time after a severe storm project. Manuscript or project report, 2023.

X. Lin, X. Pu, and X. Bai. On the efficiency impacts of berthing priority provision. *Transportation Science*, 2024.

I. Linkov, T. Bridges, F. Creutzig, J. Decker, C. Fox-Lent, W. Kröger, J. H. Lambert, A. Levermann, B. Montreuil, J. Nathwani, et al. Changing the resilience paradigm. *Nature climate change*, 4(6):407–409, 2014.

H. Liu, M. Fu, X. Jin, Y. Shang, D. Shindell, G. Faluvegi, C. Shindell, and K. He. Health and climate impacts of ocean-going vessels in east asia. *Nature climate change*, 6(11): 1037–1041, 2016.

J. Liu, B. Gu, and J. Chen. Enablers for maritime supply chain resilience during pandemic: An integrated mcdm approach. *Transportation Research Part A: Policy and Practice*, 175: 103777, 2023a.

Q. Liu, Y. Yang, A. K. Ng, and C. Jiang. An analysis on the resilience of the european port network. *Transportation Research Part A: Policy and Practice*, 175:103778, 2023b.

D. Lyu, P. Zhao, W. Zhu, W. Li, Y. Ling, L. Pang, S. Zhang, and Y. Xu. Impact of russia–ukraine conflict on global crude oil shipping carbon emissions. *Journal of Transport Geography*, 128:104311, 2025.

E. E. Malizia and S. Ke. The influence of economic diversity on unemployment and stability. *Journal of Regional Science*, 33(2):221–235, 1993. ISSN 0022-4146.

A. Mandelbaum and A. L. Stolyar. Scheduling flexible servers with convex delay costs: Heavy-traffic optimality of the generalized cμ-rule. *Operations Research*, 52(6):836–855, 2004.

C. Mayer and T. Sinai. Network effects, congestion externalities, and air traffic delays: Or why not all delays are evil. *American Economic Review*, 93(4):1194–1215, 2003.

D. J. McCauley, P. Woods, B. Sullivan, B. Bergman, C. Jablonicky, A. Roan, M. Hirshfield, K. Boerder, and B. Worm. Ending hide and seek at sea. *Science*, 351(6278):1148–1150, 2016.

S. T. McColl. Landslide causes and triggers. In *Landslide Hazards, Risks, and Disasters*, pages 13–41. Elsevier, 2022.

Q. Meng and S. Wang. Optimal operating strategy for a long-haul liner service route. *European Journal of Operational Research*, 215(1):105–114, 2011. ISSN 0377-2217. doi: https://doi.org/10.1016/j.ejor.2011.05.057.

I. Milchtaich. Internalization of social cost in congestion games. *Economic Theory*, 71: 717–760, 2021.

K. Mizuno, F. Mizutani, and N. Nakayama. Industrial diversity and metropolitan unemployment rate. *The Annals of Regional Science*, 40:157–172, 2006. ISSN 0570-1864.

D. S.-H. Moon and J. K. Woo. The impact of port operations on efficient ship operation from both economic and environmental perspectives. *Maritime Policy & Management*, 41 (5):444–461, 2014.

H. Moradlou, H. Reefke, H. Skipworth, and S. Roscoe. Geopolitical disruptions and the manufacturing location decision in multinational company supply chains: a delphi study on brexit. *International Journal of Operations & Production Management*, 41(2):102–130, 2021.

S. A. Morrison and C. Winston. Another look at airport congestion pricing. *American Economic Review*, 97(5):1970–1977, 2007.

N. Mou, H. Xu, Y. Liu, G. Li, L. Zhang, C. Ducruet, X. Zhang, Y. Wang, and T. Yang. Does the chinese coastal ports disruption affect the reliability of the maritime network? evidence from port importance and typhoon risk. *International Journal of Applied Earth Observation and Geoinformation*, 129:103846, 2024.

K. Müller, C. Xu, M. Lehbib, and Z. Chen. The global macro database: A new international macroeconomic dataset. Working Paper 33714, National Bureau of Economic Research, April 2025. URL `http://www.nber.org/papers/w33714`.

P. Nain. Interchange arguments for classical scheduling problems in queues. *Systems & control letters*, 12(2):177–184, 1989.

National Weather Service. Hurricane anatomy, 2024. URL `https://www.weather.gov/source/zhu/ZHU_Training_Page/tropical_stuff/hurricane_anatomy/hurricane_anatomy.html`. Accessed: 2025-07-18.

Natural Resources Canada. Magnitude of an earthquake, 2021. URL `https://www.earthquakescanada.nrcan.gc.ca/info-gen/scales-echelles/magnitude-en.php`. Accessed: 2025-07-18.

A. Nicita, V. Ognivtsev, M. Shirotori, et al. *Global supply chains: Trade and economic policies for developing countries*, volume 55. UN, 2013.

T. Notteboom. The relationship between seaports and the inter-modal hinterland in light of global supply chains. 2008. doi: doi:https://doi.org/10.1787/235371341338. URL `https://www.oecd-ilibrary.org/content/paper/235371341338`.

T. Notteboom and J.-P. Rodrigue. *Re-assessing port-hinterland relationships in the context of global commodity chains*, pages 67–82. Routledge, 2017. ISBN 1315246376.

T. Notteboom, T. Pallis, and J.-P. Rodrigue. Disruptions and resilience in global container shipping and ports: the covid-19 pandemic versus the 2008–2009 financial crisis. *Maritime Economics Logistics*, 23:179–210, 2021. ISSN 1479-2931.

T. Notteboom, A. Pallis, and J.-P. Rodrigue. *Port economics, management and policy*. Routledge, 2022.

T. Notteboom, G. Satta, L. Persico, B. Vottero, and A. Rossi. Operational productivity and financial performance of pure transhipment hubs versus gateway terminals: An empirical investigation on italian container ports. *Research in Transportation Business & Management*, 47:100967, 2023.

N. Olmer, B. Comer, B. Roy, X. Mao, and D. Rutherford. Greenhouse gas emissions from global shipping, 2013–2015 detailed methodology. *International Council on Clean Transportation: Washington, DC, USA*, pages 1–38, 2017.

M. Omer, A. Mostashari, R. Nilchiani, and M. Mansouri. A framework for assessing resiliency of maritime transportation systems. *Maritime Policy Management*, 39(7):685–703, 2012. ISSN 0308-8839.

H. Ouyang, N. Taník Argon, and S. Ziya. Assigning priorities (or not) in service systems with nonlinear waiting costs. *Management Science*, 68(2):1233–1255, 2022.

R. Pant, K. Barker, J. E. Ramirez-Marquez, and C. M. Rocco. Stochastic measures of resilience and their application to container terminals. *Computers Industrial Engineering*, 70:183–194, 2014. ISSN 0360-8352.

S. R. Paramati, M. Safiullah, and U. Soytas. Does geopolitical risk increase carbon emissions and public health risk? *Energy Economics*, page 108235, 2025.

E. Pels and E. T. Verhoef. The economics of airport congestion pricing. *Journal of Urban Economics*, 55(2):257–277, 2004.

H. Peng, M. Wang, and C. An. Implied threats of the red sea crisis to global maritime transport: amplified carbon emissions and possible carbon pricing dysfunction. *Environmental Research Letters*, 19(7):074053, 2024.

D. H. B. Phan, V. T. Tran, and B. N. Iyke. Geopolitical risk and bank stability. *Finance Research Letters*, 46:102453, 2022.

Philenews. Smoke from attica fires travelled 300km, 2024. URL `https://in-cyprus.philenews.com/international/smoke-from-attica-fires-travelled-300km/`. Accessed: 2025-07-18.

R. S. Pindyck. Irreversibility, uncertainty, and investment, 1990.

Port of NY & NJ. When it comes to container ships at anchor, looks are deceiving. `https://www.panynj.gov/port-authority/en/blogs/sea/when-it-comes-to-container-ships-at-anchor--looks-are-deceiving.html`, 2022. Accessed: 2025-07-18.

Y. Qin, J. Guo, M. Liang, and T. Feng. Resilience characteristics of port nodes from the perspective of shipping network: Empirical evidence from china. *Ocean & Coastal Management*, 237:106531, 2023.

R. Rhodes, C. Leiphardt, H. S. Young, J. Morten, B. Hayes, J. Dillon, W. Louttit, M. Powell, and D. J. McCauley. Investigation of a port queuing system on co2 emissions from container shipping. *Marine Pollution Bulletin*, 218:118151, 2025.

R. Robinson. Asian hub/feeder nets: the dynamics of restructuring. *Maritime Policy and Management*, 25(1):21–40, 1998.

K. L. Rødseth, P. B. Wangsness, and H. Schøyen. How do economies of density in container handling operations affect ships' time and emissions in port? evidence from norwegian container terminals. *Transportation Research Part D: Transport and Environment*, 59: 385–399, 2018.

K. L. Rødseth, P. B. Wangsness, H. Schøyen, and F. R. Førsund. Port efficiency and emissions from ships at berth: application to the norwegian port sector. *Maritime economics & logistics*, 22:585–609, 2020.

D. Roodman. How to do xtabond2: An introduction to difference and system gmm in stata. *The stata journal*, 9(1):86–136, 2009.

S. Roscoe, E. Aktas, K. J. Petersen, H. D. Skipworth, R. B. Handfield, and F. Habib. Redesigning global supply chains during compounding geopolitical disruptions: the role of supply chain logics. *International Journal of Operations & Production Management*, 42 (9):1407–1434, 2022.

L. Rousset and C. Ducruet. Disruptions in spatial networks: a comparative study of major shocks affecting ports and shipping patterns. *Networks and Spatial Economics*, 20(2): 423–447, 2020.

N. G. Rupp. Do carriers internalize congestion costs? empirical evidence on the internalization question. *Journal of Urban Economics*, 65(1):24–37, 2009.

H. Siebert. Environmental quality as a public good. In *Economics of the Environment: Theory and Policy*, pages 59–93. Springer, 1998.

H. E. Silva and E. T. Verhoef. Optimal pricing of flights and passengers at congested airports and the efficiency of atomistic charges. *Journal of Public Economics*, 106:1–13, 2013.

S. Singh, J. A. Van Mieghem, and I. Gurvich. Feature-driven priority queuing. *Available at SSRN 4998540*, 2024.

H. Song, A. L. Tucker, and K. L. Murrell. The diseconomies of queue pooling: An empirical investigation of emergency department length of stay. *Management Science*, 61(12):3032–3053, 2015.

H. Sornn-Friese, R. T. Poulsen, A. U. Nowinska, and P. de Langen. What drives ports around the world to adopt air emissions abatement measures? *Transportation Research Part D: Transport and Environment*, 90:102644, 2021.

M. Stoffel, J. A. Ballesteros Cánovas, B. H. Luckman, A. Casteller, and R. Villalba. Tree-ring correlations suggest links between moderate earthquakes and distant rockfalls in the patagonian cordillera. *Scientific Reports*, 9(1):12112, 2019.

M. Stopford. *Maritime economics 3e*. Routledge, 2008.

L. Styhre, H. Winnes, J. Black, J. Lee, and H. Le-Griffin. Greenhouse gas emissions from ships in ports–case studies in four continents. *Transportation Research Part D: Transport and Environment*, 54:212–224, 2017.

Q. R. Syed, R. Bhowmik, F. F. Adedoyin, A. A. Alola, and N. Khalid. Do economic policy uncertainty and geopolitical risk surge co2 emissions? new insights from panel quantile

regression approach. *Environmental Science and Pollution Research*, 29(19):27845–27861, 2022.

C. Sys. Is the container liner shipping industry an oligopoly? *Transport policy*, 16(5): 259–270, 2009.

W. K. Talley and M. Ng. Port multi-service congestion. *Transportation Research Part E: Logistics and Transportation Review*, 94:66–70, 2016.

T. F. Tan and B. R. Staats. Behavioral drivers of routing decisions: Evidence from restaurant table assignment. *Production and Operations Management*, 29(4):1050–1070, 2020.

The New York Times. Hurricane ida's impact: Another blow to the supply chain. `https://www.nytimes.com/2021/08/31/business/hurricane-ida-supply-chain-shortages.html`, 2021. Accessed: 2025-07-18.

K. F. Touzinsky, B. M. Scully, K. N. Mitchell, and M. M. Kress. Using empirical data to quantify port resilience: Hurricane matthew and the southeastern seaboard. *Journal of Waterway, Port, Coastal, and Ocean Engineering*, 144(4):05018003, 2018. ISSN 0733-950X.

K. Trepte and J. B. Rice Jr. An initial exploration of port capacity bottlenecks in the usa port system and the implications on resilience. *International Journal of Shipping and Transport Logistics*, 6(3):339–355, 2014.

UNCATD. Case Study 1: Ports of Los Angeles and Long Beach, United States. `https://resilientmaritimelogistics.unctad.org/guidebook/case-study-1-ports-los-angeles-and-long-beach-united-states`, 2022. Accessed: 2024-04-07.

UNCTAD. *Review of maritime transport 2017*. United Nations, New York ; Geneva, 2017. ISBN 9789211129229. OCLC: 1022725798.

UNCTAD. *Key Statistics and Trends in International Trade 2020: Trade Trends Under the COVID-19 Pandemic*. UN, 2021a.

UNCTAD. Building more diverse and resilient economies, 2021b. URL `https://unctad.org/news/building-more-diverse-and-resilient-economies`. Accessed: 2025-07-18.

UNCTAD. *Review of Maritime Transport 2022*. United Nations, Geneva, 2022. UNCTAD.

UNCTAD. Navigating troubled waters: Impact on global trade of disruption to shipping routes in the red sea and black sea, 2024. URL https://unctad.org/publication/navigating-troubled-waters-impact-global-trade-disruption-shipping-routes-red-sea-bla Accessed June 12, 2025.

UNCTAD. *Review of maritime transport 2024: Navigating maritime chokepoints*. United Nations, 2024.

E. Ursavas and S. X. Zhu. Optimal policies for the berth allocation problem under stochastic nature. *European Journal of Operational Research*, 255(2):380–387, 2016.

J. A. Van Mieghem. Dynamic scheduling with convex delay costs: The generalized c— mu rule. *The Annals of Applied Probability*, pages 809–833, 1995.

J. Verschuur, E. Koks, and J. Hall. Port disruptions due to natural disasters: Insights into port and logistics resilience. *Transportation research part D: transport and environment*, 85:102393, 2020. ISSN 1361-9209.

J. Verschuur, E. Koks, and J. Hall. Ports' criticality in international trade and global supply-chains. *Nature Communications*, 13(1):4351, 2022. ISSN 2041-1723.

J. Verschuur, E. E. Koks, S. Li, and J. W. Hall. Multi-hazard risk to global port infrastructure and resulting trade and logistics losses. *Communications Earth Environment*, 4(1):1–12, 2023. ISSN 2662-4435.

K. Wang, J. Wang, L. Huang, Y. Yuan, G. Wu, H. Xing, Z. Wang, Z. Wang, and X. Jiang. A comprehensive review on the prediction of ship energy consumption and pollution gas emissions. *Ocean Engineering*, 266:112826, 2022.

Q. Wang, X. Wang, and R. Li. Geopolitical risks and energy transition: the impact of environmental regulation and green innovation. *Humanities and Social Sciences Communications*, 11(1):1–22, 2024a.

W. Wang, Y. Niu, A. Gapich, and W. Strielkowski. Natural resources extractions and carbon neutrality: The role of geopolitical risk. *Resources Policy*, 83:103577, 2023.

X. Wang, Y. Wu, and W. Xu. Geopolitical risk and investment. *Journal of Money, Credit and Banking*, 56(8):2023–2059, 2024b.

Z. Wang and C. Guo. Minimizing the risk of seaport operations efficiency reduction affected by vessel arrival delay. *Industrial Management & Data Systems*, 118(7):1498–1509, 2018.

Z. X. Wang and W. Wei. Regional economic resilience in china: measurement and determinants. *Regional Studies*, 55(7):1228–1239, 2021. ISSN 0034-3404. doi: 10.1080/00343404.2021.1872779. URL <GotoISI>://WOS:000618993400001. Wang, Zanxin Wei, Wei Wei, Wei/I-2694-2016 Wei, Wei/0000-0001-5287-2896 1360-0591.

D. Wei, A. Rose, E. Koc, Z. Chen, and L. Soibelman. Socioeconomic impacts of resilience to seaport and highway transportation network disruption. *Transportation Research Part D: Transport and Environment*, 106:103236, 2022.

R. W. Wolff. The effect of service time regularity on system performance. Technical report, 1977.

R. Xiao, T. Xiao, P. Zhao, M. Zhang, T. Ma, and S. Qiu. Structure and resilience changes of global liquefied natural gas shipping network during the russia–ukraine conflict. *Ocean & Coastal Management*, 252:107102, 2024.

Y. Xiao and J. Drucker. Does economic diversity enhance regional disaster resilience? *Journal of the American Planning Association*, 79(2):148–160, 2013.

L. Xu, Z. Yang, J. Chen, and Z. Zou. Spatial-temporal heterogeneity of global ports resilience under pandemic: a case study of covid-19. *Maritime Policy & Management*, pages 1–14, 2023.

M. Xu, Q. Pan, A. Muscoloni, H. Xia, and C. V. Cannistraci. Modular gateway-ness connectivity and structural core organization in maritime network science. *Nature communications*, 11(1):2849, 2020.

D. Yang, L. Wu, S. Wang, H. Jia, and K. X. Li. How big data enriches maritime research–a critical review of automatic identification system (ais) data applications. *Transport Reviews*, 39(6):755–773, 2019.

D. Yang, S. Liao, Y. V. Lun, and X. Bai. Towards sustainable port management: Data-driven global container ports turnover rate assessment. *Transportation Research Part E: Logistics and Transportation Review*, 175:103169, 2023.

D. Yang, X. Yue, and W. Y. Yap. Geospatial resilience of shipping alliances: Navigating the red sea crisis. *Journal of Transport Geography*, 126:104254, 2025.

W. Y. Yap and D. Yang. Geopolitical tension and shipping network disruption: Analysis of the red sea crisis on container port calls. *Journal of Transport Geography*, 121:104004, 2024.

M. S. Yıldırım, M. M. Aydın, and Ü. Gökkuş. Simulation optimization of the berth allocation in a container terminal with flexible vessel priority management. *Maritime Policy & Management*, 47(6):833–848, 2020.

J. Yu, G. Tang, and X. Song. Collaboration of vessel speed optimization with berth allocation and quay crane assignment considering vessel service differentiation. *Transportation Research Part E: Logistics and Transportation Review*, 160:102651, 2022.

Q. Yu, G. Allon, and A. Bassamboo. How do delay announcements shape customer behavior? an empirical study. *Management Science*, 63(1):1–20, 2017.

A. Zhang and Y. Zhang. Airport capacity and congestion when carriers have market power. *Journal of urban Economics*, 60(2):229–247, 2006.

Q. Zhang, S. Wang, and L. Zhen. Evaluating eco-economic benefits of anchoring and drifting under government sulfur emission policies. *Transportation Research Part D: Transport and Environment*, 136:104442, 2024.

S. Zhang and L. Wang. The russia-ukraine war, energy poverty, and social conflict: An analysis based on global liquified natural gas maritime shipping. *Applied Geography*, 166: 103263, 2024.

K. Zhao, M. A. Wulder, T. Hu, R. Bright, Q. Wu, H. Qin, Y. Li, E. Toman, B. Mallick, X. Zhang, et al. Detecting change-point, trend, and seasonality in satellite time series data to track abrupt changes and nonlinear dynamics: A bayesian ensemble algorithm. *Remote sensing of Environment*, 232:111181, 2019.

Y. Zhou, J. Wang, and H. Yang. Resilience of transportation systems: concepts and comprehensive review. *IEEE Transactions on Intelligent Transportation Systems*, 20(12):4262–4276, 2019.

Appendix A

Supplement for Chapter 2

A.1 Layouts of berth and anchorage areas

Figure A.1 provides illustrations of terminal layouts at the Port of Busan and the Port of Los Angeles, derived from AIS data and processed through the berth and anchorage identification algorithm (Bai et al., 2023a). In Figure A.1, blue dots indicate ships at berth areas, where vessels dock for loading and unloading, and orange dots highlight ships at the anchorage areas, where ships wait for entering berth areas.

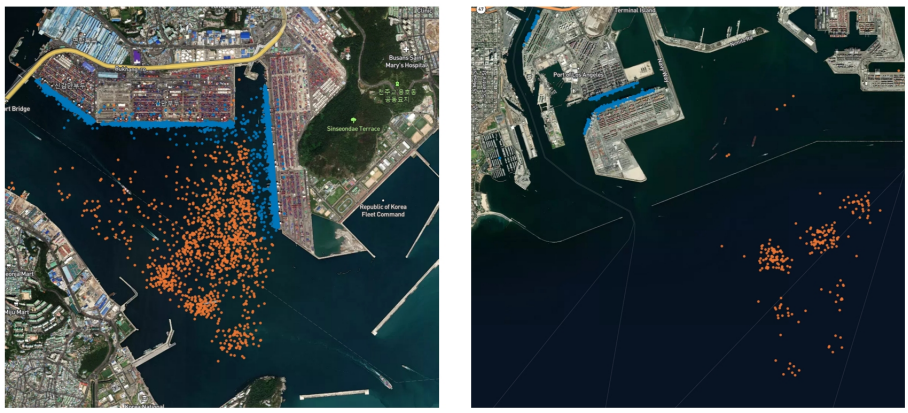

(a) Busan (b) Los Angeles

Figure A.1: Layouts of berth and anchorage areas

A.2 Average ship waiting hours

Figure A.2 illustrates the monthly average ship waiting hours at various ports from 2016 to 2020, with color intensity representing the average waiting times for each month.

For example, our estimated data aligns with reported events at the Port of Los Angeles following the onset of COVID-19. Since October 2020, ships waiting to berth at the port have experienced significant delays due to increasing demand and reduced capacity in shipping logistics (Financial Times, 2020).

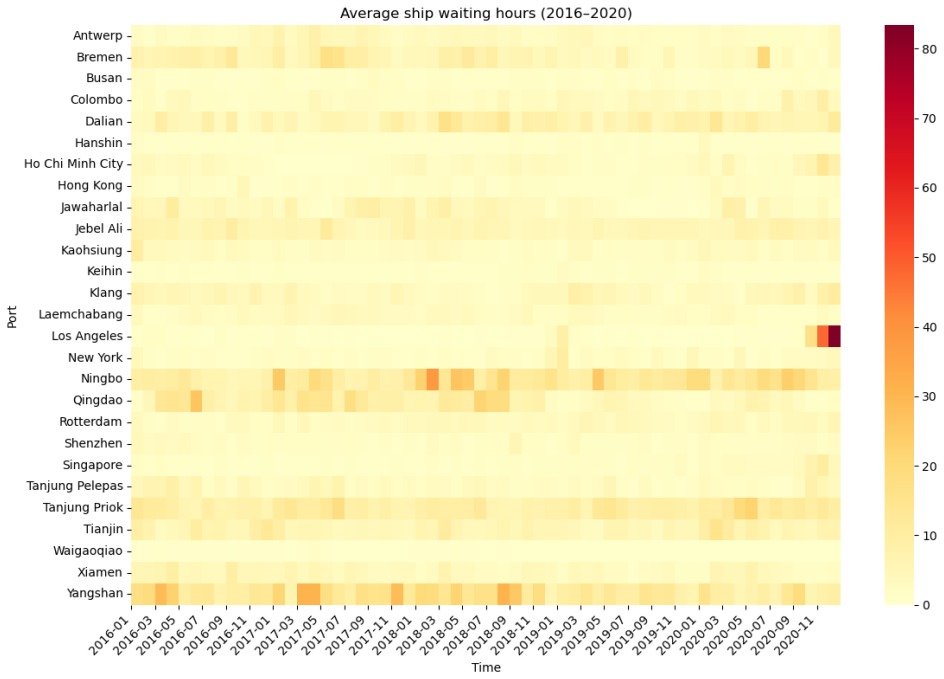

Figure A.2: Average ship waiting hours at ports

A.3 Instrument variables of priority share

$$AvgLinerPriority_{jTG} = \frac{\sum_{n \in N_{jT}, t \in T, j \in G} LinerPriority_{nGT}}{Num_{jt}} = \frac{\sum_{n \in N_{jT}, t \in T, j \in G} \left(\frac{NumPriority_{nGT}}{NumVisit_{nGT}} \right)}{Num_{jT}} \tag{A.1}$$

Eq. A.3 presents the calculation of the instrument variable for the priority share, where $AvgLinerPriority_{jTG}$ stands for shipping lines' average propensity to get priority at terminal j in group G in year T, and group G is classified by the median value of priority share, which we will introduce in the next paragraph. N_{jT} is the set of shipping lines that visited terminal j in year T and Num_{jt} is the total number of shipping lines in set N_{jT}. In particular, for each shipping line n, we calculate its annual priority propensity at group G

terminals in year T (denoted as $LinerPriority_{nGT}$) as the ratio between the number of group G terminals (excluding terminal j) at which the shipping line enjoys priority (denoted as $NumPriority_{nGT}$) and the number of group G terminals (excluding terminal j) it visits in year T (denoted as $NumVisit_{nGT}$). Then, the IV of the priority share of a terminal $j \in G$, denoted as $AvgLinerPriority_{jTG}$, is the mean annual priority propensity of all shipping lines that visited terminal j in year T.

We calculate the IV for priority share by groups classified by the levels of priority share since we notice that the relationship between the mean priority propensity of shipping lines (IV) and priority share at each terminal may be affected by the priority allocation pattern of terminals. Intuitively, in terminals with lower priority shares, the likelihood of being provided priority decreases due to fiercer competition for limited priority slots, leading shipping lines to avoid competing with others at these terminals. Therefore, obtaining priority in one terminal might reduce the likelihood of securing it in another, and the mean priority propensity of shipping lines (IV) is negatively related to the priority share at the terminal. Conversely, in terminals with higher priority shares, operators are more likely to provide priority to shipping lines and more priority slots are available. In these settings, shipping lines are more aggressive in seeking priority to reduce waiting times, fuel costs, and the risk of late deliveries. If a shipping line already has priority at multiple other less congested terminals, they are more likely to secure priority at a given terminal as well, thereby increasing the proportion of shipping lines with priority at this terminal. In this case, the mean priority propensity of shipping lines is positively related to the priority share at the terminal. Considering this, we divided all terminals into three groups based on the median value of priority share (0.1058) across all data, to reflect the diversity in terminal preferences for priority provision: 1) terminals with a priority share below the median for each year from 2016 to 2020; 2) terminals with a priority share above the median for all five years; 3) terminals with priority shares that varied around the median during the five years.

Table A.1 presents the summary statistics classified by the median value of priority share. In Table A.1, terminals with priority share consistently below the median experienced berthing waiting times exceeding 2 hours, whereas those above had significantly shorter waiting times, averaging 0.496 hours, despite similar average HHI levels in both groups. This confirms our concern about endogeneity due to the negative impact of congestion time on priority share. Additionally, those terminals with higher priority have around 8.815 shipping lines with priority on average, compared to around 2.574 shipping lines in terminals with lower priority shares. Furthermore, the average number of terminals where shipping lines have berthing priority is 0.359 for the lower priority share group, and 1.407 for terminals with higher priority shares. Aligned with our expectations, terminals with a priority share lower

(higher) than 50th percentile have a lower (higher) average number of prioritized shipping lines, and a lower (higher) average number of terminals where shipping lines enjoy berthing priority. This disparity underscores the varying patterns of priority allocation across different groups.

Table A.1: Summary statistics grouped by priority share classification

Variable	**N**	**Mean**	**SD**	**Min**	**Max**
Terminals with priority share < 50th					
WaitingTime (Hour)	115,484	2.817	6.031	0	24.649
HHI	115,484	0.065	0.051	0.020	0.587
PriorityShare	115,484	0.031	0.030	0	0.105
NumPriorityLiner	115,484	2.574	2.909	0	10
NumPriorityTerminal	115,484	0.359	0.892	0	14
HHIGlobalShare	115,484	0.060	0.044	0.027	0.706
AvgLinerPriority	115,484	0.004	0.006	0	0.058
DailyPortcall	115,484	7.232	4.178	1	28
DWT (Deadweight Tonnage)	115,484	65,677.889	49,444.759	2,743	232,606
VesselPriority	115,484	0.152	0.359	0	1
Terminals with priority share > 50th					
WaitingTime (Hour)	103,347	0.496	2.597	0	24.612
HHI	103,347	0.065	0.032	0.033	0.417
PriorityShare	103,347	0.252	0.095	0.109	0.502
NumPriorityLiner	103,347	8.815	5.636	1	22
NumPriorityTerminal	103,347	1.407	1.329	0	5
HHIGlobalShare	103,347	0.070	0.047	0.029	0.493
AvgLinerPriority	103,347	0.043	0.015	0.005	0.095
DailyPortcall	103,347	5.948	3.357	1	26
DWT (Deadweight Tonnage)	103,347	56,873.431	49,885.430	1,438	232,606
VesselPriority	103,347	0.036	0.185	0	1
Terminals with fluctuating priority share					
WaitingTime (Hour)	375,156	1.003	3.646	0	24.649
HHI	375,156	0.082	0.057	0.023	0.634
PriorityShare	375,156	0.126	0.085	0	0.632
NumPriorityLiner	375,156	5.452	4.452	0	19
NumPriorityTerminal	375,156	3.342	3.026	0	14
HHIGlobalShare	375,156	0.075	0.054	0.029	0.821
AvgLinerPriority	375,156	0.038	0.010	0	0.080
DailyPortcall	375,156	5.619	3.659	1	28
DWT (Deadweight Tonnage)	375,156	53,411.210	44,595.862	1,438	232,606
VesselPriority	375,156	0.064	0.244	0	1

Note: Terminals with fluctuating priority share refer to those whose priority share fluctuated around the 50th percentile over the five years. *NumPriorityLiner* refers to the number of shipping lines with priority at a terminal. *NumPriorityTerminal* refers to the number of priority terminals a shipping line has. Terminals with twenty or fewer monthly vessel visits were excluded as outliers.

A.4 First-stage regression results of the heterogeneity test

Table A.2 presents the first-stage regression results of our heterogeneity test in IV model. $HHIGlobalShare$ has a significant positive effect on HHI regardless of the priority share

level. However, the coefficient of $AvgLinerPriority$ becomes negative in terminals with lower priority share, and the coefficient of that in high priority share terminals remains significant and positive. This negative impact may reflect the competitive nature of priority allocation in congested terminals, where authorities are less inclined to offer priority due to high berth utilization. Data from Table A.1 reveals that, on average, shipping lines hold 0.358 priority terminals in the low priority share group compared to 1.409 in the higher priority share group. Furthermore, the number of shipping lines granted priority in lower priority share and more congested terminals is markedly lower (2.546) than in high priority share and less congested ones (8.789), demonstrating a more competitive situation of shipping lines on priority allocation in the high-demand environments. This suggests that in such congested terminals, berth utilization is high, diminishing the necessity for terminal operators to attract shipping lines through priority allocation. This suggests a tendency for shipping lines to avoid direct competition for berthing priority with others in these low-priority shares and more congested terminals. Such competitive behavior leads to a negative coefficient for the priority share instrument in the first-stage regression for terminals with lower priority shares, indicating that having priority in one terminal decreases the likelihood of securing priority in another for the same shipping line.

In contrast, terminals with a high priority share are more accommodating, often granting priority to multiple shipping lines. This phenomenon leads to a positive coefficient for the priority instrument in these terminals, aligning with our observations from pooled regression analysis. Here, shipping lines with multiple priorities in other terminals are more likely to request priority, reflecting different dynamics compared to terminals with fewer priority shares, which are less likely to host multiple priority shipping lines simultaneously.

Table A.2: First-stage regression results of the heterogeneity test using 2SLS approach

	(1)	(2)	(3)	(4)
	Priority > 50th		**Priority < 50th**	
	HHI	*PriorityShare*	*HHI*	*PriorityShare*
HHIGlobalShare	0.024***	0.001	0.062***	0.005***
	(0.001)	(0.002)	(0.003)	(0.001)
AvgLinerPriority	-0.000	0.006***	0.056***	-0.030***
	(0.001)	(0.001)	(0.004)	(0.003)
Constant	0.115***	0.142***	0.162***	-0.002
	(0.002)	(0.010)	(0.006)	(0.006)
Controls	Y	Y	Y	Y
Observations	103,347	103,347	115,484	115,484
R^2	0.775	0.397	0.860	0.486
F-statistic	464.347	158.781	863.305	261.373
Fixed Effects	Terminal / Month / Shipping line			

Note: Standard errors are clustered by terminal-month-shipping line category. * $p < 0.1$, ** $p < 0.05$, *** $p < 0.01$.

A.5 Regression results of the robustness test

Table A.3 displays the 2SLS estimation results of the robustness test. The market share of the largest shipping line at the terminal has a negative and significant effect on waiting times in both columns. The coefficient of priority share calculated by the share of shipping lines is not significant in column (1) with the full sample, but it is significant and positive in column (2) when we restrict the sample to terminals with a fixed priority policy. The regression results in Table A.3 are similar to those in Table 2.3, indicating the robustness of our models.

Table A.3: Robustness check using IV/2SLS approach

	(1) Full sample *WaitingTime*	(2) Restricted sample *WaitingTime*
MaxShare	-16.390**	-40.399***
	(7.256)	(12.577)
PriorityN	0.328	15.561**
	(2.783)	(6.094)
Constant	5.185***	5.036***
	(0.537)	(0.955)
Controls	Y	Y
Observations	593,987	218,831
R^2	0.124	0.166
F-statistic	3145.856	418.034
Kleibergen-Paap LM stat.	433.379	161.889
	(0.000)	(0.000)
Kleibergen-Paap Wald F	229.298	84.316
Fixed Effects	Terminal / Month / Shipping line	

Note: Standard errors are clustered by terminal-month-shipping line group category. * $p < 0.1$, ** $p < 0.05$, *** $p < 0.01$.
P-values of Kleibergen-Paap LM statistics are in parentheses. The Stock-Yogo weak instrument critical value for 10% maximal IV size is 7.03.

Appendix B

Supplement for Chapter 3

B.1 The affecting areas of nature disasters

Table B.1 provides a summary of the impact ranges for different types of natural disasters, including floods, storms, earthquakes, landslides, volcanic activities, wildfires, and extreme temperature events. Most disasters, such as floods, storms, volcanic activities, and wildfires, typically affect areas up to approximately 300 km in radius, while a moderate intensity of earthquakes and landslides have a smaller impact range of around 100km, and we found that the impact areas of extreme temperature events are usually determined by the temperature threshold. Considering the diverse nature of these disasters and the generally large areas they can affect, we determined that a radius of 300 km would be a reasonable threshold for assessing whether a port could be impacted by a natural disaster. This threshold ensures that the majority of potential disaster effects are accounted for.

As suggested by the existing literature, earthquakes and landslides may have a smaller impact radius. Therefore, as a robustness check, we have excluded earthquakes and landslides that occurred beyond a radius of 100 km from the port to examine the consistency of our results. As shown in Table B.2, the coefficients of the key variables remain significant and negative.

Table B.1: Summary of natural disaster impact radius used in the literature

Disaster Type	**Impact Radius Used**	**Reference**
Floods & Storms	Typically affect large areas; a radius of approximately 300 km has been used.	Li et al. (2023); National Weather Service (2024)
Earthquakes	Moderate intensity earthquakes (e.g., magnitude 6.0) can cause damage within a radius of approximately 100 km.	Natural Resources Canada (2021)
Landslides	No specific radius reported; often triggered by earthquakes and floods. A radius between 100 km and 300 km might be appropriate.	McColl (2022); Stoffel et al. (2019)
Volcanic Activities	About three-quarters of airports affected are located within 300 km of volcanoes.	Guffanti et al. (2009)
Wildfires	News sources suggest smoke and impact can travel up to 300 km.	BBC (2023); Philenews (2024)
Extreme Temperature	Little literature on affected area size; typically based on local temperature thresholds (e.g., $>40°C$ for heatwaves).	Izaguirre et al. (2021)

Table B.2: Robustness test – excluding earthquakes and landslides beyond a radius of 100 km

	(1)
	Log (Vulnerability+1)
Hinterland industrial diversity	-0.176**
	(0.065)
Port size	-0.304**
	(0.132)
Network centrality	-0.064**
	(0.026)
Constant	37.414***
	(10.292)
Controls	Y
Observations	873
R^2	0.299
F-statistic	26.049
Fixed Effects	Port / Month / Disaster

Note: Earthquakes and landslides occurring more than 100 km from ports are excluded. Standard errors are in parentheses and are clustered at the natural disaster-region level. * $p < 0.1$, ** $p < 0.05$, *** $p < 0.01$.

B.2 Algorithm for detecting change-points in daily ship visits time series

We proposed two algorithms for detecting the key change points in vessel visits post-disaster and then calculating the decrease days, closure days, and recovery days using a Bayesian Change-point Detection algorithm, i.e., BEAST. The Bayesian estimator of abrupt changes, seasonality, and trend (BEAST) algorithm is a sophisticated method for time series analysis that decomposes data into three primary components: time trends, intercept or trend changes at specific points within the series, and random errors. Unlike traditional methods that focus on a single model, BEAST evaluates numerous possible decompositions and synthesizes them into a weighted average model, rather than a "single-best" model. This approach enhances flexibility and efficacy in detecting abrupt changes within time series data.

The first algorithm focuses on ports once shutdown under natural disasters, and the second focuses on ports that remain open but experience significant decreases in vessel visits. Both algorithms start by detecting the decrease start day from potential change points with a downward trend based on BEAST. Then we use a three-day rolling average of vessel visits on the day before the disaster as a baseline for the port pre-disaster activity levels. The first algorithm identifies the zero duration or closure days post-disaster, and computes recovery days from the first instance of vessel visits post-closure to when vessel activity returns to pre-disaster levels. For the second algorithm, we set a threshold at 35% of the pre-disaster level to determine the day with minimum vessel visits, and then the recovery days is the number of days from the minimum vessel visits day until the port resumes its pre-disaster level.

Algorithm 1 Analyze vessel visits changes at ports once shutdown post-disaster

procedure PORT*EVENT_ID(*groups*)
  for each *port_event_id group* in *groups* **do**
    disaster_day ← the date that the disaster starts
    $first\_closure\_day$ ← the first day with zero vessel visits at the port post-disaster, occurring within two weeks after the disaster start day or one week after the disaster end day
    daily_change ← the changes in vessel visits compared to the day before
    pre_disaster_value ← the rolling average of vessel visits over three days on the day before the disaster
    trend_slope ← the slope of the trend fitted by Bayesian Change-point Detection method at each point of the time series
    potential_decrease_start_days ← all Bayesian change points after *disaster_day* before $first\_closure\_day$
    $first\_zero\_duration$ ← the number of days with zero vessel visits for the first time after $first\_closure\_day$
    potential_recovery_days ← all Bayesian change points after $first\_closure\_day$
    find the decrease start day that satisfies conditions before $first\_closure\_day$
    if *potential_decrease_start_days* satisfies *daily_change* < 0 or *trend_slope* < 0 or $3\_day\_rolling\_average < pre\_disaster\_value$ **then**
      decrease_start_day ← the Bayesian change point satisfies the conditions closest to $first\_closure\_day$
    end if
    decrease_days ← count days from *decrease_start_day* to $first\_closure\_day$ with *daily_change* ≤ 0
    recovery_start_day ← $first\_closure\_day + first\_zero\_duration$
    find the recovery end day after *recovery_start_day* with conditions
    if *potential_recovery_days* satisfies *daily_change* > 0 or *trend_slope* > 0 or $3\_day\_rolling\_average \geq pre\_disaster\_value$ **then**
      recovery_end_day ← the first change point in *potential_recovery_days* after *recovery_start_day*
    else
      recovery_end_day ← the first day with $3\_day\_rolling\_average \geq pre\_disaster\_value$
    end if
    recovery_days ← $recovery\_end\_day - first\_closure\_day - first\_zero\_duration + 1$
    closure_days ← count days with zero vessel visits from $first\_closure\_day$ to *recovery_end_day*
    return $decrease\_start\_day, decrease\_days, first\_closure\_day, recovery\_end\_day, recovery\_days, closure\_days$
  end for
end procedure

Algorithm 2 Analyze vessel visits changes at ports without post-disaster shutdown

procedure PORT*EVENT_ID(*groups*)
    for each *port_event_id group* in *groups* **do**
        disaster_day ← the date that the disaster starts
        daily_change ← the changes in vessel visits compared to the day before
        pre_disaster_value ← the rolling average of vessel visits over three days on the day before the disaster
        minimum_threshold ← *pre_disaster_value* ∗ 0.35
        potential_min_vessel_visit_days ← all days with vessel visits less than *minimum_threshold* post-disaster, occurring within two weeks after the disaster start day or one week after the disaster end day
        trend_slope ← the slope of the trend fitted by Bayesian Change-point Detection method at each point of the time series
        potential_decrease_start_days ← all Bayesian change points after *disaster_day* before *min_vessel_visit_day*
        potential_recovery_days ← all Bayesian change points after *min_vessel_visit_day*
        if *potential_min_vessel_visit_days* is not empty **then**
            min_vessel_visit_day ← the day with minimum vessel visits in the group *potential_min_vessel_visit_days*
        else
            The port is not affected by the natural disaster.
        end if
        find the decrease start day that satisfies conditions before *min_vessel_visit_day*
        if *potential_decrease_start_days* satisfies *daily_change* < 0 or *trend_slope* < 0 or *3_day_rolling_average* $<$ *pre_disaster_value* **then**
            decrease_start_day ← the Bayesian change point satisfies the conditions closest to *min_vessel_visit_day*
        else
            decrease_start_day = *min_vessel_visit_day* - 1
        end if
        decrease_days ← count days from *decrease_start_day* to *min_vessel_visit_day* with *daily_change* ≤ 0
        recovery_start_day ← *min_vessel_visit_day* + 1
        find the recovery end day after *recovery_start_day* with conditions
        if *potential_recovery_days* satisfies *daily_change* > 0 or *trend_slope* > 0 or *3_day_rolling_average* $\geq$ *pre_disaster_value* **then**
            recovery_end_day ← the first change point in *potential_recovery_days* after *recovery_start_day*
        else
            recovery_end_day ← the first day with *3_day_rolling_average* $\geq$ *pre_disaster_value*
        end if
        recovery_days ← *recovery_end_day* − *min_vessel_visit_day* + 1
        return *decrease_start_day*, *decrease_days*, *min_vessel_visit_day*, *recovery_end_day*, *recovery_days*
    end for
end procedure

B.3 Variables and summary statistics

Table B.3 introduces the variables used to examine the determinants of port vulnerability and the data source. The dependent variable is the Vulnerability index, calculated from the ratio of recovery days to closure days plus the ratio of recovery days to decrease days, using data from the AIS database and Lloyd's List. Major independent variables include the hinterland industrial diversity for manufacturing firms within varying radii of the port, port size, and network centrality, which are derived from AIS database and supplemented with data from Bureau van Dijk. Local economic indicators such as Hinterland GDP per capita, unemployment rate, and trade openness are sourced from various national and international databases like the World Bank, OECD, and national statistics bureau. Additionally, weather condition indicators like max wind speed, total precipitation and 2m temperature are included to assess environmental impacts, sourced from ERA5. We also control the annual vessel visits and the distance from the port to where the disaster happened. The table provides a comprehensive set of variables enabling a robust analysis of factors influencing port vulnerability in the face of disasters.

Table B.3: Main and control variables

Variable	Description	Data source
Dependent variable		
Vulnerability Index	The vulnerability index is calculated as the ratio of recovery days to closure days plus the ratio of recovery days to decrease days.	AIS Database; Lloyd's List
Main independent variable		
Hinterland industrial diversity 300km	The inverse of Herfindahl-Hirschman Index (HHI) for manufacturing firms within a radius of 300 km of the port.	Bureau van Dijk (BVD) Orbis
Port size	The maximum of vessel DWT visiting the port per year.	AIS Database
Network centrality	The network centrality is the closeness centrality, which is calculated by number of shortest paths from the given port to every other port divided by the total number of intermediary ports along these paths in each year.	AIS Database; Bai et al. (2022)
Local economic indicators		
Hinterland GDP per capita $USD	GDP ($USD) per head, constant prices, constant PPP, base year 2015, at country and regional level.	World Bank Development Indicators, OECD Regional Statistics, National Statistics Bureau
Hinterland unemployment rate %	The percentage of people in the labor force who are unemployed in the year at the country level.	OECD Regional Statistics, National Statistics Bureau
Hinterland trade openness %	Import of goods and services plus export of goods and services divided by GDP at country level.	National Statistics Bureau
Weather condition indicators		
Max wind speed ($m \cdot s^{-1}$)	The maximum speed of the 10m wind at the port.	ERA5 (monthly averaged data on single levels from 1940 to present)
Total precipitation (m)	This parameter is the total amount of liquid and frozen water, including both rain and snow, that falls to the Earth's surface at the port location.	ERA5
2m temperature (°C)	The temperature of air at 2m above the surface of port.	ERA5
Other control variables		
Annual vessel visits	The total number of vessels visiting the port in a year.	AIS Database
Distance (km)	The minimum distance from the port to the climate-related disaster affected areas.	Calculated based on AIS Database and Emergency Events Database (EM-DAT)

Table B.4 displays data on the frequency of natural disaster occurrences near 91 global container ports, totaling 919 port-disaster events. Ports such as Chiwan, Hong Kong, and Manila exhibit notably high frequencies, while many ports like Alexandria, Beirut, and Jebel Ali are listed only once in the distribution table.

Table B.4: Port distribution

Port	**Freq.**	**Port**	**Freq.**	**Port**	**Freq.**
Alexandria	1	Le Havre	6	Algeciras	6
Leixoes	1	Aliaga	2	Antwerp	7
Ashdod	2	Bangkok	6	Barcelona	7
Beirut	1	Bremerhaven	5	Busan	7
Busan new port	8	Butterworth	1	Callao	5
Casablanca	2	Charleston	1	Chittagong	12
Chiwan	32	Colombo	11	Colon	3
Da nang	2	Eemhaven Eotterdam	3	Felixstowe	4
Fort Lauderdale	14	Fukuoya	6	Gemlik	4
Genoa	11	Gioia tauro	4	Guayaquil	2
Gwangyang	6	Haifa	2	Haiphong	22
Hamburg	5	Ho Chi Minh City	5	Hong Kong	32
Incheon	3	Iskandar puteri	5	Istanbul	5
Jakarta	26	Jawarharlal nehru	4	Jebel Ali	1
Jeddah	6	Kaohsiung	13	Keelung	10
Kobe	18	Laem Chabang	6	Lagos	1
Leixoes	1	Lianyungang	1	London gateway	2
Long Beach	10	Los Angeles	3	Maasvlakte rotterdam	3
Makassar	4	Manila	37	Manzanillo	5
Mersin	1	Mundra	1	Nagoya	26
Nansha	24	NewYork	25	Ningbo zhoushan	29
Oakland	23	Osaka	18	Panama	2
Pasir gudang	1	Perama	7	Port Klang	10
Port said east	1	Qingdao	13	Ras Misalla	2
Santos	5	Savannah	26	Sines	2
St. Petersburg	1	Surabaya	20	Suzhou	18
Taichung	9	Taipei	7	Tanger med	4
Tianjin	18	Tokyo	23	Ulsan	2
Valencia	9	Waigaoqiao	42	Xiamen	22
Yangshan	29	Yantian	32	Yingkou	4
Yokohama	23	Zhangzhou	29		
Total	**919**				

Table B.5 categorizes recorded natural disasters by type in our dataset. Storms and floods are the most prevalent disaster types, constituting over 80% of the dataset, which underscores their significant impact on ports studied. Less frequent events include extreme

temperatures, landslides, and wildfires, with earthquakes and volcanic activities also noted. This distribution highlights the varied environmental challenges faced by global ports.

Table B.5: Natural disaster type distribution

Natural Disaster	**Frequency**	**Percent (%)**
Extreme temperature	65	7.07
Flood	351	38.19
Landslide	33	3.59
Storm	401	43.63
Wildfire	29	3.16
Earthquake and Volcanic activity	40	4.35
Total	**919**	**100.00**

B.4 Robustness tests

Table B.6 to B.10 displays the robustness tests conducted to validate our model's reliability in assessing the determinants of port vulnerability. Table B.6 shows the results when we substituted the pre-disaster port operation level from a three-day rolling average of ship visits on the day before the disaster to the total vessel visits and a seven-day rolling average of ship visits prior to the disaster, respectively. Table B.7 presents the results using different thresholds to determine the minimum vessel visit day for ports remaining open but experiencing significant declines in vessel visits, testing the robustness of our method by adjusting the threshold from 35% to 30% and 40% of the pre-disaster level of ports. Furthermore, we made changes in the hinterland radius of the port used for calculating the hinterland industrial diversity, expanding from 300km to 400km and 500km, and the results are shown in Table B.8. B.9 displays the results when we used a weighted average resilience index by assigning the fraction of recovery days to closure days with a higher ratio. In Table B.10, we included the total number of affected people in natural disasters as a proxy for the severity of natural disasters, retrieved from the EM-DAT natural disaster database. Additionally, to account for the effects of regional conflicts, we included a dummy variable (Conflicts) indicating whether the country or region where a port is located was involved in an armed conflict or not, sourced from the UCDP/PRIO Armed Conflict Dataset and the total number of deaths in armed conflicts in the year, sourced from the UCDP Battle-related Deaths Dataset, as control variables. The results are also presented in Table B.10. All three key determinants of port vulnerability in our models consistently exhibit significant and negative impacts on port vulnerability, indicating the robustness of our methodology and model

specifications.

We conducted an extra heterogeneity test by categorizing ports according to their primary function, specifically whether ports mainly handle transshipment cargo flows, since we suppose that the diverse roles ports play within a country or region may influence the determinants of port vulnerability. Following Ducruet and Notteboom (2012), we used network connectivity (measured by closeness centrality) as a proxy for the transshipment share of a port, considering that ports with higher convenience to other ports within the shipping network are more likely to handle more transshipment activities. Ports were subsequently divided into two groups according to the median value of network connectivity (approximately 0.46), and regression analyses were conducted separately for each group. The results are shown in Table B.11.

The findings indicate that port infrastructure significantly contributes to reducing the vulnerability of transshipment ports during natural disasters. Specifically, the coefficient for port size (-1.075) is negative and statistically significant at the 10% level, indicating that larger infrastructure helps mitigate disaster impacts for transshipment ports. For non-transshipment ports, the coefficient for network connectivity (-0.088) is statistically significant at the 5% level, suggesting that connectivity plays a crucial role in enhancing resilience.

The observed differences in the key determinants of port resilience could be attributed to the heterogeneity in port functionality. Transshipment ports appear to rely more heavily on infrastructure endowments, such as the capacity of berths and yard facilities (Notteboom et al., 2023), which are critical factors that influence shipping companies' decisions when selecting transshipment hubs. Consequently, investment in port infrastructure is essential for enhancing the resilience of ports that primarily manage transshipment flows. Conversely, for ports with limited transshipment activities, network connectivity emerges as a key determinant of resilience. These ports, being more dependent on import and export activities, face greater vulnerability during disruptions due to their limited number of shipping routes. Therefore, enhancing connectivity, such as by establishing new routes or attracting additional shipping services, could significantly improve the resilience of these ports in the face of natural disasters.

Table B.6: Robustness test – adjusting the measurement of pre-disaster level

	(1) *Log(Vulnerability+1)* Total vessel visits	(2) *Log(Vulnerability+1)* 7-day rolling average
Hinterland industrial diversity 300km	-0.152**	-0.179**
	(0.071)	(0.075)
Port size	-0.210*	-0.260*
	(0.119)	(0.149)
Network centrality	-0.070***	-0.046**
	(0.021)	(0.020)
Constant	31.169***	36.473***
	(9.604)	(10.542)
Controls	Y	Y
Observations	919	919
R^2	0.291	0.336
F-statistic	22.161	13.852
Fixed Effects	Port / Month / Disaster	

Note: Standard errors in parentheses, clustered at the natural disaster-region level. * $p < 0.1$, ** $p < 0.05$, *** $p < 0.01$. Column (1) uses the total vessel visits the day before the disaster; Column (2) uses the 7-day sum before the disaster.

Table B.7: Robustness test – adjusting the threshold for minimum vessel visit day

	(1) *Log(Vulnerability+1)* 30% threshold	(2) *Log(Vulnerability+1)* 40% threshold
Hinterland industrial diversity 300km	-0.183**	-0.164**
	(0.072)	(0.075)
Port size	-0.208*	-0.298*
	(0.124)	(0.154)
Network centrality	-0.065***	-0.047**
	(0.021)	(0.019)
Constant	34.071***	32.388***
	(10.401)	(9.311)
Controls	Y	Y
Observations	919	919
R^2	0.287	0.315
F-statistic	30.434	33.833
Fixed Effects	Port / Month / Disaster	

Note: Standard errors in parentheses, clustered at the natural disaster-region level. * $p < 0.1$, ** $p < 0.05$, *** $p < 0.01$. The minimum vessel visits volume should be reduced to lower than 30% or 40% of the three-day rolling average vessel visits volume prior to the disaster.

Table B.8: Robustness test – adjusting the hinterland radius of the port

	(1) *Log(Vulnerability+1)* 400km	(2) *Log(Vulnerability+1)* 500km
Hinterland industrial diversity 400km	-0.176**	
	(0.067)	
Hinterland industrial diversity 500km		-0.207**
		(0.088)
Port size	-0.236*	-0.247*
	(0.133)	(0.132)
Network centrality	-0.059**	-0.058**
	(0.028)	(0.028)
Constant	36.705***	38.646***
	(10.643)	(11.124)
Controls	Y	Y
Observations	919	919
R^2	0.302	0.303
F-statistic	17.954	19.022
Fixed Effects	Port / Month / Disaster	

Note: Standard errors in parentheses, clustered at the natural disaster-region level.
* $p < 0.1$, ** $p < 0.05$, *** $p < 0.01$.

Table B.9: Robustness test – a weighted average resilience index

	(1) *Log(Vulnerability+1)*	(2) *Log(Vulnerability+1)*
Hinterland industrial diversity 300km	-0.120**	-0.118**
	(0.056)	(0.057)
Port size	-0.189*	-0.184*
	(0.101)	(0.102)
Network centrality	-0.045**	-0.046**
	(0.021)	(0.021)
Constant	25.224***	24.706***
	(8.094)	(8.164)
Controls	Y	Y
Observations	919	919
R^2	0.294	0.295
F-statistic	21.942	24.747
Fixed Effects	Port / Month / Disaster	

Note: In column (1), we assigned a weighted factor of 0.55 to the fraction of recovery days to closure days and 0.45 to the fraction of recovery days to decrease days. In column (2), we assigned a weighted factor of 0.6 to the fraction of recovery days to closure days and 0.4 to the fraction of recovery days to decrease days. Standard errors in parentheses, which are clustered at natural disaster-region level. * $p < 0.1$, ** $p < 0.05$, *** $p < 0.01$.

Table B.10: Robustness test – control the severity of natural disasters and regional conflicts

	(1) *Log(Vulnerability+1)*	(2) *Log(Vulnerability+1)*	(3) *Log(Vulnerability+1)*
Hinterland industrial diversity 300km	-0.178**	-0.165**	-0.166**
	(0.067)	(0.071)	(0.071)
Port size	-0.213*	-0.240*	-0.243*
	(0.118)	(0.135)	(0.133)
Network centrality	-0.055*	-0.059**	-0.059**
	(0.032)	(0.027)	(0.027)
Log (Total affected population)	0.008		
	(0.015)		
If Conflict		-0.069	
		(0.150)	
Log (Deaths in conflicts + 1)			-0.007
			(0.038)
Constant	34.178***	34.598***	34.861***
	(10.816)	(10.515)	(10.449)
Controls	Y	Y	Y
Observations	873	919	919
R^2	0.302	0.301	0.301
F-statistic	23.220	20.397	23.311
Fixed Effects		Port / Month / Disaster	

Note: Column (1) presents the result when controlling for the severity of natural disasters using the total affected population from EM-DAT. Missing values are filled using the average within each port-disaster group; 46 observations remain missing. Column (2) controls for a dummy variable, *If Conflict*, equal to 1 if the port's region is involved in an armed conflict. Column (3) controls for the log of total deaths from conflict. Standard errors in parentheses, clustered at the natural disaster-region level. $^{*}p < 0.10$, $^{**}p < 0.05$, $^{***}p < 0.01$.

Table B.11: Heterogeneity test – sub-group regression by port function

	(1) *Log(Vulnerability+1)* Transshipment Ports	(2) *Log(Vulnerability+1)* Non-transshipment Ports
Hinterland industrial diversity 300km	-0.187	-0.132
	(0.134)	(0.184)
Port size	-1.075*	-0.125
	(0.553)	(0.194)
Network centrality	-0.011	-0.088**
	(0.024)	(0.042)
Constant	39.474*	45.468***
	(19.795)	(16.858)
Controls	Y	Y
Observations	450	469
R^2	0.322	0.358
F-statistic	26.532	15.664
Fixed Effects	Port / Month / Disaster	

Note: In column (1), transshipment ports refer to ports with a network connectivity larger than the median value, which tend to handle more transshipment flows. In column (2), non-transshipment ports refer to those ports with a network centrality lower than the median value, which are more likely to be gateway ports or mixed ports. Standard errors in parentheses, clustered at the natural disaster-region level. * $p < 0.1$, ** $p < 0.05$, *** $p < 0.01$.

Appendix C

Supplement for Chapter 4

C.1 Spatial distributions of GPR and port carbon emissions

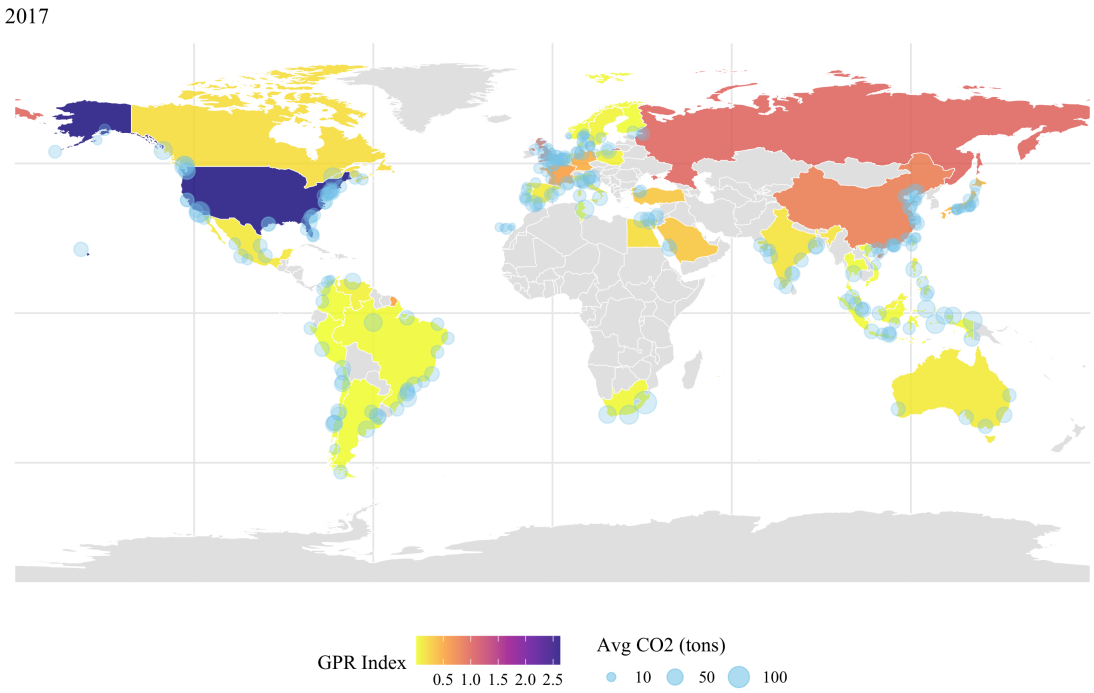

Figure C.1: Geopolitical risks and average port CO_2 emissions in 2017

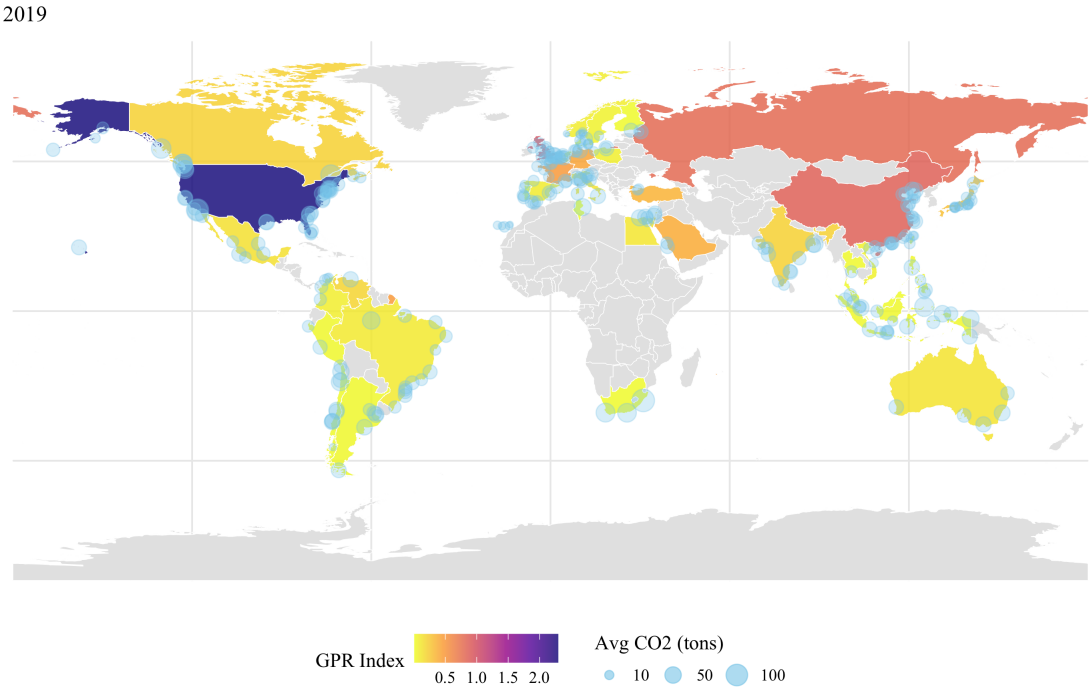

Figure C.2: Geopolitical risks and average port CO_2 emissions in 2019

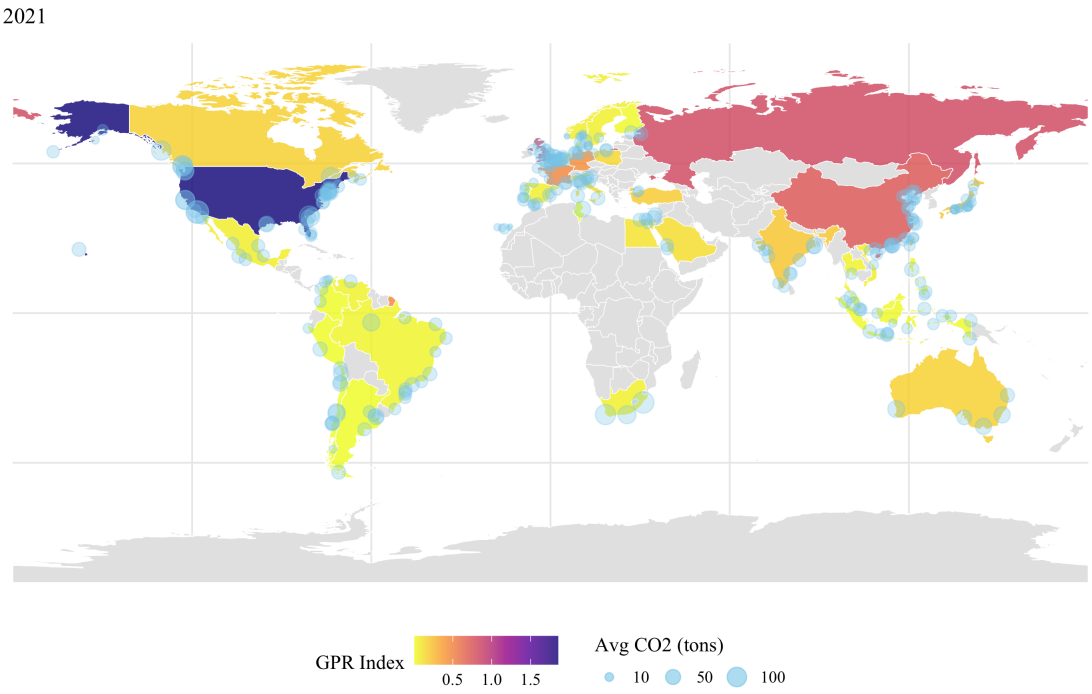

Figure C.3: Geopolitical risks and average port CO_2 emissions in 2021

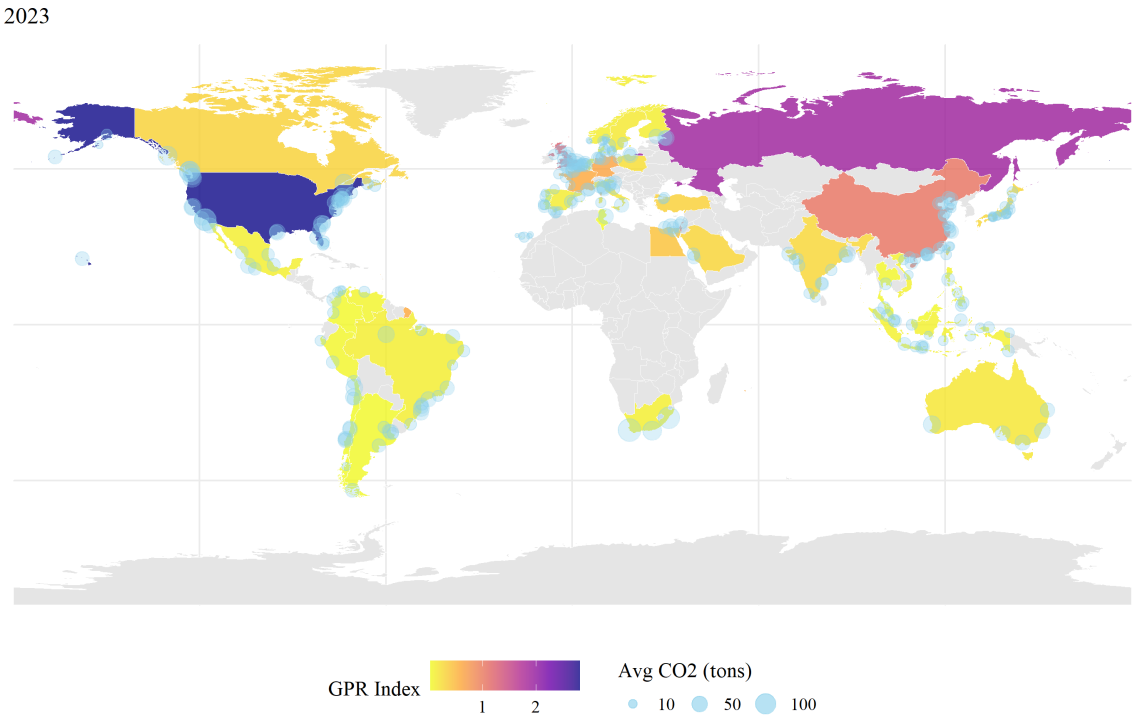

Figure C.4: Geopolitical risks and average port CO_2 emissions in 2023

C.2 Port reference table

Table C.1: Country/Region–port reference table

Country/Region - Port	**Country/Region - Port**	**Country/Region - Port**
Argentina - Buenos Aires	Argentina - La Plata	Argentina - Puerto Nacional
Argentina - Rosario	Argentina - Zarate	Australia - Botany Bay
Australia - Brisbane	Australia - Fremantle	Australia - Melbourne
Australia - Port Adelaide	Belgium - Antwerpen	Belgium - Oostende
Belgium - Zeebrugge	Brazil - Imbituba	Brazil - Itajai
Brazil - Manaus	Brazil - Paranagua	Brazil - Port De Salvador
Brazil - Porto De Mucuripe	Brazil - Porto De Suape	Brazil - Rio De Janeiro
Brazil - Rio Grande	Brazil - Santos	Brazil - Sao Francisco
Brazil - Vila Do Conde	Brazil - Vitoria	Canada - Halifax
Canada - Montreal	Canada - New Westminster	Canada - Prince Rupert
Canada - St John	Canada - Steveston	Canada - Vancouver

Country/Region - Port	Country/Region - Port	Country/Region - Port
Chile - Antofagasta	Chile - Bahia De Valparaiso	Chile - Bahia San Vicente
Chile - Coronel	Chile - Iquique	Chile - Lirquen
Chile - Mejillones	Chile - Puerto Chacabuco	Chile - Puerto San Antonio
Chile - Rada De Arica	Chile - Rada Punta Arenas	China - Bayuquan
China - Dalian	China – Huangpu Xingang	China - Huizhou
China - Jinzhou Wan	China - Lianyungang	China - Qingdao Gang
China - Qinzhou	China - Rizhao	China - Shanghai
China - Shekou	China - Taicang	China - Tangshan (Jingtang)
China - Tianjin Xin Gang	China - Weihai	China - Xiamen
China - Xiuyu	China - Yangpu	China - Yantai
China - Yantian	China - Zhangjiangang	China - Zhanjiang
China - Zhen Hai	China - Zhoushan	Colombia - Barranquilla
Colombia - Buenaventura	Colombia - El Bosque	Colombia - Santa Marta
Colombia - Turbo	Denmark - Alborg	Denmark - Arhus
Denmark - Kobenhavn	Denmark - Tuborg	Egypt - Al Iskandariyh (Alexandria)
Egypt - Bur Said (Port Said)	Egypt - Damietta	Egypt - El-Adabiya
Finland - Kotka	France - Bordeaux	France - Fos
France - Gravelines	France - Marseille	France - Montoir
France - Port Du Havre-Antifer	France - Port Of Le Havre	France - Rade De Brest
Germany - Bremerhaven	Germany - Cuxhaven	Germany - Hamburg
Germany - Wilhelmshaven	Hong Kong - Hong Kong	India - Calcutta
India - Chennai (Madras)	India - Haldia Port	India - Hazira
India - Jawaharlal Nehru Port (Nhava Shiva)	India - Kamarajar Port	India - Kochi (Cochin)
India - Mundra	India - Pipavav Bandar	India - Tuticorin
India - Vishakhapatnam	Indonesia - Ambon	Indonesia - Banjarmasin
Indonesia - Belawan	Indonesia - Bitung	Indonesia - Gresik
Indonesia - Jakarta	Indonesia - Jayapura	Indonesia - Manokwari Road
Indonesia - Merauke	Indonesia - Poleng Oil Field	Indonesia - Pontianak

Country/Region - Port	Country/Region - Port	Country/Region - Port
Indonesia - Sekupang	Indonesia - Semarang	Indonesia - Surabaya
Indonesia - Tg. Sorong	Indonesia - Ujung Pandang	Israel - Ashdod
Israel - Haifa	Italy - Ancona	Italy - Cagliari
Italy - Genova	Italy - Gioia Tauro	Italy - La Spezia
Italy - Livorno	Italy - Marina Di Carrara	Italy - Porto Di Corsini
Italy - Porto Di Lido-Venezia	Italy - Porto Di Malamocco	Italy - Trieste
Japan - Amagasaki	Japan - Chiba Ko	Japan - Eastern Part Of Niigata-Ko
Japan - Hachinohe Ko	Japan - Hitachi	Japan - Kawasaki Ko
Japan - Kobe	Japan - Nagoya Ko	Japan - Onahama Ko
Japan - Osaka	Japan - Sakai-Senboku	Japan - Sendai-Shiogama
Japan - Shimizu Ko	Japan - Tokyo Ko	Japan - Tomakomai Ko
Japan - Yokkaichi	Japan - Yokohama Ko	Malaysia - Johor
Malaysia - Port Klang	Malaysia - Pulau Pinang	Malaysia - Tanjung Pelepas
Mexico - Altamira	Mexico - Ensenada	Mexico - Lazaro Cardenas
Mexico - Manzanillo	Mexico - Mazatlan	Mexico - Veracruz
Netherlands - Europoort	Netherlands - Schiedam	Netherlands - Vlissingen
Norway - Brevik	Norway - Fredrikstad	Norway - Kopervik
Norway - Larvik	Norway - Moss	Norway - Oslo
Norway - Tananger	Peru - Paita	Peru - Puerto Del Callao
Philippines - Cebu	Philippines - Davao	Philippines - General Santos
Philippines - Manila	Poland - Gdynia	Poland - Port Polnochny
Poland - Szczecin	Portugal - Lisboa	Portugal - Porto De Leixoes
Portugal - Setubal	Portugal - Sines	Russian Federation - Lomonosov
Russian Federation - Sankt-Peterburg	Saudi Arabia - Jiddah	Saudi Arabia - Rabigh
South Africa - Cape Town	South Africa - Durban	South Africa - Port Elizabeth
Spain - Algeciras	Spain - Arrecife	Spain - Barcelona
Spain - Cadiz	Spain - Ceuta	Spain - Gijon
Spain - Las Palmas	Spain - Malaga	Spain - Puerto Del Rosario

Country/Region - Port	Country/Region - Port	Country/Region - Port
Spain - Sagunto	Spain - Santa Cruz De La Palma	Spain - Santa Cruz De Tenerife
Spain - Valencia	Spain - Vigo	Sweden - Goteborg
Sweden - Helsingborg	Sweden - Norrkoping	Taiwan, Province of China - Chi-Lung
Taiwan, Province of China - Kao-Hsiung	Taiwan, Province of China - Tai-Chung Kang	Taiwan, Province of China - Tan-Shui
Thailand - Ko Si Chang Terminal	Tunisia - Mersa Sfax	Turkey - Borusan Fertilizer Jetty
Turkey - Kaba Burnu	United Kingdom - Avonmouth	United Kingdom - Belfast
United Kingdom - Blyth	United Kingdom - Felixstowe	United Kingdom - Grangemouth
United Kingdom - Gravesend	United Kingdom - Harwich	United Kingdom - Immingham
United Kingdom - Kingston Upon Hull	United Kingdom - Liverpool	United Kingdom - Portsmouth Harbour
United Kingdom - Ramsgate	United Kingdom - Southampton	United Kingdom - Tilbury
United Kingdom - Tynemouth	United States - Alameda	United States - Anchorage
United States - Baltimore	United States - Bayonne	United States - Baytown
United States - Boston	United States - Cape Charles	United States - Charleston
United States - Chester	United States - Deepwater Point	United States - Dutch Harbor
United States - Elizabethport	United States - Gloucester	United States - Honolulu
United States - Kodiak	United States - Leonardo	United States - Long Beach
United States - Los Angeles	United States - Mayport	United States - Miami
United States - New York City	United States - Newark	United States - Norfolk
United States - Norsworthy	United States - Oakland	United States - Palm Beach

Country/Region - Port	Country/Region - Port	Country/Region - Port
United States - Port Everglades	United States - Port Hueneme	United States - Port Richmond Si
United States - Port Royal	United States - Savannah	United States - Seattle
United States - Tacoma	United States - Tampa	Venezuela, Bolivarian Republic of - La Guaira
Viet Nam - Da Nang	Viet Nam - Hai Phong	